Imprecision in Social Learning

By

Zixuan Liu

Department of Engineering Mathematics
University of Bristol

A dissertation submitted to the University of Bristol in accordance with the requirements of the degree of Doctor of Philosophy in the Faculty of Engineering.

September, 2023

Abstract

This thesis investigates the role of imprecision in social learning, which consists of two critical aspects: belief fusion with other agents and evidential updating based on direct evidence from the environment. A decentralised collective learning problem is investigated in which a population of agents attempts to learn the true state of the world and a novel parameterised fusion operator that allows varying levels of imprecision is proposed. This is used to explore the effect of fusion imprecision on learning performance in a series of agent-based simulations. In general, the results suggest that imprecise fusion operators are optimal when the frequency of fusion is high relative to the frequency with which evidence is obtained from the environment. A parallel line of study explores the role of imprecision in evidential updating in a noisy environment. Through agent-based simulations we demonstrate that the social learning model is robust to imprecise evidence. Our results also show that certain kinds of imprecise evidence can enhance the efficacy of the learning process in the presence of sensor errors. An integrated model is then proposed, combining the advantages of both the parameterised fusion operator and novel evidential updating strategies. We demonstrate that an integrated approach combining fusion and evidential imprecision can further enhance the robustness and accuracy of social learning processes. In addition, we compare various evidential updating methods for set-based belief and then propose a hybrid updating method to combine the strength of different methods. We found the hybrid methods can enhance the accuracy and robustness of social learning significantly with more time required for the agents to reach consensus. These findings have significant implications for designing intelligent systems capable of social learning and decentralised decision-making.

Dedication and acknowledgements

Embarking on the journey of my Ph.D. has been a monumental chapter in my life, replete with challenges but also extraordinary growth and enlightenment. The academic and personal support I have received from various quarters has made this experience even more fulfilling. I take this opportunity to express my appreciation to all those who have contributed to my journey. Among the people who have made this journey not just possible but truly enriching, there are a few individuals I'd like to single out for their help and support.

First, a profound thank you to Jonathan, who has been always sending my drafts back like a rainbow explosion of comments and insights. It's like getting my paper back with its own colour-coded cheat sheet. I have learned a ton from those colourful pages, and I could not be more grateful. While those colourful pages may look overwhelming, Jonathan has been a exceptional patient and encouraging supervisor so that those pages becomes more encouraging as well. His guidance inspired my interests in collective intelligence, which motivated me to shape this project. His advice and encouragement from the beginning, not to the end, but so far has contributed significantly to the development of my self-confidence. In moments when I have felt tangled in confusion or misunderstood a principle, his advice has offered both clarity and reassurance. Moreover, I have been granted an generous level of freedom, both in terms of time management and the scope of my research. This freedom has been invaluable, particularly in the flexibility it has afforded me. Not being bound to a rigid schedule or set tasks has allowed me the autonomy to prioritise my own time and research. It was a privilege that I deeply appreciate.

A special acknowledgement goes to Mike, who is not only a supervisor but friend. Most importantly, thanks for adding even more colours to my drafts and still even after making the move to fancy Tokyo. It says a lot that you are still engaged to our weekly catch-ups, despite being thousands of miles away. Beyond the professional guidance as a supervisor, he has extended a friendship and emotional support that became especially important for me during the difficult days of the COVID-19 pandemic, teaching me not only how to settle a bill in a foreign land but also how to construct the algorithms of my research. During our milk tea talks, we have shared not just scholarly challenges and successes but also life experiences, coping strategies, and even moments of humour and levity during stressful times. Our talks have been the most cherished codes in the program of my life. These 'off-the-record' conversations have often helped me cope the challenges of living in a country that I am new to, and provided fresh perspectives and rejuvenated my energy for research.

My deepest gratitude is reserved for my parents, Zhongxing and Liqing. Their unwavering support to my decisions and constant emotional support have been foundational in every step of this journey and throughout my life. I have been blessed with the freedom of choice since my formative years, thanks to the unconditional support of my family that provided such

opportunities. I look forward to the day when I can fully reciprocate their love and sacrifices. Now that I've reached an age where I can truly comprehend the complexities of life, I recognise the monumental decision it is to bring a child into this world. The choice to become parents involves untold sacrifices and endless commitment—magnitudes of responsibility that I can only now begin to grasp. I find myself with a newfound appreciation for the depth of love and courage it takes to embark on the journey of parenthood. Thank you for taking that significant step, for it has shaped my own life in ways I am only beginning to understand.

特此向我的父亲刘中兴先生和母亲付利清女士，致以深厚的谢意。他们对我的生涯决策与心理状态给予了无条件的支持。多亏了家庭的无条件支持，我自从年幼时便享有很多同龄人不曾有过的选择的自由。我企盼有朝一日，以实际行动来回报他们无私的爱和牺牲。现在，我已经到了能够真正理解人生复杂性的年龄，我认识到把孩子带到这个世界上是一个多么重大的决定。我发现自己对踏上为人父母之路所需要的深沉的爱和勇气有了新的认识，选择为人父母，需要做出难以计数的牺牲和无尽的付出，感谢你们选择把我带来这个世界并且抚养我长大。

Finally, heartfelt thanks and deep appreciation are owed to Danyang, who transformed my experience of solitude in a foreign land into a journey shared. Her love and support have been an indispensable part of both my emotional well-being and my academic journey. Our conversations in the depth of night have been my sanctuary, a place of respite where I could unburden my fears and anxieties. Our escapes—whether little trips or long getaways—have served as much-needed interludes, pulling me back from the precipice of depression time and time again. I am keenly aware that I am not always the easiest person to be around, let alone support. My words can scarcely capture the deep and transformative influence you have made on my life. Thank you, for being an irreplaceable part of my life.

Author's declaration

I declare that the work in this dissertation was carried out in accordance with the requirements of the University's Regulations and Code of Practice for Research Degree Programmes and that it has not been submitted for any other academic award. Except where indicated by specific reference in the text, the work is the candidate's own work. Work done in collaboration with, or with the assistance of, others, is indicated as such. Any views expressed in the dissertation are those of the author.

SIGNED: ..... DATE: .....

Table of Contents

List of Figures

Figure **Page**

Chapter 1

Introduction[1]

1.1 Overview

Social learning has been the subject of extensive research across various disciplines including biology, psychology, and more recently, multi-agent artificial intelligence and swarm robotic systems. Social learning is common in social animals where individuals learn collectively by both observation and imitation of others [1]. In human societies, social learning also plays an important role [2]. For example, humans acquire cultural traditions from family members and students not only learn from teachers but also engage in group projects and discussions with classmates, thus acquiring collaborative skills and diverse perspectives in school education. In addition, peer review in academic and scientific communities is a form of social learning where one's work is evaluated and critiqued by others in the field, contributing to collective knowledge. Through interacting with others, we have been able to pass down knowledge, speed up skill acquisition and ensure the continuity of cultural traditions. Social insects, such as ants, bees, and termites, use social learning to enhance their collective efforts. They excel at coordinating large groups, whether constructing complex habitats or finding the most efficient paths to gathering resources. For instance, a single ant might seem very limited in its capabilities, but a colony, through the power of social learning and self-organisation, can construct architectural marvels, wage wars, or optimise the foraging of food in surprisingly efficient ways. Ants, for instance, employ pheromone trails as a form of environmental marking to communicate with their peers about food sources or danger zones. This chemical communication allows them to collectively make decisions about the shortest paths to food or to mobilise against threats [3]. Likewise, honeybees use the "waggle dance" as a form of information sharing by which foraging bees can relay information regarding the location, distance, and quality of food sources to their hive mates, ensuring the efficient allocation of foragers to plentiful nectar sources [4]. Their achievements highlight the strength of social learning, which optimises collective behaviours.

[1]Part of this chapter has been submitted to *Swarm Intelligence* and can be accessed via Research Square: `https://doi.org/10.21203/rs.3.rs-2620622/v1`; It may appear on the Turnitin report.

For example, honeybee foragers are guided by social cues related to floral scents, conveyed through trophallaxis. This process involves successful foragers transferring nectar samples to nestmates, thereby disseminating information about nectar sources within the hive [4]. In addition, one of the most significant challenges encountered by social insect colonies is relocating their nests. This complex process involves the coordinated movement of hundreds to thousands of individuals from their existing residence to the selected best new site out of a range of potential ones. The decision-making process is driven by a few scout members who, through a sophisticated mix of individual and social learning, manage to achieve consensus on the optimal site[5]. Remarkably, this consensus is reached despite most individuals not evaluating all possible locations themselves.

In the evolving landscape of artificial intelligence, the principles of social learning are no longer reserved for biological systems and are instead finding newfound significance in the development of robust, adaptive, and efficient multi-agent AI systems. As technological advancements continue to push the boundaries of what AI can achieve, harnessing the collective intelligence of agents through social learning is becoming paramount. Just as animals benefit from the aggregated knowledge of the group, AI agents can significantly improve their performance, accuracy, and adaptability when they integrate information from diverse sources within their network. Such systems are able to solve complex tasks based on the coordinated behaviours and shared discoveries of the entire system. As we move towards a future where autonomous systems will be tasked with more complex, dynamic, and unpredictable scenarios, the ability for these systems to learn socially could be the linchpin to their success. From managing smart cities to exploring distant areas, the principles of social learning will undoubtedly play a significant role in how multi-agent AI systems collaborate, make decisions, and adapt to complex, dynamic environments.

In distributed autonomous systems, e.g. multi-agent systems (MAS) and swarm robotics, a population of AI agents operate collaboratively, often dispersed across varied locations or environments. Social learning finds pivotal applications in these aspects. One of the standout benefits of applying social learning to distributed AI systems is the ability for agents to share their beliefs. An insight or discovery by one agent can be rapidly disseminated, ensuring a swift and collective advancement in knowledge. The collective 'knowledge repository' obtained through social learning paves the way for collaborative problem-solving. Complex issues, which are often beyond the capacity of a singular agent, can be collectively solved by a population of agents thus effectively leveraging the collective intelligence and capacity of the entire system. For instance, in traffic management, individual traffic lights could function as agents, each one sensing and responding to local traffic conditions [6]. When networked together, these traffic lights can optimise for broader goals, like minimising overall commute time across the city or rerouting traffic during an emergency.

Social learning algorithms serve an important role in distributed systems like robotic swarms

that are required to make collective decisions. In real-world scenarios, dynamic environments are changing frequently and their dynamic nature requires a system that can adapt swiftly, while remaining stable in its operation. These environments are complex, often involving multiple interacting variables that change in real-time. Whether it's fluctuating stock prices in the financial markets, real-time health monitoring in intensive care units, or rapid resource allocation in disaster-stricken areas, the need for swift and adaptive decision-making is paramount. With advances in technology like AI, the complexities of these environments have only escalated. Traditional centralised systems are increasingly less-equipped to manage this complexity and the required speed of decision-making. In contrast, distributed systems and adaptive social learning models offer a compelling solution [7, 8]. A distributed system can spread new information more rapidly than a centralised system and this is thought to make them adaptive to the changes in the environment [8]. It is observed that human individuals leaned heavily on social learning to adapt spatial changes [9]. This agility in information flow is critical for localised, real-time decision-making, allowing individual nodes to adapt to immediate changes in their micro-environments. Such localised adaptability cumulatively results in a global system response that is not just swift but also robust and resilient. In this way, distributed systems are not merely keeping pace with the dynamic nature of real-world environments but are, in fact, essential for effective functioning within them.

Distributed autonomous systems can be deployed in environments which are not well suited (and perhaps even harmful) to humans, and just as humans and insects benefit from the interaction with their peers, artificial agents in MAS can be designed to learn from one another, allowing for sophisticated problem-solving strategies to emerge. For example, when seeking to detect and monitor wildfires we can opt to deploy a multi-robot fire-fighting system instead of sending human teams into danger [10]. Multi-robot teams have also been proposed for the inspection of structural integrity in hazardous environments, such as nuclear power stations [11]. However, in these scenarios there is often only very limited contact between autonomous systems and their human operators, with infrequent reporting and updating and often at great distances due to the extreme environmental conditions. The systems therefore require greater degrees of autonomy, such that they can make decisions and act based solely on the information they gather in their environment. To facilitate this, agents will need to learn an accurate description of their environment, on which the system can then base its future actions. For example, fig. 1.1 shows a wildfire search operation carried out by a swarm of Unmanned Aerial Vehicles (UAVs). The swarm disperses across a disaster-affected area to collaboratively search for sites impacted by the fire hazard. The robots explore the environment to acquire direct information and communicate with each other to combine their beliefs and gather indirect information.

In this thesis, we will focus on distributed decision making problems in which agents attempt to collectively identify the true state of the world. We employ a propositional model that a state of the world s will be an allocation of truth values to a set of predefined propositions.

Figure 1.1: The swarm disperses across a disaster-affected area to collaboratively search for sites impacted by the fire hazard. The robots explore the environment to acquire direct information and communicate with each other to combine their beliefs and gather indirect information.

In our model, we consider a proposition to represent a specific condition or variable of the environment, each of which can either be true or false. For instance, in the context of a wild fire search mission as shown in Figure 1.1, relevant propositions could include "there is a wildfire at location 2" or "there are people at location 3." These propositions serve as binary variables that can either be true or false, capturing different aspects of the environment in which the system operates. Given a set of n such predefined propositions, we can define a state of the world s as an allocation of truth values to these n propositions. With n binary propositions, there are 2^n possible states of the world. Each of these states corresponds to a unique combination of truth values allocated to the n propositions. In a scenario with five relevant propositions, 2^5 or 32 possible states, i.e. distinct allocations of the truth values, could exist—ranging from all propositions being true to all being false, or any intermediate combination thereof. Only one of these allocations will reflect the actual, true state of the world. The true state of the world then represents the correct allocation of truth values to the propositions. For example, the true state of the world reflects where survivors and fire hazards are actually located in the wildfire search scenario. This propositional model of social learning can be applied to a broad class of

applications. For example, we could model the risk of an epidemic, e.g. COVID-19, for areas around the world with a proposition of the form "this area is high risk" and the proposition can either deemed true or false (this area is not high risk) by the agents (health agencies). The true state of the world would then correspond to the actual risk profile across all areas. Agents might then be different health authorities, which would share information between them and obtain direct evidence based on data obtained about the region for which they are responsible.

The proposed model holds significant promise for swarm robotic applications, particularly in tasks that involve selecting the optimal option from a set of alternatives or classifying multiple sites when the total number of sites is predetermined. In such applications, the collective intelligence and distributed sensing capabilities of the swarm can be harnessed to assess each option or site in detail, pooling individual agents' observations to form a comprehensive understanding. This approach is particularly advantageous in scenarios where the environment may not be rapidly changing, but where the accuracy and reliability of the collected data are critical. For example, in environmental conservation efforts, a swarm of drones could evaluate various areas for a reforestation project, determining which site offers the optimal conditions based on soil quality, water availability, and existing vegetation. Furthermore, swarms of sensor-equipped drones or robots could be deployed to monitor pollutants in the environment. These swarms could cover large areas and navigate complex terrain to collect data from various locations simultaneously in order to identify and signal pollutants. The proposed model enhances these applications by ensuring that the swarm's collective decision reflects a balanced consideration of all available evidence, effectively managing the uncertainties and variabilities inherent in real-world data. This capability not only improves the quality of the decision-making process but also increases the efficiency and effectiveness of the swarm's operations in static application contexts.

Since the environment in which distributed systems will be deployed is likely to be complex and agents have limited sensory and information representation capacities, they will tend to be susceptible to noise. In the social learning literature, noise is usually modelled as Gaussian variation from a true value [12, 13] or as a probability of receiving false evidence [14]. In this paper we differentiate noise of this form, which we hereafter refer to as inaccuracy, from imprecision and we show that the latter also has an important and potential useful effect on social learning. Specifically, noise as outlined above, relates to the accuracy of the evidence obtained with reference to the true state of the world. In other words, evidence is accurate if it is consistent with the true state of the world and inaccurate otherwise. In contrast, evidence is imprecise if it fails to identify a single state of the world. From this perspective it is possible for evidence to be both accurate and imprecise since this simply means that the evidence is consistent with the true state of the world but does not uniquely identify it. In other words, the evidence is consistent with a number of possible states including the true state. In this case the degree of precision of the evidence is dependent on the number of states that are consistent

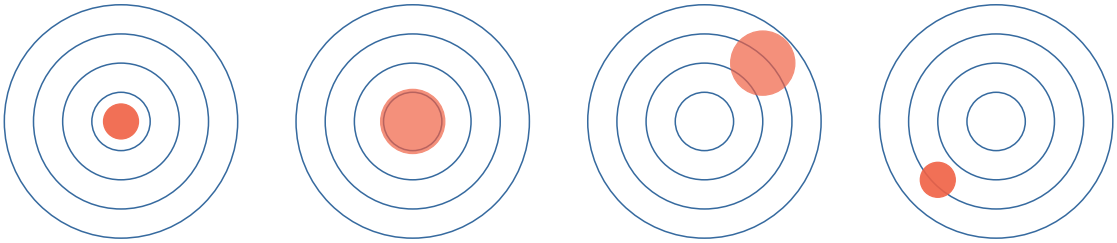

Figure 1.2: Accuracy and precision. From left to right: accurate and precise; accurate and imprecise; inaccurate and imprecise; inaccurate and precise.

with it.

From this perspective, we consider noise to consist of both *inaccuracy* and *imprecision*, where the former describes the difference between the evidence gathered and the ground truth, and the latter is where evidence fails to identify a single state of the world. Imprecise evidence is inherently less informative than precise evidence, but this means that in the presence of errors it is more likely to be consistent with the true state of the world. Figure 1.2 illustrates the distinction between accuracy and precision for noisy evidence in relation to the ground truth. The centre of the rings represents the true state of the world and an orange circle depicts the evidence gathered by an agent. The accuracy of the evidence then depends on the distance of the centre of the circle to the true state, while the imprecision of the evidence depends on the area of the circle. Hence, imprecision and inaccuracy are independent features of the evidence. Increasing/decreasing the radius of the circle results in an increase/decrease in the precision of the evidence, respectively, but the accuracy of the evidence remains unchanged. On the other hand, the distance from the centre of the orange circle to the inner-most ring is inversely proportional to the accuracy of the evidence (i.e., the greater the distance, the lower the accuracy). Imprecision naturally arises during social learning in light of the fact that evidence and beliefs are often only partial. In other words, agents often do not have sufficient knowledge to make predictions about the full state of the world. For example, in Figure 1.1 agents visit specific locations and obtain evidence about whether there is a fire at that location. However, such evidence does nothing to inform them about other locations. In other words, agents may have received sufficient information to predict the truth or falsity of some propositions, while being unable to say anything about the remaining propositions. In this paper, *imprecision* is the size of evidence or belief set, i.e. the number of possible states consistent with the evidence or agent's belief, and can be a parameter of our model. Accuracy, on the other hand, is simply a measure of the distance from an agent's current beliefs to the true state of the world and is assumed to be a feature of the interaction between the agents' sensors and the environment.

Epistemic sets are a direct way to represent the beliefs and evidence with varying levels

of imprecision, in which an agent's belief is represented by the set of states or worlds that it regards as being possible [15]. Therefore, the cardinality of the set is a straightforward measure of the imprecision of an agent's belief or evidence. As such, we adopt a set-based learning model in which beliefs about the world and evidence collected by agents are represented by sets of states. In particular, we assume that agents' beliefs take the form of sets of possible states of the world where each state is a complete allocation of truth values to the propositions under consideration. For example, let l_1 and l_2 denote propositions asserting that there is a wildfire in locations 1 and 2, respectively. In this context a state of the world is a pair of truth values, each of which is either 0 or 1, indicating whether l_1 and l_2 are false or true. An agent's belief B can be $\{\langle 1,1\rangle, \langle 1,0\rangle\}$, indicating that the agent is certain that there is a wildfire in l_1 but uncertain if there is one in l_2. Epistemic sets are one of the simplest formalism for representing uncertainty and imprecision in AI. The use of sets of states to represent beliefs dates back to Hintikka's possible worlds semantics [16], with some early applications in AI and computer science found in [17] and [18]. More recently, epistemic sets have also been applied to a simple social learning problem using an abstract agent-based simulation [19]. Using epistemic sets allows for agents to hold beliefs of varying levels of precision, which has the potential to improve system-level robustness to noise compared with other simpler models, e.g., the weighted voter model [20, 21]. Opinion diffusion logic is relevant in this context as it sometimes employs a semantic model of belief equivalent to epistemic sets [22]. In particular, an agent's belief or evidence can be represented by a logical formula F which has a model theoretic representation equivalent to the epistemic set consisting of those states (or interpretations) in which F is true [23]. The imprecision of an epistemic set then depends on the generality of the associated formula. In this case evidence $l_1 \wedge l_2$ asserts that there are wildfires in both locations, while evidence $l_1 \vee l_2$ asserts that there is a wildfire in at least one of the two locations. Clearly the second formula is more general than the first and this is reflected in the relative imprecision of the associated epistemic sets as given by $\{\langle 1,1\rangle\}$ and $\{\langle 1,1\rangle, \langle 1,0\rangle, \langle 0,1\rangle\}$, respectively.

In addition to diffusion logic models, another approach for exploring imprecision of agent's belief is Dempster-Shafer (DS) theory. The foundational concepts of the Dempster-Shafer theory of belief functions can be traced back to the work of Shafer [24], which is built upon Dempster's earlier ideas on lower and upper probabilities [25]. Unlike traditional Bayesian probability, which assigns precise probabilities to hypotheses, DS theory provides a way to allocate 'belief mass' values to sets of hypotheses. For example, in a medical diagnostic context, for instance, consider a patient showing symptoms A and B. In a conventional probabilistic framework, a probability might be allocated to the probability that the patient has a specific Disease X. However, with Dempster-Shafer theory, we can assign belief mass not solely to Disease X but to any set of diseases that could collectively explain symptoms A and B. This provides a approach that captures the inherent uncertainty and imprecision in medical diagnoses, especially when diagnostic are not definitive. In DS theory, belief and plausibility functions are utilised to

quantify uncertainty.The belief function represents the minimum amount of belief committed to a set given the available evidence. The plausibility function is a complementary measure to the belief function and provides an upper bound on the amount of belief that could be committed to a particular set when taking into account all the evidence that does not reject it. DS theory is closely related to the broader concept of imprecise probability theory which also aims to model uncertainty and imprecision more effectively than classical probability theory. In imprecise probability theory, a single hypothesis is often quantified by a set of probability measures, specifically by an upper and a lower bound. The upper probability serves as a conservative estimate that accounts for the maximum extent of belief/confidence associated with the hypothesis, whereas the lower probability provides a more optimistic measure, capturing the minimal level of belief. DS theory can be seen as a special case within this framework, where the belief measure serves as the lower probability and the plausibility measure serves as the upper probability. However, the focus of this work remains on epistemic sets. This is primarily because epistemic sets are less expressive than DS theory and offer a simpler yet effective model for capturing the essence of imprecision in social learning contexts. While DS theory provides a comprehensive and nuanced framework, the straightforward nature of epistemic sets allows for more intuitive understanding and easier implementation, especially in scenarios where computational resources may be limited. Thus, our work will continue to explore the dynamics of social learning through the lens of epistemic sets, offering insights into how imprecision can affect collective decision-making.

We consider social learning in terms of two distinct processes; evidential updating and belief fusion [26]. Evidential updating is the the process by which the robots/agents learn directly from the environment, by updating their current beliefs based on evidence received from the environment. In robotic applications evidence might take the form of signals received by various sensor modalities, such as cameras, microphones, and ultra-sound sensors. For example, in Figure 1.1 drones gather and processes direct sensory data detecting heat or smoke to determine the presence of a fire. Belief fusion complements this by facilitating inter-agent communication to merge these individual sensory findings and form a collective understanding of where fires are located. For the scenario represented by Figure 1.1, each drone shares its beliefs with others to integrate their individual findings. In a more general multi-agent context, evidence could take the form of data received directly relating to a particular instance or set of instances. The interaction between evidential updating and belief fusion has been studied based on the well known bounded confidence model [27], which suggests that the whole society will end up with a consensus on the truth with appropriate confidence level and evidence rate(so called the strength of the attraction of the truth). In addition, in the context of social epistemology, [28] argue that the communication between agents would significantly enhance the performance in truth approximation due to the ability to correct errors while propagating information across the population. For problems of this type it has been argued that approaches combining

individual evidence collection and local fusion of beliefs between individuals are more robust to noise and more efficient than those that rely on evidence collection only, since the fusion step allows for evidence propagation and error correction across the whole system [12, 21, 28]. In this thesis, we explore the impact of imprecision in both evidential updating and belief fusion on social learning. To explore the former, we propose a belief fusion operator that yields various levels of imprecise fusion results. For the latter, we present a model that accounts for varying levels of imprecision in the evidence gathered by agents.

The exploration of imprecision within artificial multi-agent systems is driven by two primary motivations. Firstly, there is an ongoing challenge in academic research to clearly differentiate between the concepts of inaccuracy and imprecision, which are often treated interchangeably, often treating them interchangeably despite their distinct implications for information processing and decision-making. Secondly, empirical studies on social insects, such as ants and bees, reveal that these organisms exploit imprecision to their advantage during tasks like food source selection. For instance, it has been suggested in the literature that some social insects may be able to adapt and even take advantage of imprecision to make more robust collective decisions [29–31]. In this context it is therefore interesting to investigate if artificial multi-agent systems can adapt to imprecise evidence and whether some forms of imprecise evidence may even enhance learning in the presence of sensor error or other types of environmental noise. In this thesis, we will propose a model in which the level of evidential imprecision can be controlled by a Hamming distance based parameter and implement the model to investigate whether artificial agents would be able to benefit from imprecise evidence.

As well as evidential updating imprecision can naturally play a role in fusion where, for example, inconsistency between two agents beliefs could result in an imprecise fused belief. For epistemic sets we can define belief fusion operators that work on the principle that disagreement or inconsistency between agents results in more imprecise beliefs, while agreement between agents increases precision. In this way [19] suggested the fusion process can help to both propagate correct information while facilitating error correction provided that belief imprecision is linked to evidence collection. In this thesis a parameterised fusion operator is introduced that returns beliefs of varying levels of imprecision. This is used to explore the effect of fusion imprecision on learning performance in a series of agent-based simulations.

1.2 Background

In this section, we introduce key concepts that are pivotal to the research presented in this thesis. Specifically, we discuss the classical logic model used to represent the state of the world, as well as the epistemic sets employed to model agents' beliefs. We then introduce the concept of consensus within multi-agent systems. To achieve consensus, agents must engage in communication to fuse their individual beliefs. Accordingly, we introduce principles that guide

various belief fusion methods.

Truth values, which are the outcomes of evaluating logical propositions as either 'true' or 'false', play a critical role in reasoning and decision-making in multi-agent systems (MAS). While various logical frameworks such as multi-valued logics, fuzzy logic, and probabilistic logics have been widely studied, the role of classic binary logic remains foundational. This framework, often considered the simplest form of logic, offers both challenges and opportunities in the context of MAS. **Classical logic,** a cornerstone of mathematical theory and Artificial Intelligence, is the study of the principles and criteria of valid inference and demonstration. Classic binary logic restricts propositions to two states: true or false. This Boolean framework is named after George Boole, who laid its mathematical foundations in the 19^{th} century. The power of this logic lies in its simplicity and computational efficiency, allowing for clear, unambiguous reasoning. In classical logic, the syntax consists of a set of well-formed formulas that obey specific structural rules. These formulas are built from atomic formulas and logical connectives like "and" ($\wedge$), "or" ($\vee$), "not" ($\neg$), "implies" ($\Rightarrow$), and "if and only if" ($\Leftrightarrow$). Semantics, on the other hand, interprets these syntactic elements to produce meaning. For example, truth tables are a semantic tool that defines the truth value of complex formulas based on the truth values of their atomic components. A defining feature of classical logic is the Principle of Bivalence, which asserts that every declarative statement is either true or false but not both. Classical logic involves various rules of inference like Modus Ponens, Modus Tollens, and Syllogism, which provide the formal machinery for logical reasoning. These rules are the building blocks of logical proofs and algorithmic problem-solving. Classical logic is broadly divided into propositional logic and predicate logic. Propositional logic deals with simple declarative propositions without considering the internal structure of the sentences. Predicate logic, on the other hand, dives deeper into the internal structure, focusing on subjects and predicates, and allows for more expressive statements involving variables and quantifiers. In today's world, classical logic has vast applications ranging from philosophy and mathematics to computer science and artificial intelligence. Its role in formal languages, database theory, and multi-agent systems is particularly significant.

Propositional logic is a subfield of classical logic and is fundamental to computer science, philosophy, mathematics, and even linguistics [32]. Propositional logic has become instrumental in various scientific domains, including multi-agents systems. In multi-agent systems, agents use propositional logic for decision-making, negotiation, and communication. It provides a formal framework for agents to represent knowledge and reason about the environment in terms of a set of propositions. For example, we assume p_1 is *it will be rainy* and p_2 is *the train will be cancelled*. If an agent deems that it will be rainy and the train will not be cancelled, using classical binary propositional logic, the agent's belief can be represented by $\{p_1 = 1, p_2 = 0\}$. In the case that another agent believes that it will be rainy and the train will be cancelled, her belief is then $\{p_1 = 1, p_2 = 1\}$. Some argue that the strict true-false framework can sometimes

be too restrictive for capturing *borderline cases* where the proposition is neither absolutely true or false [33]. Borderline cases are inherent for vague propositions, such as 'the box is heavy' or 'the phone is expensive'. A popular way to represent such borderline cases is to use three-valued logic [34] which introducing a boundary value of propositions, for example, the agent may belief that raining or not raining are both possible, i.e. $p_1 = \frac{1}{2}$. Three-valued models can also represent partial Boolean models [35], in which not all the truth values of the propositions are known. The natural generalisation of partial models consists of epistemic sets, understood as non-empty subsets of interpretations of a Boolean language. For example, $\{p_1 = \frac{1}{2}, p_2 = 1\}$ can be represented by $\{(1,1),(0,1)\}$. However, the three-valued model may overestimate the imprecision of the agent belief, for example, $\{p_1 = \frac{1}{2}, p_2 = \frac{1}{2}\}$ can be any one of $\{(1,1),\ (0,0)\}$, $\{(1,0),\ (0,1)\}$, $\{(1,1),\ (0,0),\ (1,0),\ \{(1,1),\ (0,0),\ (1,0),\ (0,1)\}$, and the latter of these is much more imprecise than the former. In this example, we see that a model employing sets of allocations based on classical Boolean truth values is more effective at characterising various degrees of imprecision. For the research outlined in this thesis, we apply epistemic sets composed of states of the world to represent an agent's beliefs. This approach effectively captures the full extent of the imprecision of an agent's belief with a cost of more complexity. In epistemic sets based model, an agent has 2^{2^n} possible beliefs rather than 3^n for the three-valued model and therefore it is more complex than the three-valued model for n . On the other hand, epistemic sets avoid some of the complexity associated with other more expressive frameworks, e.g. D.S. theory. Although D.S. theory is more expressive for the 'probabilities' associated with the belief sets, it is computationally more complex than the epistemic set models as it involves uncountable possible beliefs (mass functions). Therefore, epistemic sets is an effective middle ground between expressiveness and computational complexity, making them particularly well-suited for the analysis of imprecision in social learning scenarios.

In the context of multi-agent systems, classical propositional logic plays an essential role in formalising the conditions under which consensus can be achieved. Agents may use logical values or formulas to represent their beliefs, goals, or the state of the world, and logical inference to update these beliefs as they receive new information. Logical frameworks provide a rigorous basis for analysing the properties of consensus algorithms, such as their correctness or resilience to failures. Achieving consensus becomes more challenging as the size of the system increases, or when the system is subject to uncertainties, time-delays, or malicious attacks. There are still many open questions in the field, such as how to achieve consensus in a system with dynamically changing environments, how agents are connected and can communicate, or how to ensure that consensus is reached quickly and efficiently in very large systems. Another avenue of research is exploring alternative logical systems, like fuzzy logic or probabilistic logic, to provide a more fully integrated approach to uncertainty and imprecision.

In a multi-agent system, agents often need to collaborate to accomplish a shared task or solve a common problem. To do so effectively, they must reach a consensus on certain matters,

like what action to take or how to allocate resources [36]. The concept of consensus is thus fundamental in multi-agent systems, especially in applications where autonomous agents are expected to operate in a decentralised manner [37]. The problem of achieving consensus is often modelled mathematically. For instance, if each agent i has a belief B_i, the system achieves consensus if B_i becomes equal for all i after some finite or infinite time. Consensus is often studied in the context of a social network in the form of a graph where nodes are agents and edges represent communication channels between them [38]. Different algorithms and protocols have been developed to achieve consensus, ranging from simple averaging algorithms to more complex methods involving optimisation techniques or game theory [39]. In this thesis, we explore how a population of agents identifies the true state of the world by achieving consensus on a singleton belief set which only holds one possible state of the world. Specifically, this singleton precise belief is defined as the allocation of truth values to n propositions. Reaching a precise consensus is critical in some multi-agent systems, for example, in a network of self-driving cars navigating a busy intersection, each car needs to precisely understand the state of the traffic light and the positions of other vehicles to avoid collisions. In this study, 'consensus' refers to the requirement that this precise singleton belief is shared uniformly across all agents within the population. In order to share beliefs and then to achieve consensus, agents are required to communicate with each other via some belief fusion strategies to handle disagreements.

Belief fusion is the process of combining uncertain or incomplete information from multiple sources to extract a more accurate collective understanding. [40]. The principles of optimism, unanimity, and minimal commitment serve as guiding rules to ensure that the fusion from different sources produces outcomes that are both reliable and robust [15]. In this thesis we will focus on belief fusion of two agents, of which beliefs are modelled as epistemic sets. We denote the fused belief of a pair of agents with beliefs B_1 and B_2 as $f(B_1, B_2)$, the principles that fusion rule should satisfy are as follows:

- **Optimism:** $B_1 \cap B_2 \neq \emptyset \implies f(B_1, B_2) \subseteq B_1 \wedge f(B_1, B_2) \subseteq B_2$

The principle of optimism requires that the fusion outcome should be keeping as much information as possible from either source, i.e. being a subset of both agents' beliefs, when they are consistent. This principle asuumes that both agents are reliable and trustworthy. Capitalising on the reliability of the agents, for optimism the fusion rule aims to produce a fused belief that is as precise as possible. This precision can be particularly important when addressing complex or ambiguous issues where each piece of information may be crucial.

- **Unanimity:** $B_1 \cap B_2 \subseteq f(B_1, B_2) \subseteq B_1 \cup B_2$

Unanimity stipulates that the fusion outcome should preserve any possibility or impossibility that both agents agree upon; in other words, the fused set must be a superset of the intersection and a subset of the union of the two agents' beliefs. This principle ensures that the fusion results

include what is unanimously deemed possible while exclude what is unanimously considered impossible by the fusion pair.

- **Minimal commitment:** $f(B_1, B_2)$ is the most imprecise subset of all possible state of the world satisfying Optimism and Unanimity

Minimal commitment dictates that the fusion should remain the largest subset when the other two principles hold, i.e. the fusion results should include all possible states of world without breaking the other two principles. The principle of minimal commitment aims to keep the fused set of beliefs as imprecise as possible to maintain flexibility and reduce the risk of errors. In other words, it avoids making unwarranted assumptions by preserving a level of imprecision, allowing the system to adapt more easily to new information.

When dealing with set-based beliefs from two sources, the only canonical fusion rule that satisfies the criteria of optimism, unanimity, and minimal commitment is to take the intersection when the sets are consistent and the union when they are not [15]. In this thesis, we will provide a formal definition of the fusion operator as described in [15] in social learning context and adopt it as the standard operator. In real-world scenarios, the sources of fusion may not be reliable, especially in environments where the information is not accurately received by agents. In order to explore the role of imprecision to deal with such inaccuracy, we then parameterise the standard fusion operator and propose a new one designed to yield more imprecise fusion outcomes, with breaking the principle of optimism.

1.3 Related Work

Collective decision making

Collective decision making refers to the process where a group of agents collectively reaches a decision which can either be selecting an optimal option or determining a suitable course of action. For example, honeybees collectively choose and commit to a single suitable nectar site using collective and distributed information processing[41] while fish and birds moves collectively as groups using local interactions with their neighbours[42]. These two types of collective behaviours are classified as consensus achievement and task allocation [43]. Inspired by the animal behaviours, decentralised social learning and decision-making are well-studied tasks in multi-agent and swarm robotic systems. One common family of problems considered which have influenced this research are best-of-n problems, in which a population of robots must collectively identify the best out of n distinct options on the basis of local interactions and limited feedback [44]. In the literature on collective decision making, options often have associated quality values. These values can take a variety of forms, such as the brightness of lights [44, 45], intensity of colours [12], the dimensions of specific areas [46], or the proportions of a particular feature within a defined space [47]. Quality values can also be modelled directly

as numbers [12, 19, 47] and based on these quantities agents form beliefs about the best option. This type of problem is often explored within the confines of a binary scenario, where $n = 2$. Typically, the agents must decide between two options based on certain criteria, such as selecting the option with the lowest cost or the highest quality [48]. However, in recent years, more studies have started investigating more challenging best-of-n problems where $n > 2$ [12, 19, 49].

In this thesis we will instead focus on a more challenging collective problem on in which a population of agents must learn and reach consensus on the truth values of each proposition being investigated (i.e., the true state of the world which will be defined in Chapter 2) rather than simply identifying the best out of a set of n alternatives. In cases where $n = 2$, the problems of best-of-n is essentially converge to the same issue as the state of the world problems with 1 propositions. This is because with only two alternatives, it can be represented by the proposition 'Option 1 is the best' , which inherently provides a complete description of that world's state. However, as n increases, the complexity of these problems diverges significantly, and it is this more complex scenario that the thesis will explore. Identifying the best out of n alternatives may not always be the most efficient approach, especially when comprehensive information is desired on all options. For instance, during search and rescue operations, merely identifying the 'best' option could overlook other viable options. A more comprehensive understanding of all possible options might be crucial to ensure optimal outcomes in such scenarios. Therefore, ranking-n problems, as a variant of best-of-n problems have recently emerged into the domain of social learning [50, 51]. Rather than only identifying the 'best' option out of n, this novel approach seeks to understand how individuals or entities might socially learn the entire hierarchy or 'ranking' of the n options available. This perspective is particularly relevant in contexts where understanding the ordinal relationships between choices is as important, if not more so, than identifying the singular best option. For instance, in market analysis, a company might be more interested in understanding the ranked preferences of consumers across a spectrum of products, rather than just knowing the most popular product. The propositional model we proposed in this thesis can also be applied to a preference learning problem when treating the preference/partial order between every pair of options as a unique proposition. The state-of-the-world encompasses a challenging general class of problems than either best-of-n or the ranking problem. In particular, for n options the size of the space of possible answers is n, for best-of-n, and $n!$ for ranking problems. However, for a general n proposition problem the solution space of possible states of the world is 2^n.

Evidence and belief models

Social learning and collective decision-making are commonly viewed in the context of two specific processes: evidential updating and belief fusion. Evidential updating is the mechanism by which an agent updates its existing beliefs based on new evidence from the environment. Belief fusion is the method through which agents exchange its knowledge with their peers and

drives consensus. In this framework, how an agent's beliefs are modelled becomes especially crucial.

In multi-agent systems, the modelling of an agent's belief is pivotal for decision-making. The most direct way is to model agent's belief as a proposition, 'option i is the best option' [52], sometimes together with the corresponding quality value [13]. Based on this representation, there are two primary strategies for belief updating: Direct Comparison and Cross Inhibition. For the Direct Comparison approach, agents assess the quality values of their preferred option against either the belief of another agent or newly acquired information. They subsequently update their belief in favour of the option with superior quality. For Cross-inhibition agents' beliefs shift from precise/certain to imprecise/uncertain when dealing with inconsistency such that directly comparing quality values is not necessary. [13] used cross-inhibition to solve a best-of-n problem of up to 12 options and shows that cross-inhibition is more robust to noisy quality values than direct comparison. In this thesis, the proposed model also moves away from using quality values of which obtaining accurate measurements in noisy environments can be inherently challenging.

Another way to model agent belief is to use a probability distribution on the options and then to use Bayesian updating where the agents refine the beliefs given new evidence [12]. The agent's belief can be an $1 \times n$ vector representing the probabilities that the agent considers each of options $1, \ldots, n$ being the best option. Then agents can update their beliefs based on the Bayes' Theorem using a preset likelihood and pool their beliefs of distributions by various pooling operators [53]. Possibility theory is an alternative framework to represent agent's belief in social learning model's.[54] introduced a methodology based on a possibility distribution, assigning a degree of possibility to each set of possible states of the world. Compared to the probability framework, the possibility measure provides both upper and lower probabilities respectively. Results suggest that the possibility theory based method is more robust to environmental inaccuracy in scenarios in which agents can rarely gather evidence [54].

These studies provide some evidence that in certain scenarios imprecise beliefs can enhance performance in social learning. We see that the cross-inhibition model allows agents to hold imprecise beliefs and is more robust to inaccuracy compared to the Direct comparison model [13]. A more imprecise version of probability method, the possibility theory based method, enhanced the model's robustness to noise and malfunction agents [54]. Furthermore, simulations in [21] shows that a three-value model that allows the agent to hold an imprecise belief can be more robust to the presence of malfunctioning or noisy individuals in the population than the weighted voter model [20] with a cost of slower convergence.

In this thesis, we use epistemic sets as agents' beliefs. The use of sets of states to represent beliefs, referred to as epistemic sets, dates back to Hintikka's possible worlds semantics [16] and some early applications in AI and computer science can be found in [17] and [18]. More recently, epistemic sets have been applied to the best-of-n collective learning problem [19].

Using epistemic sets allows agents to hold beliefs of varying levels of imprecision, which has the potential to improve system-level robustness to noise compared with other simpler models, e.g the weighted voter model.

For belief fusion we make the distinction between symmetric and asymmetric methods. For the former agents usually receive other agents' beliefs and update its own independently, such as majority rule [47] for which agent updates its belief to the majority of its neighbours', and the weighted voter model [20] for which agents adopts the belief of a neighbour with a probability proportional to their weights. The latter is usually conducted within a pool, such as a ranking voting model [51], in which an agent's belief is modeled as a vector representing the ranking of the options. Pairs of agents vote using inverse Borda count [55] to generate a fused ranking vector.

When belief is modelled as probability, possibility, or epistemic sets, there are usually various symmetric combination operators. For epistemic sets, there is a strong relationship with Dempster-Shafer theory since in the latter beliefs can be thought of as being characterised by mass functions defined over epistemic sets and therefore The fusion operators proposed for Dempster-Shafer theory can also be applied to these epistemic sets. A large number of fusion operators have been proposed in the literature, an overview of which is given by [56].

In this section, we reviewed belief and updating models for collective decision making studies and found that a more imprecise belief representation framework may result in more accurate and robust learning performance. In the next section, we will discuss more about imprecision applied in the social learning models.

Imprecision in Learning

Imprecision refers to the inherent vagueness or lack of exactness in data or decision-making processes. In multi-agent systems, this could mean inexact sensor readings, ambiguous communication between agents, or non-specific rules for action. The ability to deal with imprecision is crucial for robust and effective operation, especially in environments where exact information is either not available or too costly to obtain. Multi-agent systems often operate in real-world scenarios that are fraught with uncertainty, inaccuracy, and imprecision. Addressing imprecision appropriately can make systems more resilient, adaptable, and effective in achieving their goals. In formal settings, imprecision can be represented by epistemic sets which contain more than one possible state of the world. Dealing with imprecision introduces computational and conceptual challenges. Algorithms need to be robust enough to handle imprecision but also efficient enough to be practical. In this thesis we will focus on developing more efficient algorithms that are robust to imprecision that emerges during social learning and on investigating how varying levels of imprecision affect overall performance.

The idea that imprecise evidence can sometimes be beneficial in social learning is found in the study of social insects[31, 57]. For example, the honeybee's waggle dance to communicate

information about potential food sources is imprecise in its direction indication, and this results in variation in the angles indicated when the dance is repeated. This imprecision can be observed in either a series of waggle runs by a single dancing bee or between individuals with there typically being a variation of between 10° and 15°[29]. The "tuned error" hypothesis [58] states that this imprecision is used for spreading recruits over a certain spatial configuration and is selected for by natural selection. [59] reported experiments that supported the hypothesis by finding smaller divergence angles in dances indicating potential home sites than in dances indicating food sources. The former are always point locations and the latter are often patches. However, other studies shed doubt on this hypothesis by suggesting that the imprecision of honey bee dances is the result of physical constraints and the honeybees' limited capacity to perform what is a complex sensory task [41, 60, 61]. Despite the debate concerning this hypothesis, simulation studies have suggested that an imprecision level of 10° is beneficial while a higher degree of imprecision is only beneficial when the food source is scarce [57].

Ants have also been reported to take advantage of imprecision in environmental information in order to adapt to dynamic environments. [31] suggested that the imprecision caused by variation in the trail of ants following behaviour between individuals, as well as by the behaviour of individuals over time, plays an important role in enabling the effective tracking of changes in the environment. [30] suggests that the crucial role of imprecision is not tied to a particular organism or species but can be relevant across a wide range of systems. In human behaviours, imprecision is also valuable for swift adaptations to the dynamic environment and optimising short-term predictability [62].

Communication constraints in Social Learning

In most agent-based collective learning models, agent communications are typically assumed to be entirely stochastic. At each iteration, a predetermined number of agents are equally likely to be selected into a pool to consolidate their beliefs. The size of this pool can range from as few as 2 agents, as the models in studies such as [19, 21, 51], or can be determined based on specific design parameters as discussed in [63]. However, in realistic robotic scenarios, setting a fixed number of participants for a belief fusion event can be challenging. Therefore, in this thesis, we probabilistically model the communication constraints, capturing the constraints inherent in real-world robots and their operating environments.

In practical social learning scenarios, conventional wisdom suggests that highly connected networks facilitate more efficient information dissemination [47, 64]. However, recent studies have begun to challenge this prevailing viewpoint. Using small world network treating agents as nodes and their communication links as edges, [38] suggests totally-connected networks result in lower average accuracy with more time cost when compared to less connected networks and limitation on the network connectivity improves the model's robustness to inaccuracy. In a swarm robotic scenario, [8] suggests that the constrained communication can enhance model's

adaptability to the dynamic environments.

1.4 Thesis outline

In this chapter, we have introduced several topics related to social learning and imprecision. We have found in these studies that imprecision can play a positive role in the collective decision making problems. Drawing on the insights from the studies highlighted in this chapter, it becomes evident that imprecision in belief representations has potential for improving the performance of collective decision-making or social learning models.

In the rest of this thesis we investigate a decentralised social learning problem in which a population of agents attempts to learn the true state of the world based on direct evidence from the environment and belief fusion carried out during local interactions between agents. We particularly focus on the role of imprecision which is defined as the cardinality of a set that can represent the agent's beliefs or evidence received. We investigate the influence of imprecision in both the evidential updating and belief fusion processes, which are two primary components of the social learning model.

In **Chapter 2** a parameterised fusion operator is introduced that returns beliefs of varying levels of imprecision. This is used to explore the effect of fusion imprecision on learning performance in a series of agent-based simulations. In this chapter we also described the propositional social learning model that we also employ in Chapters 3 to 5. We carry out agent-based simulations and then analyse the results in depth with a particular focus on how performance varies for different levels of imprecision in the fusion operator under different learning conditions.

Based on the social learning model proposed in Chapter 2, in **Chapter 3** we introduce an evidence model in which the evidence gathered by agents can exhibit varying degrees of imprecision. We first explore this model through agent-based simulations to investigate the robustness of the social learning model to evidence that varies in the levels of imprecision. Furthermore, we also conduct multi-robot simulation experiments focusing on a location classification task, in which the number of locations is greater than the number of robots. In these robotic experiments, the evidence collected by each robot naturally varies in its degree of imprecision. In order to investigate the potential benefits of evidential imprecision for the social learning model, we introduce an imprecise evidence model based on a Hamming distance neighbourhood surrounding an estimated state of the world. This estimated state is directly derived from evidence from the environment. We then show that agents building in imprecision of this kind into evidential updating can result in improved social learning performance, in terms of accuracy and robustness to the environment.

In **Chapter 4**, we introduce an integrated model that combines the imprecise fusion operator from Chapter 2 and the imprecise evidential updating model discussed in Chapter 3. The goal

is to investigate how these two components work in tandem within the larger system. To this end, we use a similar methodology to that employed in earlier chapters, to study the effects of combined imprecision in both evidential and fusion processes. Through these experiments we investigate how imprecision at different stages of social learning can influence the overall system dynamics, including agents' ability to reach consensus, robustness to noisy data, and to make reliable collective decisions. The integration of imprecise mechanisms in both evidence gathering and belief fusion processes seeks to provide a deeper understanding of how real-world uncertainty and partial information can be navigated effectively.

In **Chapter 5**, we explore alternative approaches for evidential updating for different levels of evidential imprecision. We begin by applying a well-known mathematical operator in evidence theory, which leads more imprecise outcome of evidential updating when there is disagreement between evidence received and the agent's current belief. We then proceed to compare this method with traditional updating strategies through simulation experiments. Based on our findings, we propose a novel approach that combines the strengths of both methods. This new strategy allows agents to hold 'rough beliefs', which are then incorporated into the belief fusion process. We therefore blur the lines between belief fusion and evidential updating, creating a more integrated model. We validate this hybrid model through simulations, assessing its performance in terms of both decision-making speed and accuracy.

In the concluding **Chapter 6**, we summarise the key findings of our research with identifying some remain challenges and discuss several possible avenues for future research on the topic.

1.5 Contributions

In this thesis, we contribute to the fields of social learning and multi-agent systems by developing new models for evidential updating and belief fusion between pairs of agents, introducing imprecise evidential updating method and imprecise fusion operators, and showcasing potential practical applications. These efforts collectively enhance our understanding of the benefits of incorporating imprecision into complex distributed decision-making systems. The main contributions of this thesis are as follows:

- We use epistemic sets to model agent beliefs, allowing for the representation of imprecision through the cardinality of evidence sets. This enables us to differentiate between imprecision and error (inaccuracy). The former in our set-based model can be modelled directly by the cardinality of the evidence/belief sets while the latter describes the difference between the evidence gathered and the true state of the world.

- We show that the well-known intersection-union fusion operator results in effective social learning across a range of scenarios in which there is erroneous and relatively limited direct evidence in Chapter 2. Our results indicate that the accuracy of social learning is

affected by the relationship between the relative frequency of evidential updating and belief fusion. We then introduce a novel parameterised fusion operator that can return beliefs of different levels of precision or imprecision. Our results indicate that imprecise fusion operators leads to the best outcomes when belief fusion is more frequently compared to evidential updating. If the frequency of belief fusion is relatively high compared to evidential updating, optimal results are obtained by a more imprecise operator.

- In Chapter 3 we demonstrate that social learning is robust to varying levels of imprecise evidence. A neighbourhood-based imprecise evidential updating model that intentionally infuse imprecision to evidence is proposed and demonstrated to be beneficial for improving the accuracy of social learning systems under certain conditions. Using agent-based simulations, we establish that there exists an optimal level of evidential imprecision that maximises both the speed of convergence and the overall accuracy of the system. Importantly, this optimal level varies depending on the the level of evidential inaccuracy. Additionally, we conduct a robustness analysis for different levels of system tolerance to error, showing that different levels of evidential imprecision should be applied for various application requirements.

- In Chapter 3 we also construct a multi-robot location classification problem for which a small population of agents must solve a classification task with a greater number of locations. Here, we take into account realistic constraints such as hardware limitations and environmental conditions that could introduce imprecision in the evidence collected by robots. Our simulation results indicate that our approach remains robust even in the presence of noisy evidence and outperforms the expected error when the number of robots is less than the number of locations under investigation. Our robot simulation experiments therefore show that that our approach has strong potential to be applied to location classification tasks conducted by multi-robot systems.

- In Chapter 4 our findings suggest that incorporating both imprecision in evidence and belief fusion into the same model yields notable improvements in learning accuracy, particularly in noisy conditions. The findings demonstrate the value of a combined approach that incorporates imprecision in both evidential updating and belief fusion. Furthermore, we observe trade-offs between speed and accuracy in the model. Specifically, the optimal level of evidential updating that maximise accuracy also enhances speed. However, the optimal fusion imprecision requires more time to reach a consensus compare to the precise fusion.

- In Chapter 5, we identify the limitations of two established evidential updating methods, i.e., their poor performance in high-error scenarios, specifically issues related to convergence and low learning accuracy. To overcome the limitations, a novel evidential updating and belief fusion approach is proposed. We then demonstrate that in high-error scenarios

the new approach enhances the learning accuracy significantly at the cost of increased learning time.

Chapter 2

Imprecise Fusion in Social Learning[1]

In this chapter, a decentralised social learning problem is investigated in which a population of agents attempts to learn the true state of the world based on direct evidence from the environment and belief fusion carried out during local interactions between agents. A parameterised fusion operator is introduced that returns beliefs of varying levels of imprecision. This is used to explore the effect of fusion imprecision on learning performance in a series of agent-based simulations. In general, the results suggest that imprecise fusion operators are optimal when the frequency of fusion is high relative to the frequency with which evidence is obtained from the environment.

We will focus on a propositional model described in Chapter 1, in which agents attempt to collectively identify the true state of the world in the form of the correct allocation of truth values to a set of predefined propositions. In this chapter we formalise this model and then investigate the model with $n = 5$ propositions so that there are $2^5 = 32$ possible states. Each state then corresponds to an allocation of truth values to the 5 propositional variables, where only one allocation reflects the ground truth. We first formalise the set-based belief models and then introduce an operator for belief fusion and a strategy of evidential updating, before detailing simulation experiments in which this model is applied to social learning. Representing beliefs by sets of states provides a natural way of modelling imprecision in terms of cardinality. The higher the cardinality of a belief, i.e., the more states it deems to be possible, the more imprecise that belief is. Hence, in this context a fusion operator is imprecise if it tends to result in beliefs of high cardinality. Furthermore, we propose a Jaccard similarity-based threshold fusion operator and explore the impact of imprecise fusion on the population-level learning performance. Our results show that fusion imprecision can improve the accuracy social learning when the agents can only receive evidence infrequently from environments.

An outline of the rest of the chapter is as follows: In the next section, we give an overview of some relevant existing literature on collective learning and decision making. We then describe

[1]This chapter has been published on ALife 2021: `https://doi.org/10.1162/isal_a_00407`; It may appear on the Turnitin report.

a propositional model and introduce an imprecise operator for belief fusion and evidential updating, before detailing simulation experiments in which this model is applied to collective learning. The results from these simulation experiments are then considered in detail with a particular focus on how they pertain to the use of imprecision in belief fusion for collective learning. Finally, we give some conclusions and outline possible future directions.

2.1 Related Work

Belief fusion is studied within the broader context of information fusion, a field that encompasses diverse applications, such as image fusion [65], robotic sensor fusion [66] and opinion diffusion logics [23, 67]. In general, the fusion process provides a means of resolving inconsistencies between different sources and hence achieving consensus. The fusion of agents' beliefs can be modelled by pairwise operators. Several such fusion operators have been proposed and [15] introduces a number of desirable properties that any information fusion process should satisfy, i.e. optimism, unanimity, and minimal commitment for set-based beliefs. In this chapter, we propose a fusion operator for epistemic sets which results in different levels of imprecise fusion results based on the one proposed by [68, eq. 56], which was proved to be the only pairwise operator for set-based information items, which satisfies the desirable properties [15].

There are several well-established fusion strategies applied to collective decision-making problems. A primary type of these strategies is voting-based methods. The majority rule, for instance, is a straightforward method where the most commonly held belief among all neighbours of an agent is selected as the fused belief [47]. Although simple, this method can be effective under certain conditions, especially when the population of agents is large and their individual beliefs are reasonably accurate. Another popular voting-based approach is the weighted voter model [20, 21]. Unlike the majority rule, which use the belief of majority as the fused belief directly, the weighted voter model is probabilistic with assigning varying degrees of probability to selecting different beliefs based on the number of votes of each belief, i.e. the proportion of agents within the neighbourhood that hold the belief. The truth value based fusion model has been shown to be more robust to noise then the weighted voter model [21]. In addition to voting-based frameworks, agents may also engage in belief fusion with their peers through fusion operators, typically involving a fixed number of agents for fusion. For instance, in the study by Lee et al. [12], in which agents' beliefs are modelled using probabilities, agents update their beliefs based on Bayes' theorem and engage in belief fusion using the multi-hypothesis product operator [69]. This approach is particularly beneficial in environments with noise and the frequent receipt by agents of erroneous quality values for different options. Similarly, in belief models based on Possibility Theory or Dempster-Shafer Theory, pairwise fusion operators can be employed [26, 54]. Possibility theory can also be interpret as a 'imprecise' version of probability theory featured with upper and lower probabilities, which has been shown

outperforming a similar probabilistic model when the evidence is not frequently received [54]. The robustness to evidential inaccuracy of several of these operators applied to the best-of-n problem has been compared by [26]. In particular, the best performance under noisy conditions was achieved by Yager's operator [70] and by Dubois & Prade's operator [68].

In this chapter we model the agent's belief by sets of possible states and propose a pairwise operator to investigate the impact and benefits of fusion imprecision. The operator proposed work on the principle that higher levels of disagreement or inconsistency between agents' beliefs result in more imprecise fused beliefs, while agreement between agents increases precision. In this way the fusion process can help to both propagate correct information while also correcting errors [19].

2.2 Social Learning Model

In this section, we introduce a social learning model tailored for collective decision-making in multi-agent systems. We first outline the set-based belief model in Section 2.2.1, followed by the fusion operator Section 2.2.2. We then introduce an evidential updating strategy and compare it with an more established method in Section 2.2.3

2.2.1 Belief Representation

Consider a population of agents attempting to collectively learn the state of their environment which we assume can be described by a finite set of propositions $\mathcal{P} = \{p_1, ..., p_n\}$. We assume that the propositions are not changing during the learning process. From this perspective a state s is the allocation of Boolean truth values to each of the propositions. In other words, a state is a function $s : \mathcal{P} \to \{0, 1\}^n$. For notational convenience we represent a state s by the n-tuple $\langle s(p_1), \ldots, s(p_n)\rangle$. Let $\mathbb{S}$ denote the set of all states so that $|\mathbb{S}| = 2^n$.

An agent's belief $B \subseteq \mathbb{S}$ is then the set of states which the agent believes can possibly be the true state s^*. We therefore represent uncertain beliefs as being subsets of $\mathbb{S}$ with cardinality $|B| > 1$ while a singleton belief $B = \{s\}$ means that the agent is certain that s is the true state. We assume that agents adopt a closed-world assumption which in this context means assuming that $\mathbb{S}$ covers all possible states of the world. Therefore, agents' beliefs are constrained such that $B \neq \emptyset$ since it cannot be the case that all states in $\mathbb{S}$ are impossible. Note that a given belief $\emptyset \neq B \subseteq \mathbb{S}$ classifies each proposition p_i as being either true, if $s(p_i) = 1$ for all $s \in B$, false, if $s(p_i) = 0$ for all s in B, or uncertain otherwise. Hence, the more imprecise an agent's belief the more propositions they will tend to be uncertain about. This indicates a natural relationship between the epistemic model of beliefs and three-valued approaches [21]. For example, consider the search and rescue scenario with 5 location outlined above where p_i denotes the proposition 'casualties are in location i for $i = 1, \ldots, 5$. Now consider the belief B given by,

$$B = \{\langle 1, 0, 0, 0, 0\rangle, \langle 0, 1, 0, 0, 0\rangle\}$$

In case this B corresponds to the belief that there are casualties either in location 1 or location 2 but not both, and there are no casualties in any other location. Therefore, according to B no propositions are classified as being certainly true, p_3, p_4 and p_5 are classified as being certainly false, and p_1 and p_2 are uncertain.

2.2.2 Belief Fusion Operators

We now introduce a parameterized fusion operator for combining epistemic sets which returns beliefs of varying levels of imprecision. This requires a measure of the similarity between epistemic sets for which we use the well-known Jaccard similarity [71] defined as follows: For $B_1, B_2 \subseteq \mathbb{S}$,

$$J(B_1, B_2) = \frac{|B_1 \cap B_2|}{|B_1 \cup B_2|} \tag{2.1}$$

We now define the similarity threshold operator as follows: for $\gamma \in [0, 1]$,

$$B_1 \odot_\gamma B_2 = \begin{cases} B_1 \cap B_2 & : \quad J(B_1, B_2) > \gamma \\ B_1 \cup B_2 & : \quad J(B_1, B_2) \leqslant \gamma \end{cases} \tag{2.2}$$

For example, let $B_1 = \{s_1, s_2, s_3\}$ and $B_2 = \{s_2, s_3, s_4, s_5\}$ then,

$$J(B_1, B_2) = \frac{|\{s_2, s_3\}|}{|\{s_1, s_2, s_3, s_4, s_5\}|} = \frac{2}{5}$$

and hence $B_1 \odot_\gamma B_2 = \{s_2, s_3\}$ if $\gamma < \frac{2}{5}$ and $B_1 \odot_\gamma B_2 = \{s_1, s_2, s_3, s_4, s_5\}$ for $\gamma \geqslant \frac{2}{5}$.

Note that for $\gamma = 0$ this operator corresponds to the intersection-union operator [68, eq. 56] as given by:

$$B_1 \odot_0 B_2 = \begin{cases} B_1 \cap B_2 & : \quad B_1 \cap B_2 \neq \emptyset \\ B_1 \cup B_2 & : \quad B_1 \cap B_2 = \emptyset \end{cases} \tag{2.3}$$

On the other hand, for $\gamma = 1$ we have that $B_1 \odot_1 B_2 = B_1 \cup B_2$. In general, γ controls the level of generality or precision of the operator such that for $\gamma \leqslant \gamma'$, $B_1 \odot_\gamma B_2 \subseteq B_1 \odot_{\gamma'} B_2$ for all sets $B_1, B_2 \subseteq \mathbb{S}$. The use of Jaccard similarity to deal with inconsistency has also been proposed by [72] who applies similarity-based enlargement of the sets of interpretations to resolve inconsistencies in fusion problems.

2.2.3 Evidential Updating Method

In addition to combining their beliefs with others, agents also gather evidence from the environment. Here we assume that this evidence E takes the form of an assertion of the truth

value of one proposition $p_1, \ldots, p_n$, i.e., $\mathrm{E} = \{s \in \mathbb{S} : s(p_i) = v\}$ for some p_i and where $v \in \{0, 1\}$. Given E we then propose that an agent updates their belief B to $B|\,\mathrm{E}$ such that:

$$B|\,\mathrm{E} = \{s|\,\mathrm{E} : s \in B\}. \tag{2.4}$$

and where,

$$s|\,\mathrm{E}(p_j) = \begin{cases} v : j = i \\ s(p_j) : \text{otherwise} \end{cases} \tag{2.5}$$

In contrast to more established belief updating methods such as where

$$B|\,\mathrm{E} = \begin{cases} B \cap \mathrm{E} : B \cap \mathrm{E} \neq \emptyset \\ B : \text{otherwise} \end{cases} \tag{2.6}$$

as applied in [19], the above approach has the advantage that it preserves beliefs about the propositions which are consistent with E. To see this consider the case where we have two propositional variables and where $B = \{\langle 1, 0\rangle, \langle 0, 1\rangle\}$, i.e., in this case both p_1 and p_2 are uncertain since for both there are states in B where they are true and also states where they are false. Suppose evidence E is "p_1 is true", then applying intersection-based updating results in $B|\,\mathrm{E} = \{\langle 1, 0\rangle\}$ and therefore removes the uncertainty about p_2. More specifically, according to B, p_2 is now certainly false. However, since E makes no reference to p_2 this seems counter-intuitive. In contrast applying our proposed updating method results in $B|\,\mathrm{E} = \{\langle 1, 0\rangle, \langle 1, 1\rangle\}$, hence preserving the uncertainty about p_2. In general, provided that the proposition p_i to which the evidence pertains is classified uncertain by belief B then updating on the basis of eq. (2.4) will result in more imprecise beliefs than updating on the basis of eq. (2.6). Less restrictive updating of this kind can be advantageous in collective learning scenarios in which evidence is noisy and where agents focus on investigating propositions about which they are currently uncertain.

2.3 Agent-based Simulation Experiments

In this section, we present the results for a series of agent-based simulation experiments in which a population of agents attempts to reach a consensus about a propositional state description of the world. In practice, both evidence and agent interactions may be sparse or limited. Figure 2.1 shows the iterative model of social learning, which is modelled probabilistically as follows: Each agent conducts evidential updating and belief fusion iteratively. During each iteration, every agent starts from exploration state for which they randomly chooses a proposition about which it is uncertain to investigate and has probability ρ (the *evidence rate*) of successfully obtaining evidence from the environment, and the agent will stop collecting evidence if it

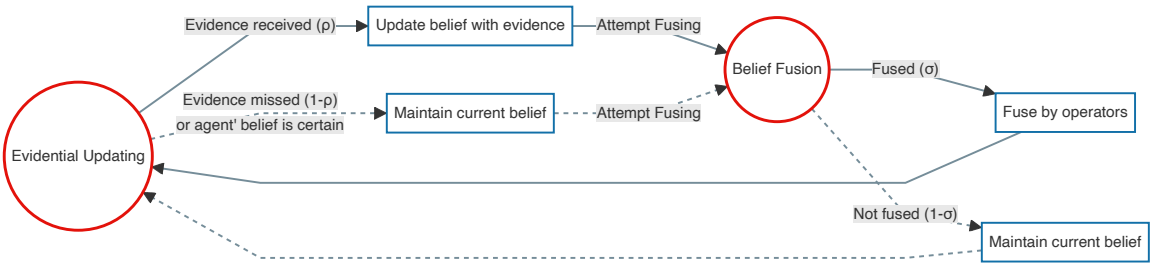

Figure 2.1: Diagram of a updating-fusion iteration. During the iteration, agents uncertain about propositions seek evidence with success rate ρ and then all agents attempt fusing beliefs with peers at a rate σ.

is certain about every proposition, i.e. it has a singleton belief. Agents also learn from the evidence being gathered by their peers using belief fusion. Every agent in the population has probability σ (the *fusion rate*) of being placed in a pool to fuse their belief with the belief of another agent. Each agent within the pool will be randomly paired with another agent and then each pair will combine their beliefs using the fusion operator in Equation (2.2). For every pair, both agents will adopt the result of this fusion as their new belief. If the number of agents in the pool is odd, then one agent will not take part in fusion. Such pairwise belief fusion is applied in many similar models, such as in [19, 38]. Belief fusion of multiple sources is not studied within the scope of this thesis. The parameter of fusion rate is used to realistically simulate communication constraints within multi-agent systems, reflecting factors such as limited bandwidth, resource conservation, signal interference, network scalability, and security concerns, which are all prevalent in real-world scenarios. The fusion rate also serves as a control mechanism for the frequency of belief updates in multi-agent systems. Limiting the frequency of fusion, as identified in recent research [73], results in improved robustness to error in evidence. There are 4 possible transitions, as shown in Figure 2.2. For example, with a probability of $\rho \times \sigma$ the agent will both receive evidence and entering the fusion pool(represented by gray arrows). In addition, we use the error rate ϵ as a simple model of environmental or sensor errors(the evidential inaccuracy). We define error rate as a probability ϵ that the evidence received could be incorrect. More specifically, let the true state be denoted by s^* then if an agent receives evidence about proposition p_i, they will receive $\mathrm{E} = \{s : s(p_i) = s^*(p_i)\}$ with probability $1 - \epsilon$ and $\mathrm{E} = \{s : s(p_i) = 1 - s^*(p_i)\}$ with probability ϵ.

The population of agents are initialised to hold completely ignorant beliefs, i.e., $B = \mathbb{S}$ at time $t = 0$. In other words, the agents are initialised as having no prior knowledge about the world. Experiments are then run multiple times to reduce random variation of results.

We evaluate performance on this learning task using the average Hamming distance H from the agents' belief values to the true state s^*. Furthermore, without loss of generality, we assume

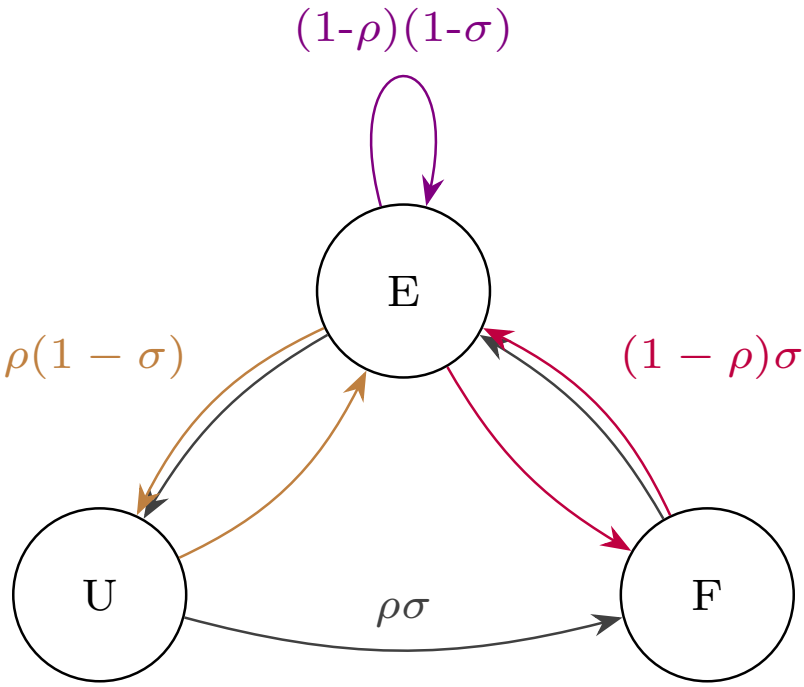

Figure 2.2: Transition Model of Social Learning: *E*, *U*, and *F* represent Exploration, Evidential Updating, and Belief Fusion, respectively. Each possible transition is marked with its probability and is colour-coded.

that s^* is such that $s^*(p_i) = 1$ for $i = 1, \ldots, n$. In this context, the Hamming distance between states is defined as follows: Let $s_1 = \langle s_1(p_1), \ldots, s_1(p_n)\rangle$ and $s_2 = \langle s_2(p_1), \ldots, s_2(p_n)\rangle$ be two states, then the Hamming distance between them is given by:

$$H(s_1, s_2) = \sum_{i=1}^{n} |s_1(p_i) - s_2(p_i)| \tag{2.7}$$

For example, supposing $s_1 = \langle 1, 0, 0, 0, 0\rangle$ and $s_2 = \langle 0, 1, 0, 0, 0\rangle$, the Hamming distance between s_1 and s_2 is $H(s_1, s_2) = 2$. We then extend this to give a normalised Hamming distance between an epistemic set $B \subseteq \mathbb{S}$ and the true state of the world s^* as follows:

$$H(B, s^*) = \frac{1}{|B|}\frac{1}{n}\sum_{s\in B} H(s, s^*) \tag{2.8}$$

Furthermore, we evaluate the performance at the population level as the average Hamming distance between the population of agents $\mathcal{A}$ of size k, and s^* such that:

$$H(\mathcal{A}, s^*) = \frac{1}{k}\sum_{B\in\mathcal{A}} H(B, s^*) \tag{2.9}$$

2.4 Results

In this section, we present the results obtained from agent-based simulation experiments conducted to evaluate the performance and efficacy of the intersection-union fusion operator in Section 2.4.1, and the imprecise operators in Section 2.4.2 in the context of our social learning model. These results show the trade-offs and advantages of different fusion approaches within multi-agent systems.

2.4.1 Results for the Intersection-Union Operator

In this section we present the simulation results of our model for social learning using the intersection-union operator in Equation (2.3) to which we shall later compare the proposed similarity threshold operator in Equation (2.2). Recent Studies usually found that an increase in population size can improve the systems accuracy in noisy environments [19, 50, 63]. However, these studies usually use a constant number of agents participating in belief fusion, the proportion of actively fusing agents decreases as the population size grows and therefore the communication frequency for individual agents decreases (fusion rate). In other physical simulations, a common practice involves using a parameter such as communication range to model real-world constraints on fusion [8]. However, in this case, with a fixed size for the simulation area, the "fusion rate" of individuals can vary based on the population size, as agents may be more sparsely or densely distributed. In our study, for a larger population, the fusion pool is also larger because the fusion rate is fixed. In Figure 2.3 we see that the learning outcome is not sensitive to population size $k \in [20, 100]$ for different combinations of evidence and fusion rates. We choose the population size $k = 50$ for all the experiments in this section, unless otherwise specified. Furthermore, a comparison between Figure 2.3a and Figure 2.3d reveals significant disparities in learning accuracy, suggesting that learning accuracy may be influenced by the relative relationship between ρ and σ.

Figure 2.4 shows a heat map of the average Hamming distance H of the population's beliefs (from Equation (2.9)) to the true state s^* after 3000 time steps, for varying ρ and ϵ. Here, a darker colour indicates that the average belief of the population is at a lower distance from the true state and therefore the population is performing better under these conditions, while a lighter colour indicates a greater distance to the true state and poorer performance. For an evidence rate $0.02 < \rho < 0.04$ we see that increasing the evidence rate also leads to an increase in robustness to different error rates in that good performance is maintained for higher values of ϵ. However, when $\rho > 0.04$, the robustness to inaccuracy surprisingly decreases as the evidence rate increases further. In these experiments, the fusion rate $\sigma = 0.04$ is fixed and relatively low corresponding on average to only one fusion operation per time step. This suggests that in noisy scenarios the relative frequency of fusion and evidential updating has an impact on overall performance. We hypothesise that fusion plays an error-correcting role when ϵ is high

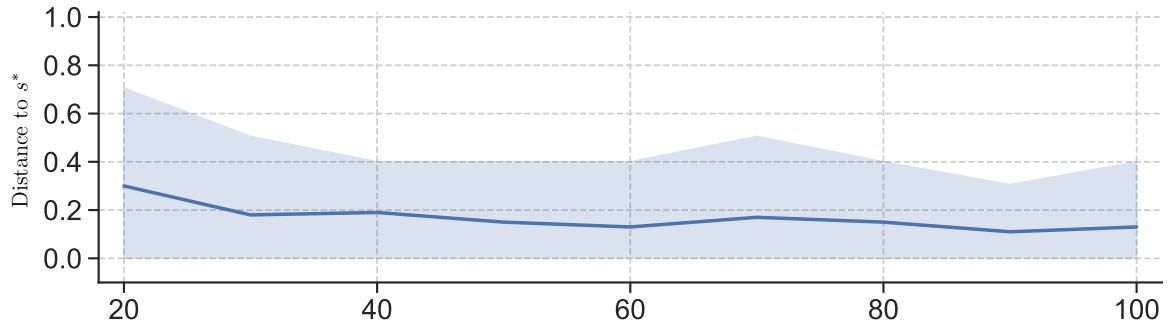

(a) $\rho = 0.1, \sigma = 0.1$

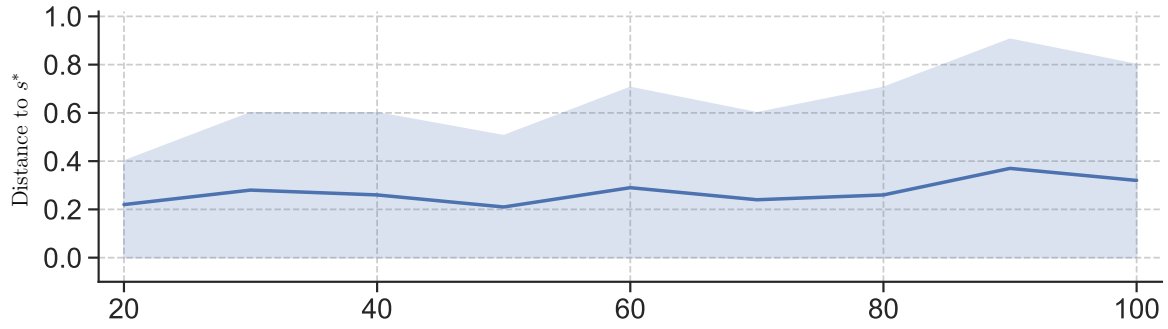

(b) $\rho = 0.1, \sigma = 0.9$

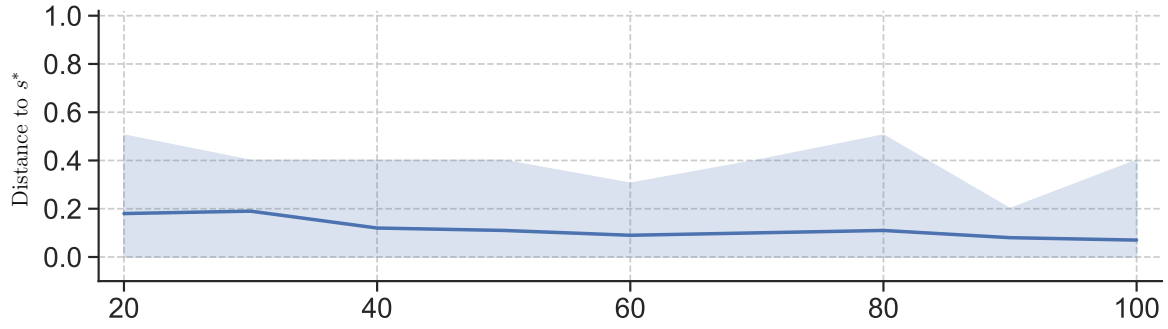

(c) $\rho = 0.9, \sigma = 0.9$

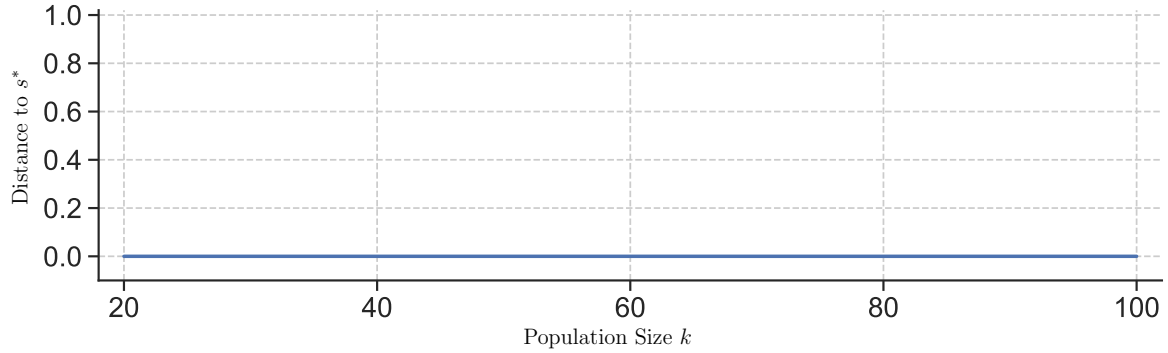

(d) $\rho = 0.9, \sigma = 0.1$

Figure 2.3: Distance to s^* for population sizes $k \in [5, 100]$ with $\{\rho, \sigma\} \in \{0.9, 0.1\}^2$ and error rate $\epsilon = 0.3$ The 5^{th} and 95^{th} percentiles are presented. For each combination of evidence and fusion rates, the performance is barely sensitive to k.

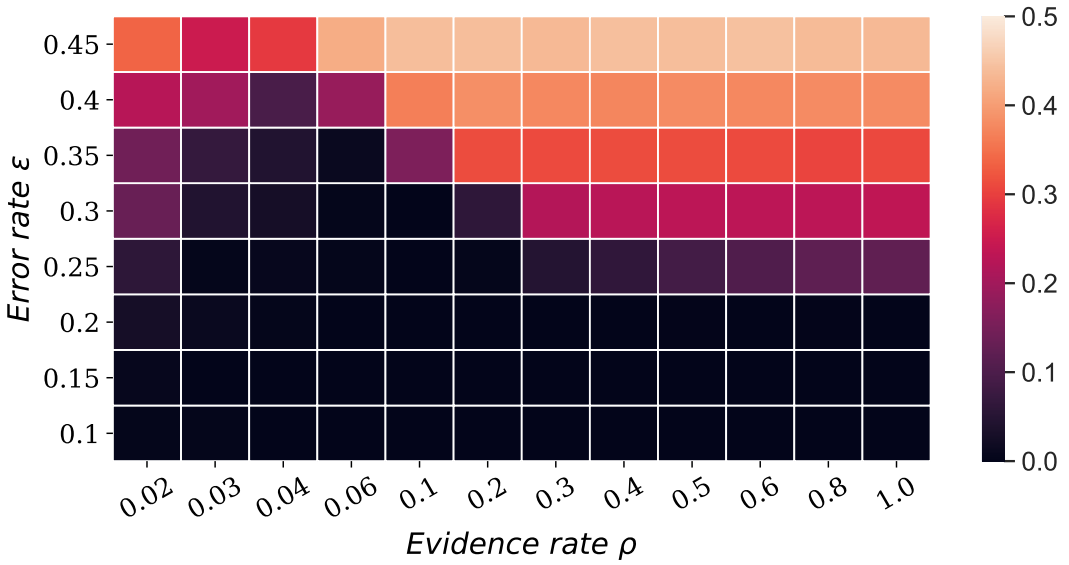

Figure 2.4: Average distance H to the true state with fusion rate $\sigma = 0.04$. In this case, the system exhibits optimal robustness to evidential inaccuracy at evidence rate $\rho = 0.04$, with system performance declining at rates above and below it.

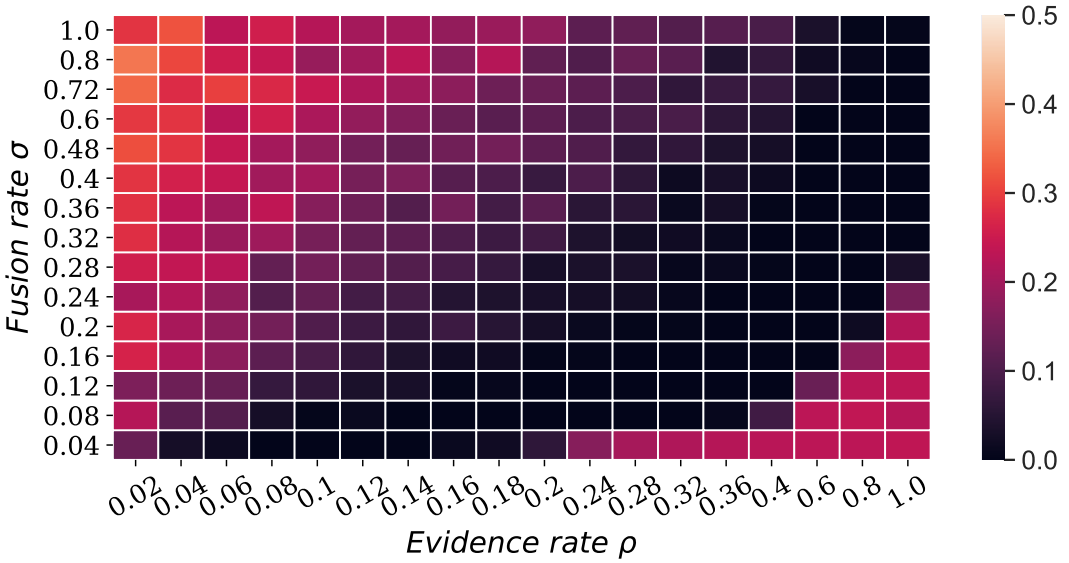

Figure 2.5: Average distance H to the true state with error rate $\epsilon = 0.3$ for different evidence and error rates. When the evidence rate is low, less frequent belief fusion can improve the accuracy for the learning model.

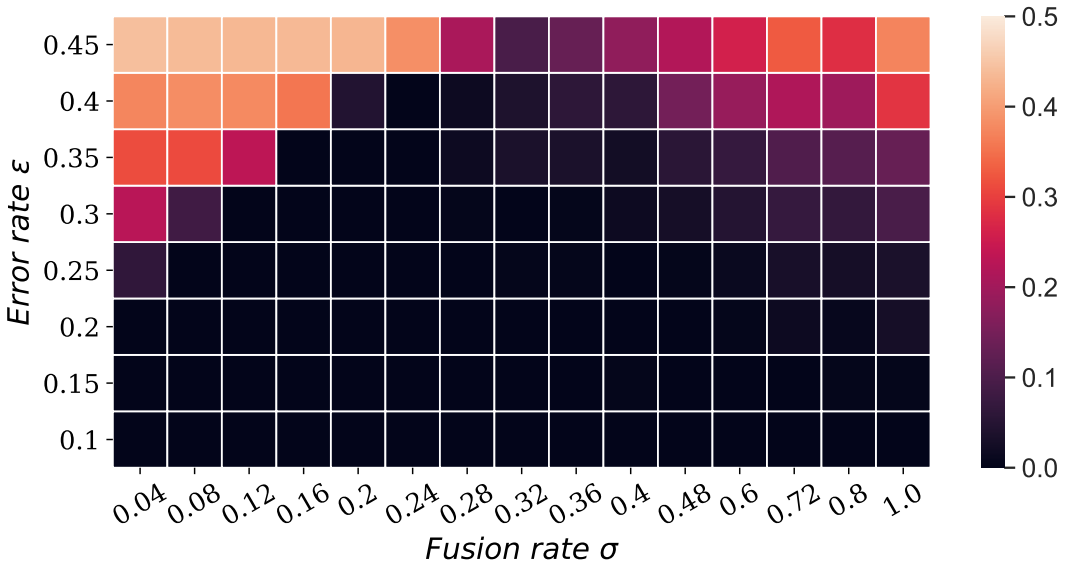

Figure 2.6: Average distance H to the true state with evidence level $\rho = 0.4$. The system exhibits optimal robustness to evidential inaccuracy at fusion rate $\sigma = 0.32$, with system performance declining at rates above and below it.

[19, 21], but if evidence is obtained at too high a rate then fusion is not sufficiently frequent to correct for the inaccuracy. On the other hand, if the evidence rate is too low then fusion drives the system to consensus too quickly before there has been time for agents to receive a sufficient amount of evidence to identify the true state. To investigate this directly, we now vary the fusion rate σ and present the results in Figures 2.5 and 2.6.

Figure 2.5 shows population performance at $t = 3000$ for varying values of σ and ρ with the fixed $\epsilon = 0.3$ and $k = 50$. The figure suggests that lower evidence rates require a lower fusion rate in order to achieve good performance and vice versa. We suggest that again this effect may be due to the relative frequency of updating and fusion from the perspective of an individual agent. More specifically, Figure 2.5 suggests that for a given evidence rate ρ there is an interval of fusion rates σ for which optimal performance can be obtained. If the fusion rate is too high relative to the evidence rate then the population converges too quickly before there is time to collect sufficient evidence. On the other hand, if the fusion rate is too low relative to the evidence rate then there is insufficient fusion to correct for the errors introduced by evidential inaccuracy.

Figure 2.6 shows that higher error rates lead to smaller optimal intervals for σ. The performance is poorer on the top left and right regions of the figure where the fusion rate is either too low or too high respectively. Figure 2.7 shows H plotted against $\frac{\rho}{\sigma}$ when $\epsilon = 0.3$. This suggests that performance is best when $\frac{\rho}{\sigma} \in [2, 3]$, i.e., when the evidence rate is between 2 and 3 times the fusion rate. The average distance to the true state increases significantly more

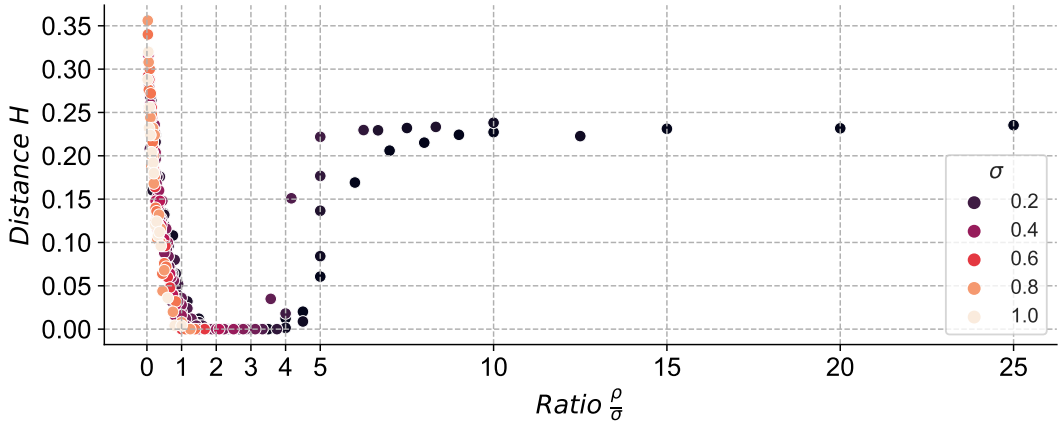

Figure 2.7: The average distance H to the true state against the ratio of evidential updating to belief fusion $\frac{\rho}{\sigma}$, for a fixed error rate $\epsilon = 0.3$. The system obtains optimal performance at specific ratios ($\frac{\rho}{\sigma} \in [1, 4]$) of evidence rate to error rate.

slowly when $\frac{\rho}{\sigma} > 10$ and $H(\mathcal{A}, s^*)$ tends to 0.25. We suggest that evidence updating dominates in such cases so that fusion has little impact on the population and the distance to the true state converges to $\epsilon = 0.3$ as would be expected if learning is based only on evidential updating without the error correction provided by fusion. Therefore, the performance of collective learning in this case can potentially be optimised by controlling the relative frequency at which evidential updating and fusion take place. Performance is relatively poor as $\frac{\rho}{\sigma}$ tends to 0. In such cases it is likely that beliefs across the population are converging before sufficient information becomes available to the population in the form of direct evidence. The Intersection-Union Operator operates on the basis of the optimism principle, which assumes that the beliefs of both agents involved are reliable. As a result, the operator retains only the consistent elements between the two beliefs, even if the overlap/consistency is minimal. When the consistency of agents is minimal, the discontinuity of the operator can also be problematic in such situations since it can lead to loss of information. For example, $B_1 \odot B_2 = \{s_i\}$ if $B_1 = \{s_1, ..., s_i\}$ and $B_2 = \{s_i, ..., s_n\}$, while if $B_1 = \{s_1, ..., s_i\}$ and $B_2 = \{s_{i+1}, ..., s_n\}$ then $B_1 \odot B_2 = \mathbb{S}$. Therefore, we hypothesise that an imprecise operator will improve the performance and we propose using the threshold operator as given in Equation (2.2) to vary the imprecision and to reduce the discontinuity effect of the operator.

2.4.2 Results of the Imprecise Operator

In this section we investigate the effect on performance of systematically varying the imprecision of the fusion operator under different learning scenarios. More specifically, we consider the threshold fusion operator in Equation (2.2) for a range of different values of γ between 0 and 1. By a series of simulation experiments we show that in high error rate and low evidence rate

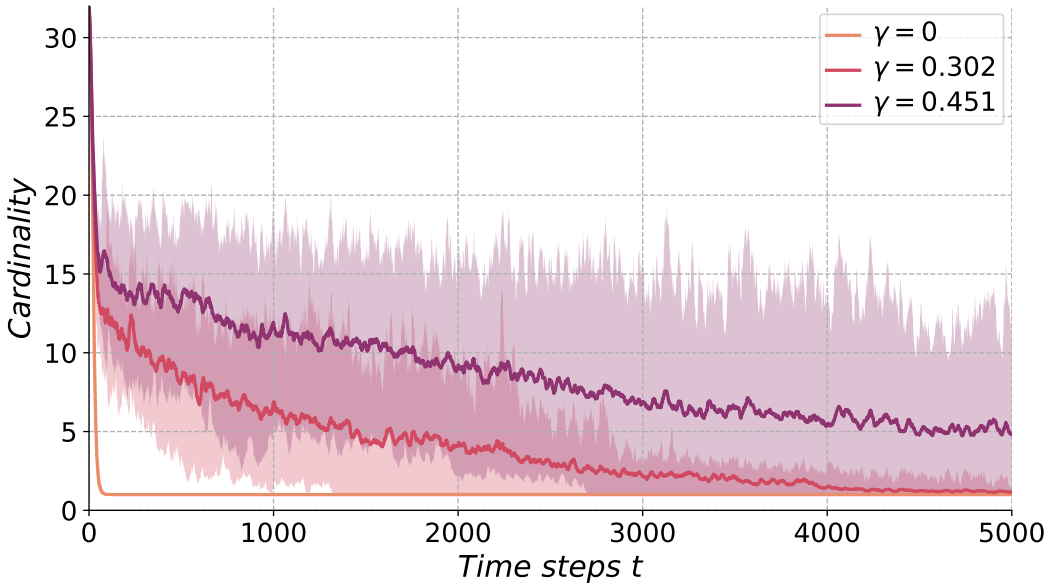

Figure 2.8: Average belief cardinality of the population against time steps for $\rho = 0.01, \sigma = 0.2, \epsilon = 0.3$, and $n = 5$. It is noted that increasing the fusion threshold reduces the speed of reaching consensus.

scenarios performance is optimal for an intermediate level of fusion imprecision, especially when performance is measured in terms of an F_β score which gives significantly higher importance to not being incorrect than to being correct. For this we will use the F_3 score. In the following results we will consider the fusion operators $\odot_\gamma$ for $\gamma \in \{\frac{j}{i} | i \in [1, 2^n], j \in [0, i], i, j \in \mathbb{Z}\}$.

Figure 2.8 shows the average cardinality of beliefs in the population decreasing over time for different thresholds. Recall that for epistemic sets, i.e. belief represented by sets of states, cardinality provides a measure of imprecision. Hence, we see a general trend by which the precision of the agents' beliefs increases during social learning. The red line ($\gamma = 0.302$) declines slower than the orange line ($\gamma = 0$) which is equivalent to the intersection-union operator and they both reach a cardinality of 1 after 5000 iterations. However, the purple line ($\gamma = 0.451$) decreases even more slowly to an average cardinality of around 5 after 5000 iterations. Hence, decreasing the precision of the fusion operator has the effect of slowing convergence and also tends to result in agents holding more imprecise beliefs over time.

As can be seen from Figure 2.8, the agents' beliefs may not always be precise after 5000 iterations with imprecise fusion, i.e. the cardinality of the belief set may be greater than one, i.e., $|B| > 1$. Therefore, in order to thoroughly evaluate the performance of different levels of imprecise fusion, we use multiple metrics. In addition to the Hamming distance, we also assess performance by measuring the proportion of correct propositions in each belief and by utilising an F-measure which give different importance of correctly identifying propositions and the not

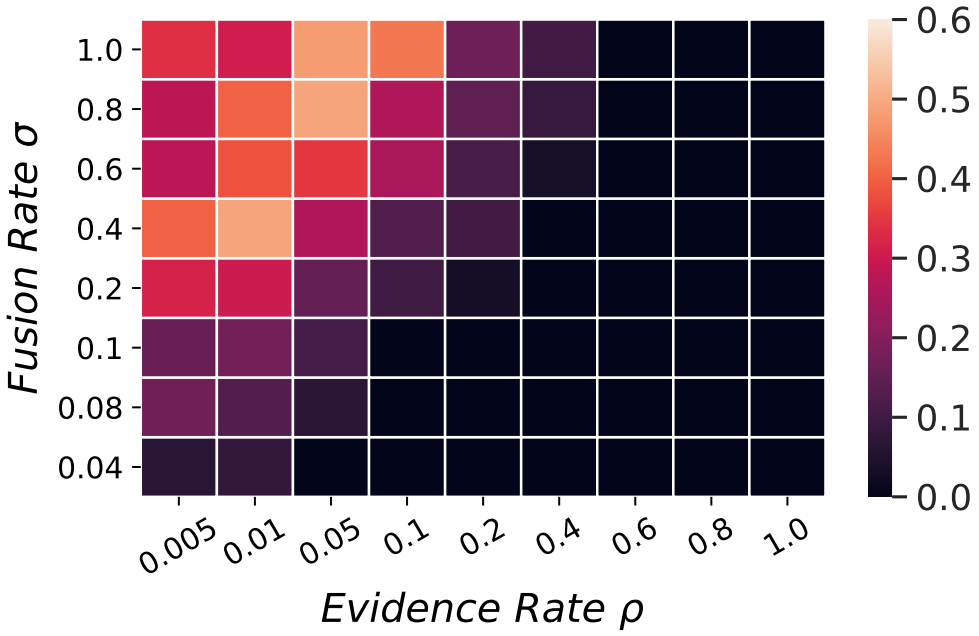

(a) Optimal thresholds γ_α for α.

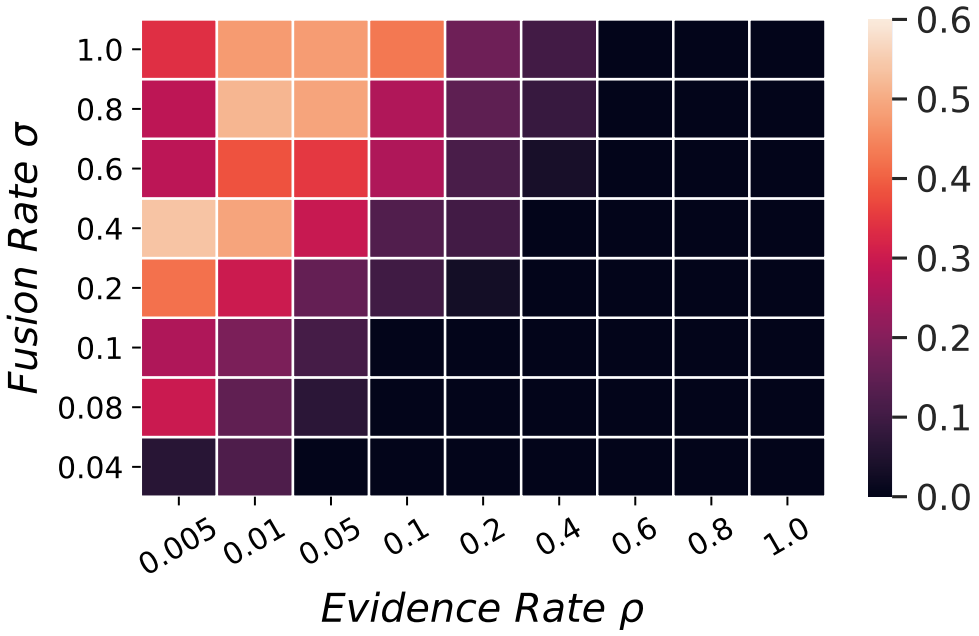

(b) Optimal thresholds γ_{F_3} for F_3.

Figure 2.9: Optimal thresholds for $\rho \in [0.005, 1]$ and fusion rate $\sigma \in [0.04, 1.0]$ where $\epsilon = 0.3$. We see that imprecise fusion is optimal when the evidence rate is relatively low compared to the fusion rate.

incorrectly identifying propositions.

More specifically, for an epistemic set B we define the following:

$$C(B) = \{p_i : s(p_i) = s^*(p_i) \text{ for all } s \in B\} \tag{2.10}$$

$$I(B) = \{p_i : s(p_i) = 1 - s^*(p_i) \text{ for all } s \in B\} \tag{2.11}$$

If agent $a_i \in \mathcal{A}$ has belief B_i then let,

$$\alpha = \frac{1}{n}\frac{1}{k}\sum_{a_i \in \mathcal{A}} |C(B)| \quad \text{and} \quad \theta = 1 - \frac{1}{n}\frac{1}{k}\sum_{a_i \in \mathcal{A}} |I(B)| \tag{2.12}$$

$C(B)$ is the number of propositions about which belief B is both certain and correct, while $I(B)$ is the number of propositions about which B is both certain and incorrect. Hence, α is the average proportion of propositions about which agents are both certain and correct, while θ is the average proportion of propositions about which agents are either correct or uncertain, i.e., not incorrect. From this we can then define the F_β score according to:

$$F_\beta = (1 + \beta^2)\frac{\alpha \cdot \theta}{\beta^2 \cdot \alpha + \theta}. \tag{2.13}$$

Here β is a parameter that allows us to give different degrees of importance to α and θ such that F_β attributes β times as much importance to not being incorrect as to being correct.

Let γ_{F_3} denote the value of γ at which F_3 is maximal at $t = 5000$, and let γ_α denote the value of γ at which α is maximal at $t = 5000$. Figure 2.9 shows two heat maps of performance, i.e. values of α and F_3 respectively, with $\epsilon = 0.3$ plotted against fusion rate σ and evidence rate ρ. For low evidence rate and relatively high fusion rate we have that $\gamma_\alpha > 0$ and $\gamma_{F_3} > 0$. This is consistent with the hypothesis that more imprecise operators are optimal when ρ is significantly less than σ, i.e. when $\frac{\rho}{\sigma}$ is low.

Figure 2.10 shows both the average correct proportion α and the F_3 score at $t = 5000$ plotted against different values of γ for evidence rate $\rho = 0.01$ and fusion rate $\sigma = 0.2$. Both measures are maximal for an intermediate value of γ, and this is particularly pronounced for the F_3 score. Figure 2.10 also shows the average proportion of determined propositions as corresponding to those propositions about which an agent is certain (orange line). This is given by $\alpha + 1 - \theta$. Notice that this decreases as γ increases thus resulting in more imprecise fusion and $\alpha = F_3$ when agents are certain on all the propositions, i.e., $\alpha = \theta$. However, at the values of γ for which α or F_3 are maximal, around $\gamma = 0.3$ and $\gamma = 0.4$ respectively, the number of determined propositions remains high (more than 0.95 and 0.75 respectively), suggesting that the population is still learning the true state with a high degree of precision.

Figures 2.11 to 2.13 shows γ_{F_3} (purple lines), and γ_α (red lines) for varying fusion σ, evidence ρ, and error rates ϵ. Figure 2.11 plots γ_{F_3} and γ_α against fusion rate σ for $\rho = 0.01$ and $\epsilon = 0.3$, and shows that in this case both metrics increase with σ for $\sigma < 0.4$. γ_{F_3} stops changing and

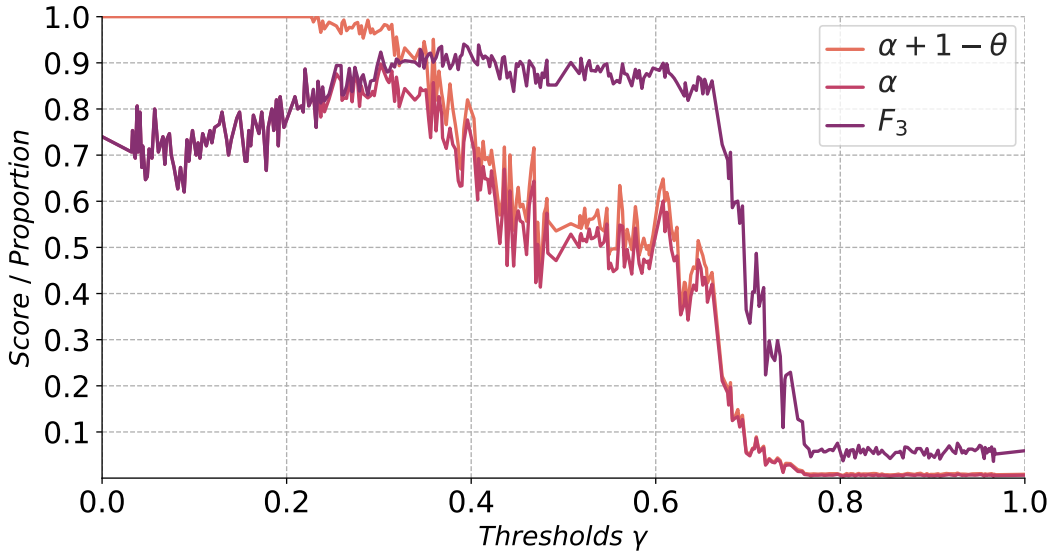

Figure 2.10: Average score (F_3) or proportion (α, $\alpha + 1 - \theta$) for a population of $k = 50$ agents, language size $n = 5$, fusion rate $\sigma = 0.2$, evidence rate $\rho = 0.01$, and error rate $\epsilon = 0.3$. Both metrics peak at a mid-range value of γ, with the effect being especially marked for the F_3 score.

γ_α decreases slightly with σ for $\sigma > 0.4$. Figure 2.11 suggests that as the fusion rate increases relative to the evidence rate then optimal performance requires an increasingly imprecise fusion operator. In other words, if fusion is frequent relative to evidence acquisition then it is better if the result of the fusion is imprecise, whereas if fusion is rare relative to evidence acquisition then it is better if the result of the fusion is precise. Figure 2.12 illustrates this relationship between σ and ρ from a different perspective by plotting γ_{F_3} and γ_α against evidence rate ρ. Again we see that as the evidence rate increases relative to the fusion rate, optional performance is obtained using increasingly precise fusion operators. This trend suggests that the efficacy of the imprecise fusion operator is not just an isolated property but rather depends on the specific conditions under which it is deployed. In scenarios where agents frequently update their beliefs with new evidence, a more precise fusion operator seems enough to superior performance. This may be attributed to the higher confidence we can place in each piece of evidence as they become more abundant, thereby allowing the system to more safely narrow down the belief sets without risking the exclusion of the true state of the world.

Figure 2.13 shows optimal threshold values for fixed σ and ρ plotted against the error rate ϵ. This suggests a subtle relationship between fusion imprecision and evidential inaccuracy. For example, as the error rate increases the optimal imprecision value γ_{F_3} increases. In other words, as evidential inaccuracy increases then more imprecise fusion operators are required in order to optimise the F_3 score. On the other hand, optimising the proportion of correctly classified propositions α requires more precise operators in high error rate scenarios, although these are

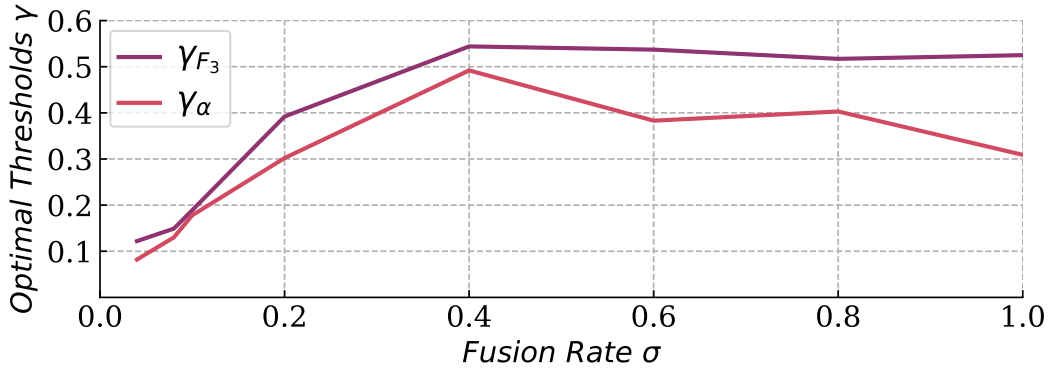

Figure 2.11: Optimal thresholds γ according to F_3 (γ_{F_3}) and α (γ_α) against fusion rate σ for evidence rate $\rho = 0.01$ and error rate $\epsilon = 0.3$. For $\sigma < 0.4$, an increase in σ leads to an increase in the optimal fusion thresholds. For $\sigma > 0.4$, γ_{F_3} stabilises while γ_α marginally declines with increasing σ.

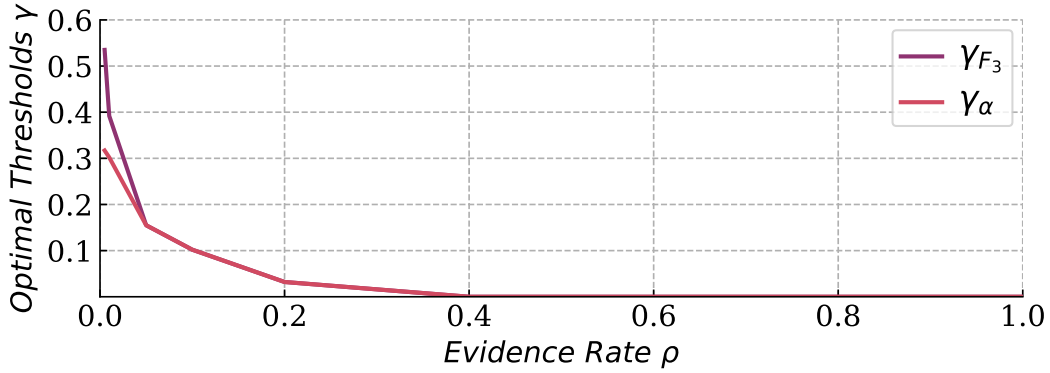

Figure 2.12: Optimal thresholds γ according to F_3 (γ_{F_3}) and α (γ_α) against evidence rate ρ for fusion rate $\sigma = 0.2$ and error rate $\epsilon = 0.3$. Optimal performance with higher ρ requires more precise fusion operators.

still more imprecise than the intersection-union operator. These results are likely to be due to a trade-off between error and uncertainty. For very imprecise fusion operators agents will tend to hold beliefs with higher cardinality (see Figure 2.8) and therefore have a higher proportion of uncertain propositions. Ideally, these uncertain propositions should be those for which a given agent has received conflicting information and would therefore have had a higher chance of incorrectly classifying them if they held more precise beliefs. The F_3 score takes into account this potential trade-off between accuracy and uncertainty, while on the other hand, α will tend to decrease as γ increases since the proportion of correctly classified propositions is bounded by

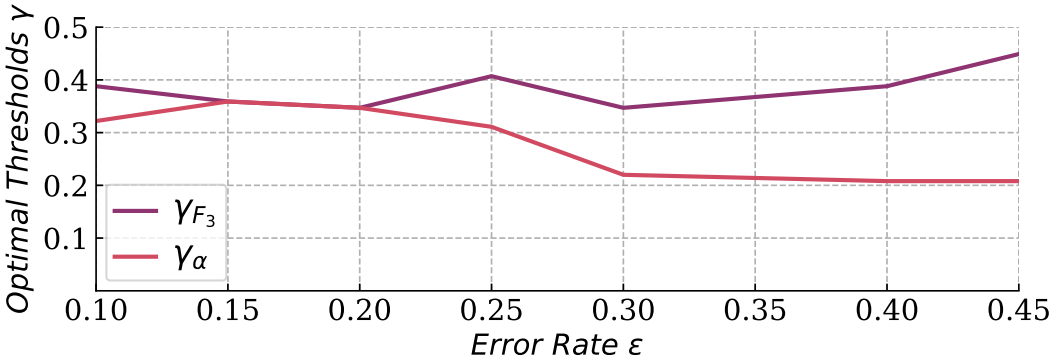

Figure 2.13: Optimal thresholds γ according to F_3 (γ_{F_3}) and α (γ_α) against error rate ϵ for fusion rate $\sigma = 0.2$ and evidence rate $\rho = 0.01$. Both thresholds are less sensitive to various error rates; γ_{F_3} slightly increases and γ_α slightly decreases with the ϵ increases.

the proportion of propositions which are determined, i.e., which are classified as being true or false rather than uncertain (see Figure 2.10).

2.5 Conclusion

In this chapter we have investigated social learning of the state of the world in a propositional model. Agents' beliefs have been represented by epistemic sets corresponding to the set of states that each agent believes are possibly the true state. Agents learn from two distinct sources: directly from the environment using belief updating, and from other agents by applying a fusion operator to combine their beliefs with those of other agents.

Our analysis demonstrated that the well-known intersection-union(Dubois&Prade) fusion operator results in effective social learning across a range of scenarios in which there is inaccurate and relatively limited direct evidence. However, performance is affected by the relative relationship between the evidence rate ρ and the fusion rate σ. More specifically, our results suggest that for a given value of ρ there is a bounded interval of values of σ for which performance is good.

We then extended our investigation to the role of imprecision in belief fusion. A novel parameterised fusion operator was introduced, which can generate beliefs of different levels of precision or imprecision. Our results then show that if σ is high relative to ρ then optimal results are obtained by a more imprecise operator, comparing to the state-of-the-art standard Dubois&Prade operator. In general, the optimal level of imprecision is strongly dependent on the frequency of evidence relative to the frequency of fusion, so that the higher the frequency of fusion is compared to the frequency of evidence the more imprecise the operator should be, and much less clearly dependent of the level of evidential inaccuracy.

One of the limitations of this work is that it does not account for the noise that can occur during the fusion process. In real-world scenarios, communication channels are often imperfect, and the information exchanged between agents may be subject to distortion, interruptions, or other forms of interference. These conditions can significantly impact the reliability of belief fusion and, consequently, the learning accuracy of the system. Future research could explore the integration of models considering the possible failure of communication, e.g., introducing a failure rate for fusion, to enhance the robustness and applicability of the proposed algorithms in more realistic settings. In addition, the communication topology is assumed to be a fully connected network. However, in real-world scenarios, communication topology is often limited, and recent studies have shown that less connected networks may achieve better accuracy, although this comes with the trade-off of increased learning time[38].

Following this work, we intend to investigate other imprecise fusion operators based on alternative measures of similarity or distance, e.g., a threshold operator based on the Hamming distance. Another direction of future work may focus on empirically validating these results in real-world scenarios and extending the model to accommodate more complex types of evidence and agent interactions.

Additionally, having shown that preserving imprecision during belief fusion leads to greater performance in the context of collective learning, we seek to explore whether imprecise forms of evidential updating may lead to similar improvements in the learning process. Finally, simulated robot experiments will enable us to investigate a more grounded collective learning scenario in which to better understand the implications of our model when external constraints such as communication bandwidth and inaccuracy from on-board sensors are imposed by the robot hardware.

Chapter 3

Imprecise Evidence in Social Learning[1]

In the Chapter 2, we proposed a social learning model characterised by set-based agent beliefs. We introduced a Jaccard similarity-based operator for imprecise belief fusion, which yields belief combinations with varying levels of imprecision. This approach enables the agents' beliefs to be fused into a more conservative result when their intersection is relatively precise. Our simulation results have demonstrated that the social learning model can benefit from low to intermediate levels of imprecision in terms of the accuracy of the learning outcomes when the evidence rate ρ is low. In addition, the evidence acquired by agents may also be imprecise, as real-world information is often subject to various sources of uncertainty and noise in practical applications. Such imprecision may arise due to factors such as limited sensor capabilities, constrained communication bandwidth, or the inherent complexity of the underlying phenomena being observed. Consequently, it is crucial to explore the robustness of our social learning model in the context of imprecise evidence. In this chapter we separate imprecision from inaccuracy in noisy real-world evidence and investigate the impact of imprecise evidence on social learning. In particular, we propose social learning models in which evidence collected by agents are represented by a set of possible states, and therefore the evidence collected can vary in its level of imprecision. We investigate this model using agent-based an robot simulations and demonstrate that it is robust to imprecise evidence. Furthermore, we propose a method that intentionally incorporates imprecision into the evidential updating. Our results also show that this type of imprecise evidence can enhance the efficacy of the learning process in the presence of sensor errors.

Imprecise evidence in social learning can arise from multiple sources. The inherent variability in how individuals perceive, process, and transmit information; the complexities of the environment in which learning takes place; and the intricacies of the social network structure all

[1]This chapter has been submitted to *Swarm Intelligence* and can be accessed via Research Square: `https://doi.org/10.21203/rs.3.rs-2620622/v1`; It may appear on the Turnitin report.

contribute to the landscape of imprecision of evidence. In this chapter we not only investigate the robustness of the model but also propose a novel method for evidential updating, which uses purposefully designed imprecise evidence as a tool, enabling multi-agent systems to cope with and possibly counterbalance the challenges posed by evidential inaccuracy. Through this research, we aim to better understand the role of evidential imprecision in social learning and exploring ways to utilising it. In this chapter, we extend the social learning model discussed in Chapter 2 to explore its robustness under varying degrees of evidential imprecision. Using both agent-based and multi-robot simulation experiments, we demonstrate the model's robustness to imprecise evidence and its effectiveness in location classification tasks, even when the evidence is inherently imprecise. To further investigate the role of imprecision, we introduce a Hamming-distance-based strategy to convert precise evidence into imprecise forms, thereby allowing us to control the desired level of imprecision. Our findings suggest that systems utilising imprecise evidence can achieve higher levels of robustness and accuracy under certain conditions, depending on their tolerance for error.

An outline of the remainder of the chapter is as follows: In Section 3.2 we outlines the set-based model for social learning and discusses belief fusion and evidential updating. In Section 3.3, we describe a series of simulations experiments that investigate the robustness of social learning to imprecise evidence with different degrees of imprecision. As well as agent-based simulations this also includes multi-robot simulation experiments of a location classification task. Then in Section 3.4 we introduce imprecise evidence in the form of a Hamming distance neighbourhood of an estimated state of the world, where the latter obtain as direct evidence from the environment. In Section 3.5 we then show that agent's building in imprecision of this kind into the evidence updating can result in improved social learning performance. Finally, we give some conclusions and outline possible future directions in Section 3.6.

3.1 Related Work

In a general multi-agent context, evidence could take the form of data received directly relating to a particular instance or set of instances. In more specific robotic applications evidence might take the form of signals received by various sensor modalities, such as cameras, microphones, and ultra-sound sensors. For problems of this type it has been argued that approaches combining individual evidence collection and local fusion of beliefs between individuals are more robust to noise and more efficient than those that rely on evidence collection only, since the fusion step allows for evidence propagation and error correction across the whole system [12, 21, 28]. The interaction between evidential updating and belief fusion has been studied based on the well known bounded confidence model [27], which suggests that the whole society will end up with a consensus on the truth with appropriate confidence level and evidence rate(so called the strength of the attraction of the truth).

The use of robots has become increasingly prevalent in various fields. Multi-robot systems are a specific type of multi-agent system that uses robots as agents. Such systems are usually used for the purposes of surveillance [74], formation [75], exploration, search and rescue tasks [76], and best-of-n problems [48]. A social learning model with agents' belief being modelled as a number $\in [0, 1]$ has been applied in a best-of-n problem [12] by E-pucks. The location classification task explored in this chapter can be considered a variant of the best-of-n problem. The best-of-n problem focusing on identifying the best option of n alternatives while our task focus on classifying every location either being labelled as *red* or *green* by identifying the correct allocation of colours out of 2^n possible ones.

There is a significant body of literature discussing the impact of evidence inaccuracy in practical environments, typically focused on the topic of the speed-accuracy trade-off in collective decision-making tasks [48, 77]. The robustness to evidential inaccuracy of several belief fusion operators applied to the best-of-n problem has been compared by [26]. In particular, best performance in noisy conditions was achieved by Yager's operator [70] and by Dubois & Prade's operator [68]. In this chapter, with the set-based belief representation framework, we will focus on the impact of evidential imprecision rather than inaccuracy. Imprecise evidence has been shown to be advantageous in the social learning processes of certain insect species. For example, studies on bees [59] and ants [31] have suggested that the utilisation of imprecise evidence can improve collective decision-making and problem-solving abilities. These findings suggest that there may be underlying adaptive advantages to employing imprecise evidence in social learning contexts, offering potential insights for the design of multi-agent systems.

3.2 Model

In this chapter, agent beliefs are also represented by a set of possible states $B \subseteq \mathbb{S}$ as described in Section 2.2. A group of agents socially seeks to learn their environment, which can be described by a series of propositions $\mathcal{P} = \{p_1, ..., p_n\}$. Each environmental state is $s : \mathcal{P} \to \{0, 1\}^n$. Agents hold beliefs about the possible states of the environment, represented as subsets of all possible states. A belief containing multiple states indicates ambiguity, while a single-state belief signifies conviction. For example, in a multi-location search and rescue context, a belief set $B = \{\langle 1, 0, 0, 0, 0\rangle, \langle 0, 1, 0, 0, 0\rangle\}$ would indicate the agent's uncertainty about casualties being in either the first or second location. Agents' beliefs will be fused by the same pairwise fusion operator described by Equation (2.3), we recall it as follows:

$$B_1 \odot B_2 = \begin{cases} B_1 \cap B_2 & : \quad B_1 \cap B_2 \neq \emptyset \\ B_1 \cup B_2 & : \quad B_1 \cap B_2 = \emptyset \end{cases}$$

In addition to fusing with other agents, agents receive direct information from the environment as evidence. For evidential updating, in this chapter we assume that the evidence

takes the form of a set of assertions about the true state of the world s^*. Suppose, for example, agents receive a set of states that can possibly be the true state.

Since evidence corresponds to a set of states, we can then naturally measure its imprecision by its cardinality $|E|$, i.e. the greater $|E|$ the more imprecise the evidence is. We then extend the language size of this problem from $n = 5$ in Chapter 2 to $n = 8$ to obtain more possibilities of potential evidential imprecision, i.e. from $|E| \in \{1, \ldots, 32\}$ to $|E| \in \{1, \ldots, 255\}$.

Given the form of E we then propose that an agent updates its belief B to $B|E$ by applying the operator defined by Equation (2.6), we recall it as follows:

$$B|E = \begin{cases} B \cap E : B \cap E \neq \emptyset \\ B : \text{otherwise.} \end{cases}$$

This method of evidence updating in which certain states are ruled out as part of the learning process has already been applied effectively in social learning for best-of-n problems [19].

In this chapter, we evaluate performance on this learning task at the population level using the average Hamming distance H from the population of agents $\mathcal{A}$ belief values to the true state s^* defined by Equation (2.9), re-scaled as an accuracy α measure such that,

$$\alpha = 1 - H(\mathcal{A}, s^*) \tag{3.1}$$

In order to investigate the impact of imprecision on social learning we will focus on the state-of-the-world problem in which agents attempt to learn the truth values of a set of propositions. In Section 3.3.1 we then investigate how tolerant of this form of social learning is to the presence of imprecise evidence. In Section 3.3.2, we instantiate this problem using a robot simulator to investigate the potential of applying this model in robotic applications and its robustness to imprecise evidence in practice.

3.3 Learning with imprecise evidence

In this section, we introduce two simulation scenarios where imprecise evidence is naturally encountered by the agents/robots. In Section 3.3.1, the agents receive accurate but imprecise evidence. In other words, the cardinality of the evidence set will vary while it will always include the true state of the world. We use simulations experiments to investigate how robust the social learning model is to imprecise evidence before introducing a robotic classification task Section 3.3.2 where the imprecision of evidence is dependent on the number of locations visited by robots in a single evidence collection episode.

3.3.1 Agent-based simulation with imprecise evidence

This section describes simulations of a multi-agent system with $k = 100$ agents attempting to socially learn the truth values of $n = 8$ propositions. The choice of $n = 8$ propositions provides

a broad range of levels of imprecision ($|E| \in \{1, 2, 3, \ldots, 256\}$) while maintains acceptable computational costs. The agents are initialised without any priory knowledge, In order to investigate the model's robustness to imprecise evidence, the degree of evidence imprecision received, as measured by $|E|$, is varied. For example, we might think of this as occurring when agents gradually learn facts about the world from different sources and expressed as logical formulas with different levels of generality. In this section, we only consider an error-free scenario such that the evidence obtained by the agents will be guaranteed to include the true state of the world s^*, while each of the other states has equal probability of being sampled without replacement. The number of states that are not s^* included in the evidence set will depend on a model parameter controlling the level of imprecision. In examining the relationship between the cardinality of evidence ($|E|$) and its precision, the principles of Shannon entropy offer a compelling framework for analysis. Shannon's concept, central to information theory, provides a quantitative measure of the uncertainty or unpredictability inherent in an information source. In this context, each piece of evidence is considered as an individual message that contributes to the overall information about a hypothesis, i.e. possible states of the world in this context. High entropy, characterised by a large set of evidence, suggests increased imprecision in the information conveyed. Conversely, a small set of evidence might exhibit low entropy, indicating greater precision and reduced uncertainty. In this thesis, we apply the cardinality of evidence to represent the imprecision of the evidence for its simplicity.

As previously described in Section 2.3, in practice, both evidence and agent interactions may be sparse or limited. We model this probabilistically as follows: Each agent conducts evidential updating and belief fusion iteratively. During each iteration, every agent has probability ρ (the *evidence rate*) of successfully obtaining evidence from the environment, and the agent will stop collecting evidence if it is certain about every proposition, i.e. it has a singleton belief. Agents also learn from the evidence being gathered by their peers using belief fusion. Every agent in the population has probability σ (the *fusion rate*) of being placed in a pool to fuse their belief with the belief of another agent. Each agent within the pool will be randomly paired with another agent and then each pair will combine their beliefs using the fusion operator in Equation (2.3). For every pair, both agents will adopt the result of this fusion as their new belief. If the number of agents in the pool is odd, then one agent will not take part in fusion.

The evidence received by the agents will be modelled as follows: The degree of the imprecision of evidence is pre-defined and varied to investigate the robustness of the set-based social learning model to different degrees of evidential imprecision. The evidential imprecision is constant across all iterations and across the population. In this section, we present error-free simulation results of which the true state of the world is guaranteed to be included in the evidence sets and the rest of the states will be randomly selected until the pre-defined evidential imprecision $|E|$ is satisfied.

In Figure 3.1 we show the average accuracy α of the agents' beliefs against time t for

different values of evidential imprecision $|E|$ and different combinations of evidence rate, ρ, and fusion rate, σ. For each combination of parameters we ran the experiments 50 times and the results are averaged over those 50 runs. We see that the population converges to $\alpha = 1$ at steady state for every combination of ρ, σ, and $|E|$. Since the only belief for which $\alpha = 1$ is $B = \{s^*\}$ it follows that the population has reached consensus by correctly and precisely identifying the true state of the world. Furthermore, this suggests that this social learning model is robust to various levels of evidential imprecision, provided that the agents always receive accurate evidence, i.e. $s^* \in E$.

In Figure 3.1a we see that the population converges more slowly as evidence imprecision increases, such as when evidence is sparse ($\rho = 0.1$) and fusion is infrequent ($\sigma = 0.1$). For $|E| = 1$, the population converges quickly to consensus by around $t = 25$. Convergence time increases to around 80 time steps when $|E| = 255$, this corresponding to the most imprecise non-vacuous evidence for $n = 8$ propositions since only one state of the world is emitted. In a scenario where evidential updating is frequent while fusion is infrequent, as shown in Figure 3.1b, the population converges faster for all levels of evidence imprecision than when evidential updating is infrequent; within 10 time steps for $|E| = 1$ and within 25 iterations for $|E| = 255$. When evidence is sparse and fusion is more frequent, Figure 3.1c shows that population also reaches consensus faster than those shown in Figure 3.1a whereas all levels of imprecision converges after around the same number of time steps. In Figure 3.1d, both evidential updating and fusion are frequent, resulting in fast convergence to the belief indicating the true state of the world, with little difference between the different levels of evidential imprecision. The effect of evidence imprecision on the convergence time decreases as we increase ρ or σ, as seen in Figures 3.1b to 3.1d. Furthermore, from Figure 3.1b and Figure 3.1c we see that both more frequent evidence and more frequent fusion can reduce the differences in the learning speed of the population. Furthermore, the frequency of belief fusion has the greater effect. Comparing Figure 3.1b and Figure 3.1c, we see that the convergence speeds are less affected by the level of evidential imprecision when agents learns more socially ($\rho = 0.1, \sigma = 0.9$) than when they learn more independently ($\rho = 0.9, \sigma = 0.1$).

So far, the evidence received by agents in this section has been error-free. However, in real-world situations it is highly likely that the evidence received could be subject to error; often due to noisy sensing equipment or even environmental noise. In the following section we will investigate social learning in a multi-robot scenario in which both evidential inaccuracy and imprecision are present.

3.3.2 Location classification task by multi-robot system

In real-world scenarios, such as a swarm of drones collaboratively mapping an uncharted terrain, a potential source of imprecision is when agents receive only partial information about the state of the world during the evidence collection process. In this section we consider a particular form

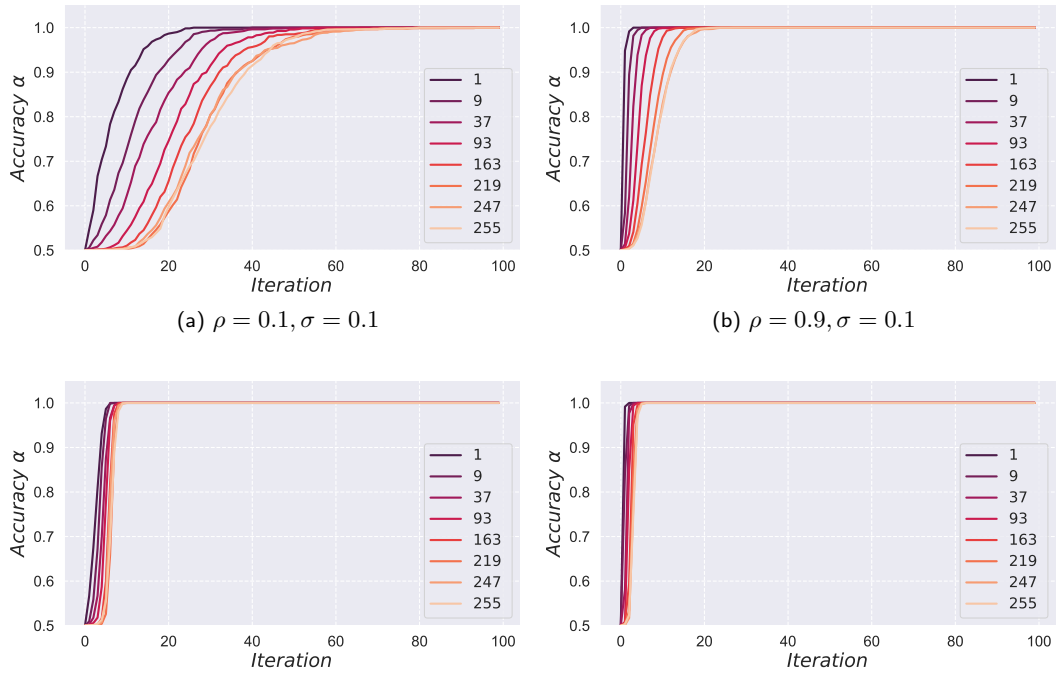

(a) $\rho = 0.1, \sigma = 0.1$

(b) $\rho = 0.9, \sigma = 0.1$

(c) $\rho = 0.1, \sigma = 0.9$.

(d) $\rho = 0.9, \sigma = 0.9$.

Figure 3.1: Average accuracy at steady state against time t for evidence rate $\rho \in \{0.1, 0.9\}$, fusion rate $\sigma \in \{0.1, 0.9\}$, and evidential imprecision $|E| = 1, \ldots, 255$. The model maintains high learning accuracy across different levels of evidential imprecision for various evidence and fusion rates.

of imprecise evidence arising from partial knowledge in a multi-robot systems in which robots are investigating properties of a number of different locations. During an evidence collection episode individual robots are only able to visit a limited number of locations and, hence, obtain only partial information about the full state of the world. In this context our results show that for a simple robot arena environment, social learning is robust to a range of different evidence collection bounds while being more effective than an approach based on individual, evidence-based learning alone.

We now describe a series of experiments in which $k = 5$ or 10 e-puck robots investigate $n = 4$, 8 or 12 locations arranged in a circle, each coloured either red or green. This is a similar configuration to that used by [12] .We conduct simulation experiments for a multi-robot system needing to make a collective decision about the true state of the world by attempting to classify n locations as either being red or green. Specifically, the proposition p_i asserts that location l_i *is red* and $\neg p_i$ asserts that l_i *is green*. In this case a state s_i is the Boolean allocation of the two colours to each location and beliefs are the set of the allocations deemed possible. Evidence is collected using the e-puck's in-built camera and with an additional error imposed on the classification process. To model this we introduce an error rate ϵ corresponding to the probability

of receiving evidence that is inconsistent with the true state of the world. More specifically, let the true state be denoted by s^*, then in the case that an agent receives information about location l_i they will receive $s(l_i) = s^*(l_i)$ with probability $1 - \epsilon$, and $s(l_i) = 1 - s^*(l_i)$ with probability ϵ. Between evidence collection episodes individuals move to the centre of the circle for fusion. The goal is for the whole system to reach consensus by identifying the true state of the world, i.e., the correct colour of each location from the $2^n = 16$, 256, or 4096 possibilities for $n = 4, 8$ or 12, respectively.

We simulate e-puck robots [78] which are well-suited to a classification task of this kind since they are equipped with a range of sensors. Experiments were performed in the CoppeliaSim[2] simulation environment which models the physical characteristics of the e-pucks, including motion, communication and sensing. Figure 3.2 shows the experimental arena which has $n = 8$ locations equally distributed around a 1.12 m circle with the $k = 5$ e-pucks' fusing positions spaced evenly around a 0.3 m disc at the centre. Each e-puck returns to their fusing positions after an evidence collection episode to fuse their beliefs with another robot also at their positions at that time. The robots will only be able to communicate when they are at the fusing positions, i.e., around the central area of the arena, with this restriction providing a basic model of a scenario in which communication is limited.

A group of e-pucks are initialised without any prior knowledge and hence with initial beliefs corresponding to the set of all possible states, representing total ignorance. They are given the coordinates of all locations and relevant fusing positions and apply simple path planning to travel between sites and the fusing positions. The e-pucks featured have 8 IR proximity sensors and therefore we apply Braitenberg-based collision avoidance algorithms [79]. The system learns the environment iteratively with individuals alternating between episodes of evidence collection and fusion. During an evidence collection episode a robot visits some of the sites about which they are currently uncertain, where the number of locations visited is less than a pre-specified upper bound N_u.

This parameter N_u is defined as the maximum number of locations that a robot is able to visit during each evidence collection episode, this modelling plausible real-life constraints imposed by both robot hardware, and the scale and complexity of the environment, on distance that can be travel during evidence collection. A natural consequence of this bound is that evidence collected during each episode will typically only provide partial information in the form of noisy data concerning the class of only some of the locations. The representation of this partial information will take the form of imprecise evidence. We can then determine the impact that imprecise evidence has on the population by varying N_u. Robots will obtain precise evidence if they visited a relatively high numbers of locations since the evidence E they received would then identify a small number of possible states, i.e., have low cardinality. More specifically, the relationship between the number of sites visited v and the cardinality of the evidence set is

[2]https://www.coppeliarobotics.com/

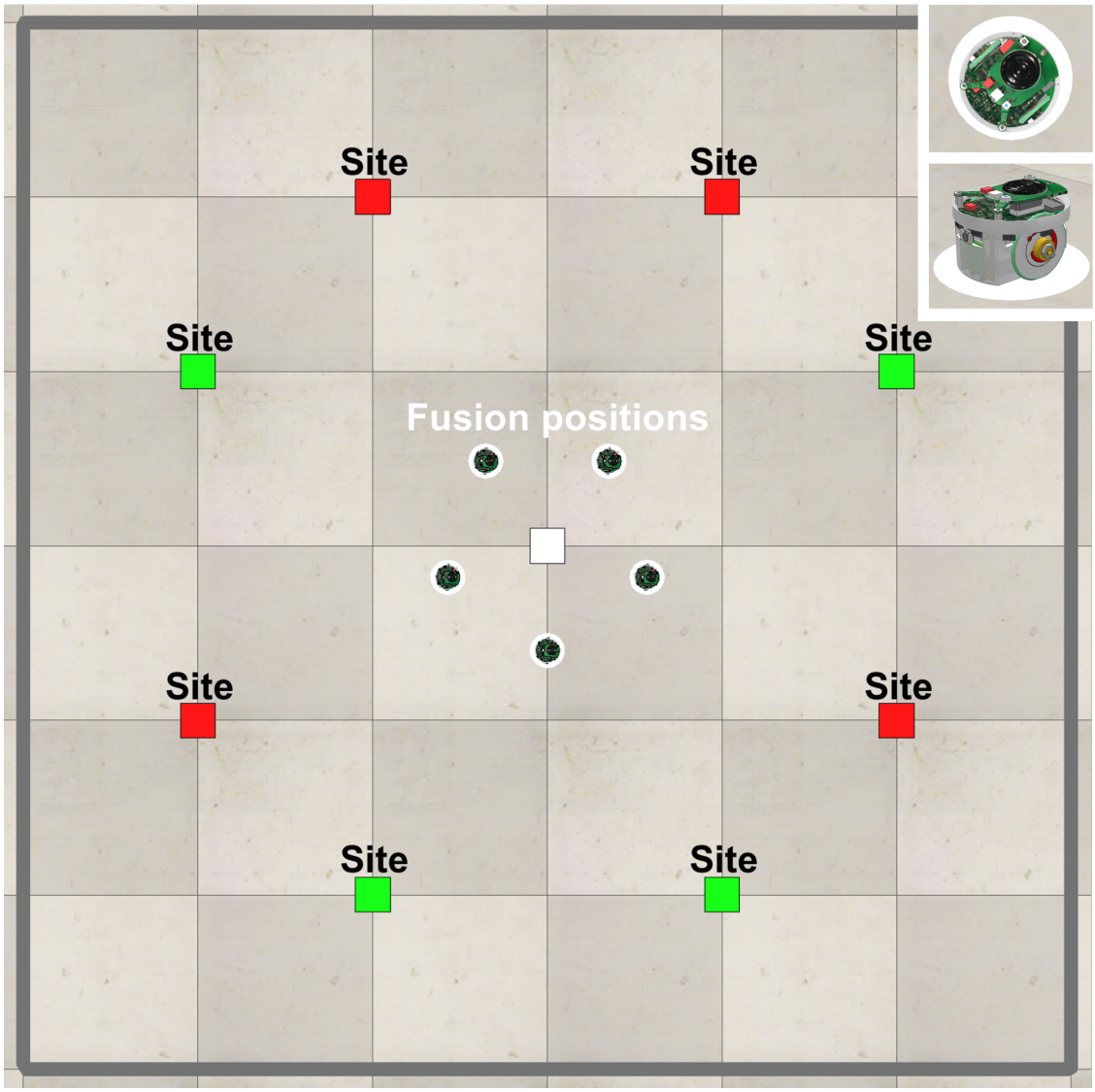

Figure 3.2: Top-down view of the experimental setup for $n = 8$ sites. The red/green squares indicate the location of the sites, and the white circles show the fusion positions. An e-puck resides at each fusion position.

given by $|E| = 2^{n-v}$. Each robot selects up to N_u locations from the set of locations for which either class is still possible according to their current belief B. At each location an e-puck uses its camera to capture a colour value indicating the class to which that particular site belongs. After visiting all the locations that they have selected, they update their belief according to Equation (2.6) and return to their pre-specified central location. Each robot then broadcasts its belief along with a flag message identifying the broadcaster as being ready to fuse. In our model we simulate the communication between e-pucks using the built-in CoppeliaSim functions while physical e-pucks can achieve the same communication via on-board Wi-Fi or Bluetooth

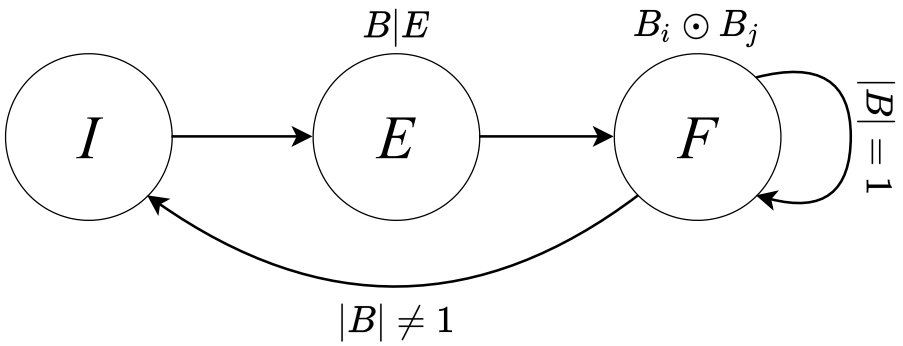

Figure 3.3: The robot's state transition model. (I) When the robot visits all of the locations it has planned to visit. Evidential updating (E), and Belief fusion (F).

functionality. They also listen for any other robots currently broadcasting and fuse their belief with the transmitted belief in the first such message they receive.

Figure 3.3 shows a state transition diagram for the above process. Robots have 3 internal states: Investigation (I); Evidential updating (E); and Belief fusion (F). Robots are initialised in state I before they select locations to investigate and visit them in order, collecting class information as they go. Once all selected locations have been visited the robot transitions to state E and updates their belief based on the evidence collected. They then transition to the state F, return to their fusing positions and perform fusion. If their belief now identifies a single complete set of classifications for all the locations they remain in their fusing positions in state F and carry out another fusion, otherwise they transition to state I for another evidence collection episode.

We use the accuracy metric defined in Equation (3.1) to measure the performance of the whole population of robots. Notice that for evidence-only learning, when the belief fusion process is disabled and robots learn independently based *only* on the evidence they receive, the simulations lead to Bernoulli experiments with the success probability $p = 1 - \epsilon$. The expected value of the Hamming distance between a robot's belief and the true state is then as follows:

$$\mathbb{E}(H(B, s^*)) = \frac{1}{n} \sum_{i=0}^{n} \binom{n}{i} i(1-\epsilon)^{(n-i)} \epsilon^i = \epsilon \tag{3.2}$$

We therefore employ $1 - \epsilon$ as a benchmark to illustrate the improvement in performance which results from robots interacting with one another and fusing their beliefs to achieve social learning.

We now present results from simulation experiments conducted with $k = 5$ or 10 e-pucks, $n = 4$, 8, or 12 sites and different upper bounds N_u on the number of sites visited during an evidence collection episode. For each combination of parameters we ran the experiments 20 times. The results presented herein are then averaged across runs with error bands corresponding to the 5^{th} and 95^{th} percentiles.

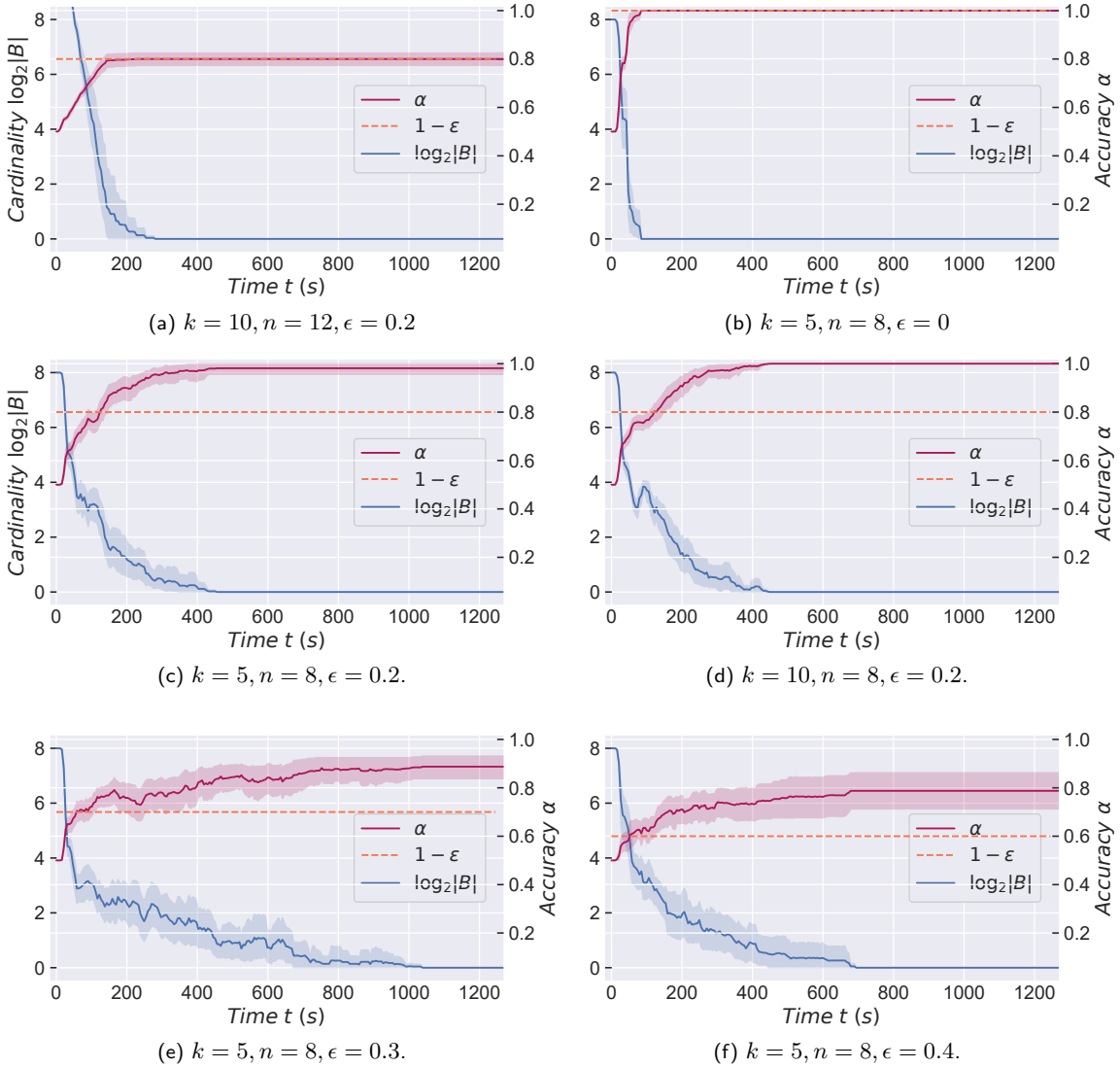

(a) $k = 10, n = 12, \epsilon = 0.2$

(b) $k = 5, n = 8, \epsilon = 0$

(c) $k = 5, n = 8, \epsilon = 0.2$.

(d) $k = 10, n = 8, \epsilon = 0.2$.

(e) $k = 5, n = 8, \epsilon = 0.3$.

(f) $k = 5, n = 8, \epsilon = 0.4$.

Figure 3.4: Average log cardinality $log_2|B|$ and average accuracy α plotted against iteration for $N_u = 3$ with different numbers of agents k, locations n and error rate ϵ. (a) Evidence-only learning (without fusion). (b–f) Social learning (with fusion).

Figure 3.4 shows the log average cardinality $log_2|B|$ (blue line) and the average accuracy α (purple line) of the robots' beliefs against time t for $n \in \{8, 12\}$ locations with an upper bound $N_u = 3$. For all plots in Figure 3.4 the dotted orange lines indicate the value of $1 - \epsilon$; i.e. the expected accuracy when agents learn individually from direct evidence alone. For instance, in Figure 3.4a we present results from an evidence-only learning scenario where we see that, for $n = 12$ locations, $k = 10$ e-pucks and error rate $\epsilon = 0.2$, the cardinality of the population decreases to 0 over time while the average accuracy of the system converges to the expected accuracy of $1 - \epsilon$. This is because, without belief fusion, agents are dependent on the evidence

that they receive directly, without any communication with other agents. This leads to agents adopting erroneous beliefs about the state of the world. An accuracy value above the dotted line is therefore indicative of the system's ability to correct for errors as a direct result of social learning.

From Figures 3.4b to 3.4f we see that, across all runs and for all parameter combinations, the robots converge to a belief of cardinality $|B| = 1$, i.e., a singleton belief, as shown by the blue lines decreasing to $log_2|B| = 0$. This means that, under our model, all of the e-pucks eventually remain stationary at their central fusing positions having reached a consensus about the state of the world that they believe to be true. Of course, the primary purpose of location classification is for the system to *accurately* identify the true state of the world. The purple lines in Figures 3.4b to 3.4f show the average accuracy of the population plotted against time. Broadly, we see that the system is able to correctly classify locations with high accuracy. Starting with an error-free scenario in Figure 3.4b with 8 locations and an upper bound of $N_u = 3$ as well as $k = 5$ e-pucks, the robots always identify the true state of the world s^* with accuracy $\alpha = 1$ in under 100 seconds across all 20 experiments. This is perhaps unsurprising when robots obtain perfect information during evidence collection. In Figures 3.4c and 3.4d we show a moderately noisy scenario with $\epsilon = 0.2$ and an upper bound $N_u = 3$. In Figure 3.4c we see with noisy evidence the system is slower to reach a consensus but still manages to converge on a belief with an average accuracy of 0.98 after roughly 400 seconds and in Figure 3.4d with greater number of robots the system achieves higher accuracy of 1 with less variations after roughly the same time as system with 5 robots. With higher error rates $\epsilon = 0.3$ and $\epsilon = 0.4$, the robots converges with a lower accuracy $\alpha = 0.9$ and $\alpha = 0.8$ and more variation across multiple runs, as shown in Figure 3.4e and Figure 3.4f. However, the systems are still manage to reach consensus at a singleton belief in these scenarios of higher error rates

The upper bound on the number of locations N_u also has an impact on accuracy when the population size k is small, with higher accuracy being achieved for intermediate values of N_u. For example, Figure 3.5a shows the average accuracy against the upper bound N_u taking values from $[1, n]$, for $k = 5$ and $n \in \{4, 8, 12\}$, with moderate error rate $\epsilon = 0.2$. In Figure 3.5a the best performance is obtained when the visit bound $N_u = 2, 3$ where, at steady state, the system achieves an accuracy $\alpha = 1$ on average across 20 runs. That means the system reaches consensus on s^* across all 20 experiments. For $N_u = 1$ and $N_u = 4$, however, the accuracy falls to around 0.87 and 0.95, respectively. More generally, good performance across all N_u values shows that this form of social learning is still accurate under imprecise evidence. Although, there is some reduction in performance for the most imprecise case when a maximum of only 1 location is visited in each evidence collection episode. The model is more robust to varying imprecise evidence when there are $k = 10$ e-pucks, with similarly high accuracy observed for all N_u and for all $n \in \{4, 8, 12\}$ as shown in Figure 3.5b. Increasing the number of robots k can improve the overall performance of social learning and decrease the variance in accuracy. The

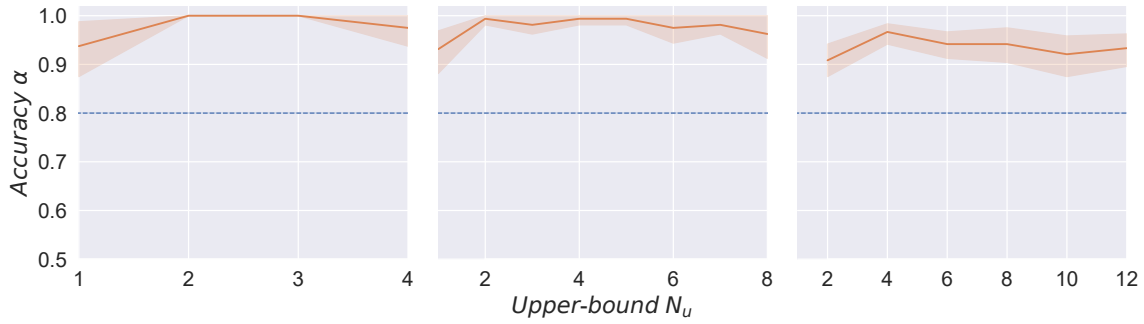

(a) $k = 5$.

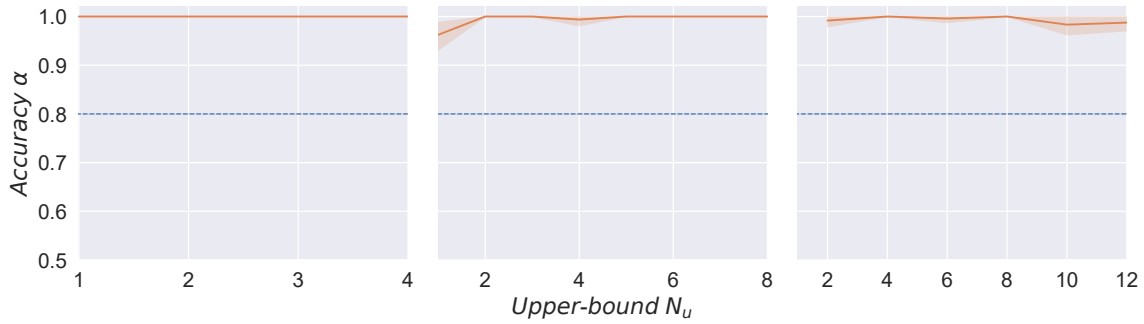

(b) $k = 10$.

Figure 3.5: Average accuracy at steady state for various upper bounds N_u and error rate $\epsilon = 0.2$. (a) $n \in \{4, 8, 12\}$ from left to right with $k = 5$. (b) $n \in \{4, 8, 12\}$ from left to right with $k = 10$.

system achieves greater accuracy for all upper bounds with $k = 10$ robots than $k = 5$ robots. The performance is also less variant across simulations and across different N_u.

It is also important to consider whether there are different costs associated with the different levels of imprecision. In Figure 3.6 we show the average number of evidence collection episodes required to reach a system-wide consensus against the upper bound N_u with error rate $\epsilon = 0.2$. We see that for systems of $k = 5$ and $k = 10$ e-pucks the average number of evidence collection episodes performed by each e-puck are very similar for $n = 4$ and $n = 8$ locations and for $n = 12$ locations the robots performed more evidence collection episodes when $k = 10$ than when $k = 5$. For example, for $n = 12$ and $N_u = 4$, with $k = 10$ e-pucks each robot performed 14 evidence collection episodes on average whereas for $k = 5$ the average was only 11, meaning that having more e-pucks does not reduce the number of evidence collection episodes performed by each e-puck on average. Therefore, with double the number of e-pucks the system obtains roughly twice as much information in the form of direct evidence and roughly twice the opportunities for error correction via belief fusion.

As each evidence collection episode requires the robots to leave and reenter the central fusing positions, we now consider the cost that N_u incurs in terms of the average distance

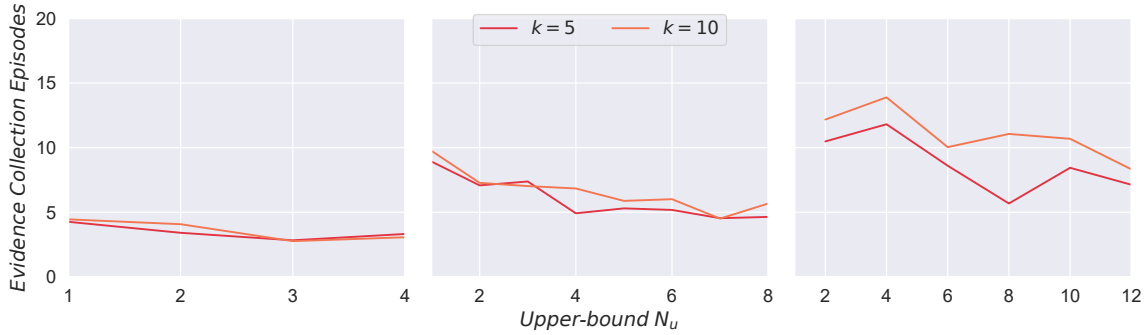

Figure 3.6: Average number of evidence collection episodes performed by one e-puck prior to reaching consensus for $\epsilon = 0.2$, $k \in \{5, 10\}$ with $n \in \{4, 8, 12\}$ from left to right.

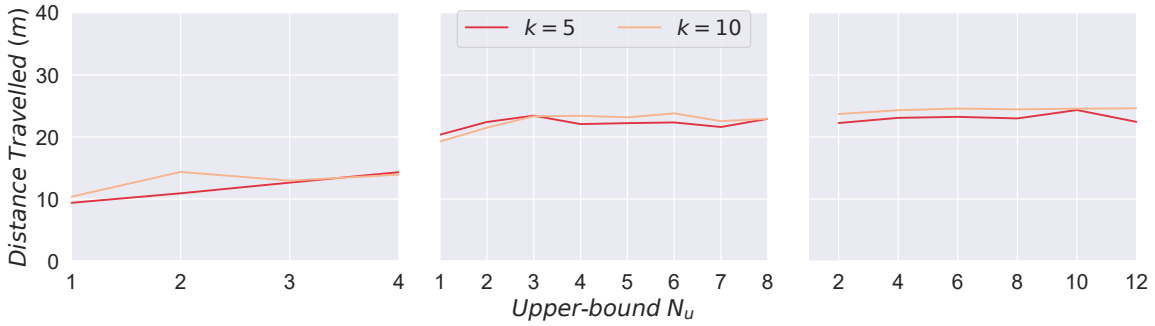

Figure 3.7: Average distance travelled prior to consensus against upper bounds N_u for $\epsilon = 0.2$, $k \in \{5, 10\}$ with $n \in \{4, 8, 12\}$ from left to right.

travelled by the robots for $n \in \{4, 8, 12\}$ and $k \in \{5, 10\}$ as shown in Figure 3.7. We see that the average distance travelled is robust to both population size n and the visit upper bound N_u. As we increase N_u the robots must travel between sites before returning to their fusing positions, covering increasing distances proportionate to N_u. However, the increased distance travelled in a single evidence collection episode is offset by the reduction in the average number of evidence collection episodes, as shown in Figure 3.6. The total evidence collection episodes performed are trending down with increasing N_u. We therefore see relatively little change in the average distance travelled across different values of N_u. Finally, in Figure 3.8 we show the average convergence time for the system against N_u. This is the time it takes for the robots to reach a consensus. For $\epsilon = 0.2$ we see a relatively consistent convergence time for different N_u, which demonstrates the robustness of the social learning model to noisy evidence and insensitivity to the level of evidential precision. Although the time cost increase for higher number of locations needed to be classified, in general, the time cost is insensitive to both the population size and different constraints on the number of locations that can be visited in an evidence collecting episode. In other words, the convergence time is insensitive to the different

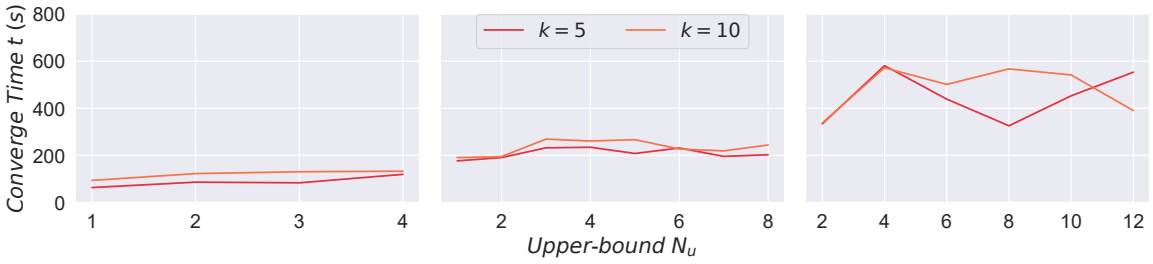

Figure 3.8: Average time to convergence against upper bound N_u for $\epsilon = 0.2$, $k \in \{5, 10\}$ with $n \in \{4, 8, 12\}$ from left to right.

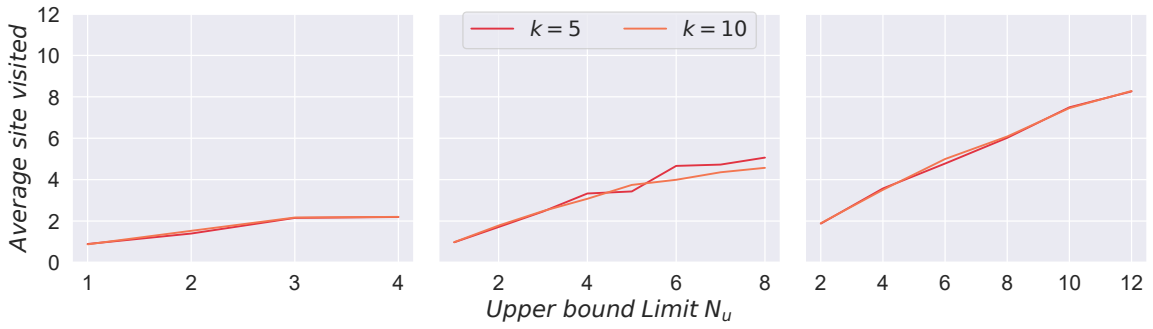

Figure 3.9: Average numbers of site visited per episodes against N_u for $\epsilon = 0.2$, $k \in \{5, 10\}$ with $n \in \{4, 8, 12\}$ from left to right

levels of evidential imprecision.

Due to the evidence gathering strategy applied, the e-pucks sometimes do not visit the maximum number of sites that N_u allows them to visit. We therefore present the average number of sites actually being visited per evidence collection episode for $n \in \{4, 8, 12\}$ and $k \in \{5, 10\}$ with error rate $\epsilon = 0.2$ in Figure 3.9. We see that for the highest visit bounds $N_u = 4, 8, 12$, e-pucks only visit around 2.5, 5, and 8 locations, respectively, on average. The robots visit locations adaptively according to their current belief, and this may explain the system's robustness to N_u as shown in Figure 3.5.

We then carried out experiments with a higher error rate $\epsilon = 0.3$ for $n = 8$ locations and $k = 5$ e-pucks to consider the model robustness to an even noisier environment. In Figure 3.10 we present the accuracy against the visit bound N_u for $\epsilon = 0.3$. Here higher accuracy can also be obtained by intermediate visit bounds where the multi-robot system achieves $\alpha > 0.9$ on average for $N_u = 4$ and $N_u = 5$. However, across the range of upper bounds N_u performance always exceeds that of the expected accuracy, even in the high error rate scenario where $\epsilon = 0.3$, suggesting that this model is robust to error . In Figure 3.11, we see that the time to convergence does increase for a higher $\epsilon = 0.3$.

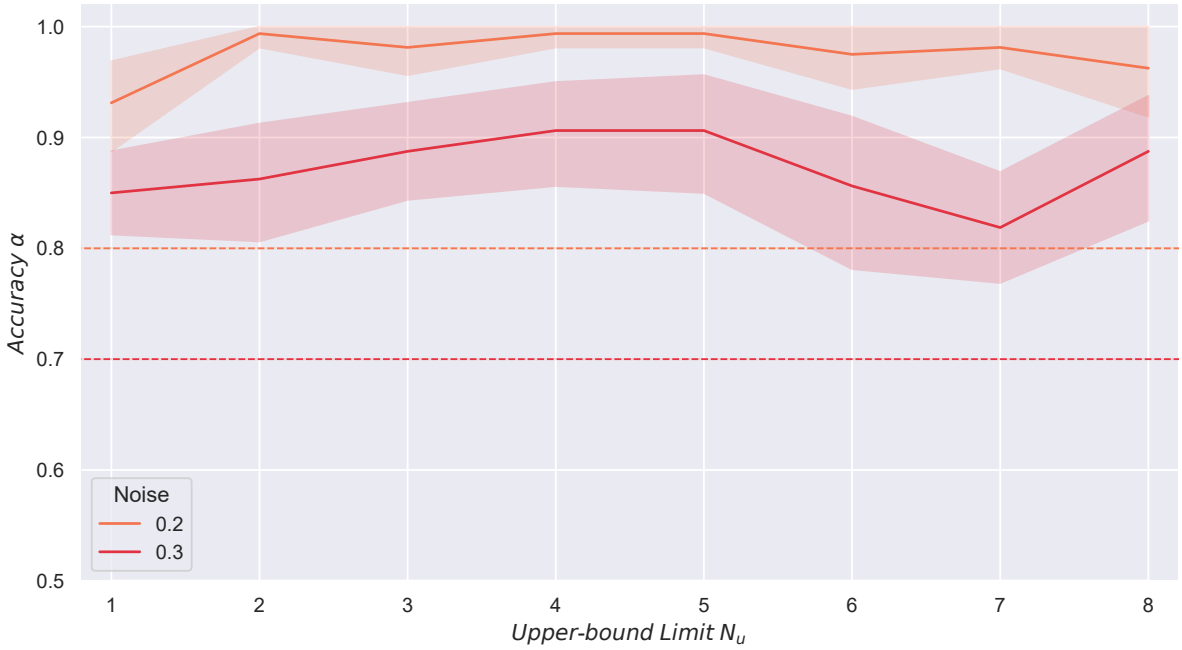

Figure 3.10: Average accuracy at steady state for various upper bounds N_u and error rate $\epsilon \in \{0.2, 0.3\}$

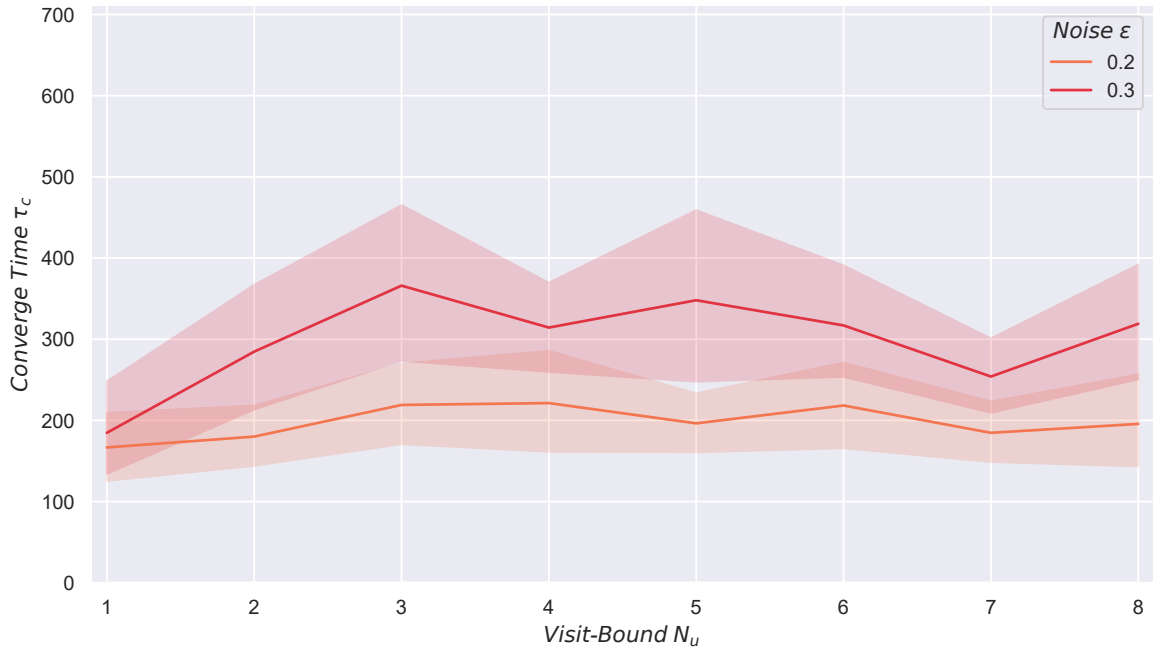

Figure 3.11: Average time to convergence for various upper bounds N_u and error rate $\epsilon \in \{0.2, 0.3\}$

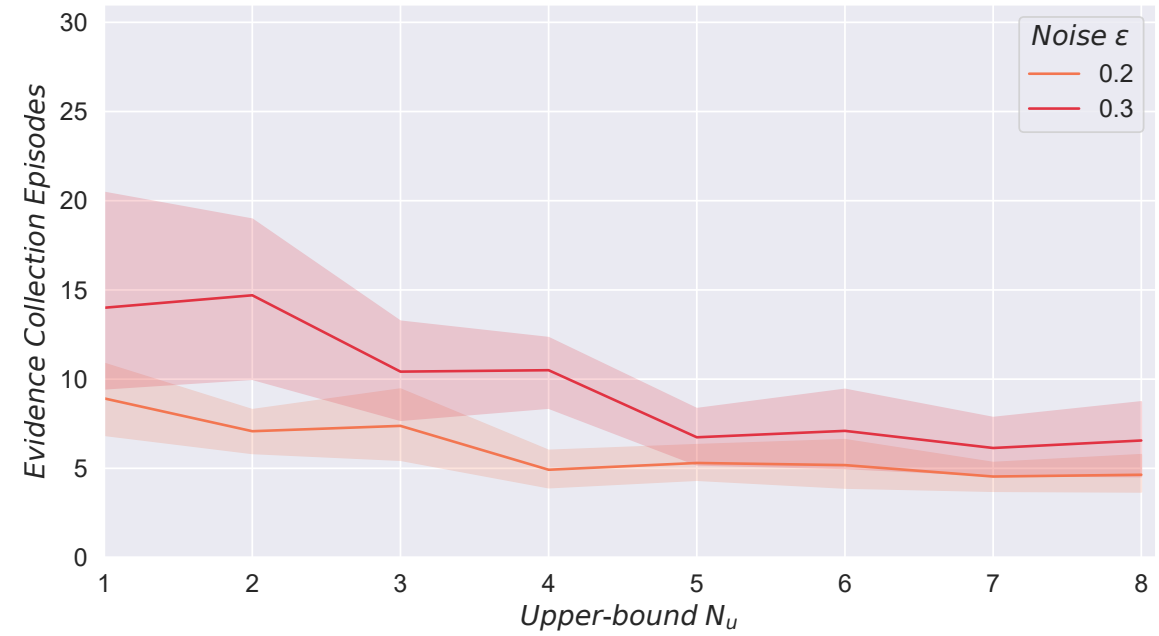

Figure 3.12: Average accuracy(a) and Average time to convergence(b) at steady state for various upper bounds N_u and error rate $\epsilon = 0.3$

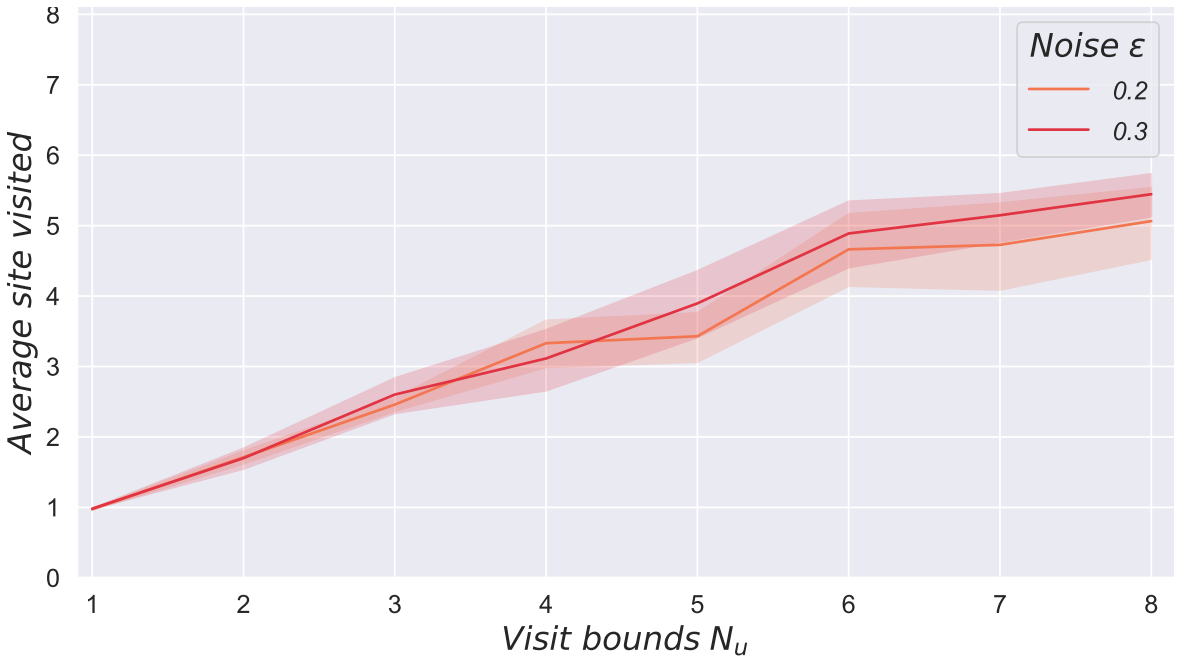

Figure 3.13: Average numbers of site visited per episodes against upper bounds N_u for $\epsilon \in \{0.2, 0.3\}$, $k = 5$, and $n = 8$

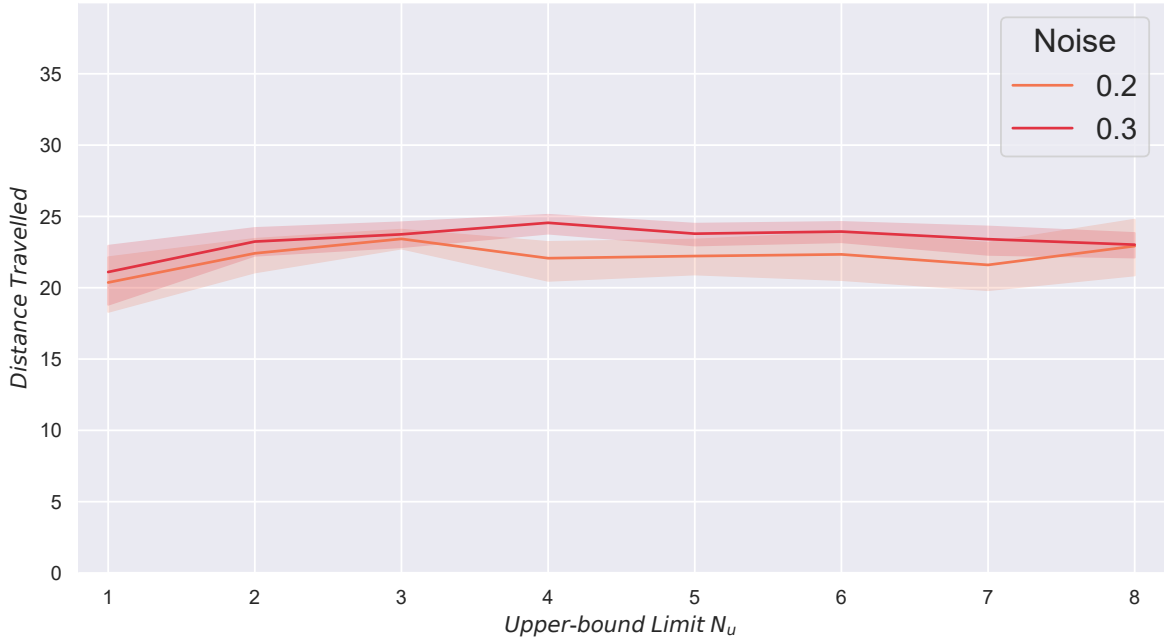

Figure 3.14: Average distance travelled prior to consensus against upper bounds N_u for $\epsilon \in \{0.2, 0.3\}$, $k = 5$, and $n = 8$

In Figure 3.12 we show the average number of evidence collection episodes required to reach a consensus in the system against the upper-bound limit N_u and for error rate $\epsilon \in \{0.2, 0.3\}$. We see that the swarm conduct more evidence collection episodes for $\epsilon = 0.3$ than for $\epsilon = 0.2$. Specifically, when N_u is, the required number of episodes is considerably higher for $\epsilon = 0.3$ than for $\epsilon = 0.2$. For greater N_u bounds, the increase becomes modest. This suggests that the robots demand more evidence collection episodes for consensus for higher error rate.

In addition to the average number of evidential collection episodes, we now consider the cost that N_u incurs in terms of the average distance travelled by the robots for different error rate $\epsilon = 0.2$ and $\epsilon = 0.3$ as shown in Figure 3.14, as well as the average number of sites visited in each evidence collection episodes for different N_u as shown in Figure 3.13. Between the two examined error rates, Figures 3.13 and 3.14 indicates that the average distance travelled and number of sites visited by the robots is not sensitive to changes in the error rate ϵ. While higher error rates necessitate more evidence collection episodes, the results suggests that this increase does not drastically inflate the overall distance covered by the robots during their task. The system effectively balances the need for additional evidence collection against the operational constraints of travel distance. This robustness demonstrates that the cost implications of noise are manageable, thereby highlighting the scalability and reliability of our social learning model in varying environments and operational conditions.

Overall, the results of the robot simulation experiments show that this form of multi-robot social learning achieves high accuracy across all different imprecision levels. The cost of the

classification task is robust to both error rate and different constraints on the number of locations that can be visited in an evidence collecting episode. The approach therefore has the potential to be effectively applied to location classification tasks conducted by multi-robot systems. In this approach, each robot does not have to investigate every location for the system to reach consensus. There can be good performance in scenarios in which access to some locations is restricted, either by the range of the robots (e.g., due to power constraints) or a heterogeneous system possessing different levels of access or capabilities. Furthermore, the approach scales well scenarios in which the number of locations is greater than the number of robots. This scalability is crucial because it enables efficient resource allocation, allowing a smaller robotic team to effectively monitor or operate in a large and complex environment without compromising performance.

the simulation can be easily transferred to a real world implementation, using a similar set-up as applied in [12].

In this section, we have demonstrated that social learning is capable of delivering robust performance, even when robots are dealing with imprecise and noisy evidence. Remarkably, the level of imprecision can be significantly high, and the system's performance still remains accurate. In other words, social learning can be robust to evidence that is both imprecise and noisy. Subsequently, we show that social learning performance can actually be improved by incorporating imprecise evidence of a particular type and degree in Section 3.4.

3.4 The benefits of imprecise evidence in social learning

In this section, we detail a method employing the Hamming distance to infuse imprecision into the evidence collected by agents. In Section 3.4.1, this approach is formulated with the intent of harnessing deliberately infused imprecision into the evidence, particularly when agents acquire precise evidence. We hen carry out agent-based simulations in Section 3.4.2 and demonstrate that certain degrees of evidential imprecision can mitigate the adverse effects caused by the inaccuracy of the evidence in the social learning process.

3.4.1 Model for Imprecise Evidence and the Neighbourhood Approach

In this section, we introduce a method to use evidence imprecision as a design parameter for social learning and conduct agent-based simulations. Here we assume the information receive by the agent is precise, identifying a single state s_e which may or may not deviate from the true state of the world, depending on whether or not there is environmental inaccuracy i.e. $\epsilon > 0$. The estimate s_e is generated by independently sampling the truth value of each proposition and then recording the correct truth value with probability $1 - \epsilon$ and incorrect truth value with probability ϵ. Let $H_e = H(s^*, s_e)$ denote the Hamming distance between the true state of the

world and the state identified during evidence collection. In the case that the error rate $\epsilon > 0$ then H_e is a random variable with the following probability distribution:

$$P(H_e(s_e, s^*)|\epsilon) = \binom{n}{i}\epsilon^i(1-\epsilon)^{n-i} \tag{3.3}$$

Based on Equation (3.3), the maximum likelihood estimation of H_e is $\hat{H}_e = 0$, $\hat{H}_e = 1$, and $\hat{H}_e = 2$ for $\epsilon = 0.1$, 0.2, and 0.3 respectively if $n = 8$. In other words, the probability that $s^* = s_e$, i.e. $H_e = 0$, can be relatively small compared to $s^* \neq s_e$ ($H_e > 0$) if the values of n and ϵ are high. Figure 3.15 shows the relationship between the observed state and the true state of the world. s_e^1, s_e^2, and s_e^3 are three states independently collected as evidence, assuming $\epsilon > 0$. All three states are different from the true state s^* with the distance shown as concentric circles centred on s^*. However, if we consider imprecise evidence in the form of a neighbourhood of the evidence states, then as the radius of that neighbourhood increases so will the probability that s^* is contained in the evidence set (see the brown circle around s_e^1). We hypothesise that this increase in probability of the evidence being consistent with the true state of the world can be potentially beneficial in social learning.

In general, given an estimated state of the world s_e obtained from evidence, then an associated imprecise evidence set $E(s_e, \tilde{H})$ can be defined as a Hamming distance neighbourhood of s_e based on distance threshold $\tilde{H}$ in the following way:

$$E(s_e, \tilde{H}) = \{s|s : H(s, s^e) \leqslant \tilde{H}\}, \text{where } \tilde{H} \in \{0, \ldots, n-1\} \tag{3.4}$$

We use $\tilde{H}$ as a representation parameter to control the imprecision of the evidence received by the agents. An agent receives precise evidence s_e and uses it as an estimate of the state of the world. This parameter essentially serves as a tuning knob, allowing for varying degrees of evidential imprecision by varying its cardinality. The cardinality of the evidence increases with $\tilde{H}$; for example, in the case that $n = 8$, the cardinality of the evidence is $|E(s_e, \tilde{H})| = \sum_{i=0}^{\tilde{H}} \binom{n}{i}$, specifically, $|E(s, 0)| = 1$, $|E(s, 1)| = 9$, $|E(s, 2)| = 37$, $|E(s, 3)| = 93$, $|E(s, 4)| = 163$, $|E(s, 5)| = 219$, $|E(s, 6)| = 247$, and $|E(s, 7)| = 255$.

3.4.2 Simulation Results of the Hamming Neighbourhood Approach

We now describe a number of agent-based simulation experiments to investigate the effect of varying the threshold $\tilde{H}$ in social learning. Here we will assume a population of $k = 100$ agents will investigate the truth-values of $n = 8$ propositions. The evidential updating and belief fusion methods defined in Equation (2.3) and Equation (2.6) are also applied in this simulation with an evidence rate $\rho \in [0.02, 1)$ and a fusion rate $\sigma \in [0.02, 1)$. The population of agents is initialised as having no prior knowledge about the world and hence hold completely

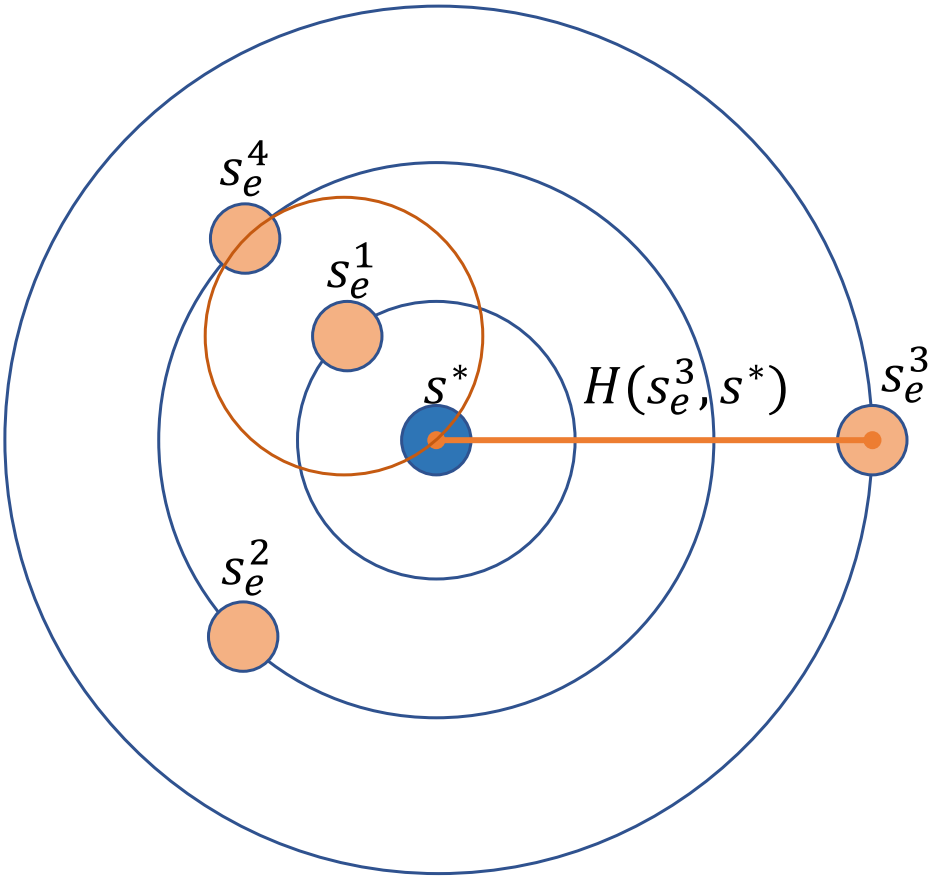

Figure 3.15: Diagram showing the relationship between the observed state s_e and the true state s^*

ignorant beliefs, i.e., $B = \mathbb{S}$, at time $t = 0$. Experiments are run 50 times and the results are averaged over those runs to account for variation in performance.

Figure 3.16 shows heat maps of average accuracy for varying fusion and evidence rates, at different levels of evidential imprecision as parameterised by different Hamming distance thresholds and different error rates. For each single heat map, with a step size of 0.02 we have evidence rates $\rho \in [0.02, 1)$ for the vertical axis and fusion rates $\sigma \in [0.02, 1)$ for the horizontal axis. The top-left plot in Figure 3.16 includes axis labels for clarity. The Hamming distance threshold increases from left to right for Figures 3.16a to 3.16d. Here lighter and darker colours indicate higher and lower accuracy, respectively. Across the heat maps, when evidence is of low to intermediate imprecision, we see that the system is more accurate when the evidence rate is relatively high in relation to the fusion rate. In other words, lower fusion rates increase the system's robustness across various evidence rates, error rates, and levels of evidential imprecision. On the other hand, in areas where the evidence rate is relatively low compared to the fusion rates, the system requires significantly low fusion rates to reach higher accuracy. In regions of the parameter space in which the fusion rate is higher than

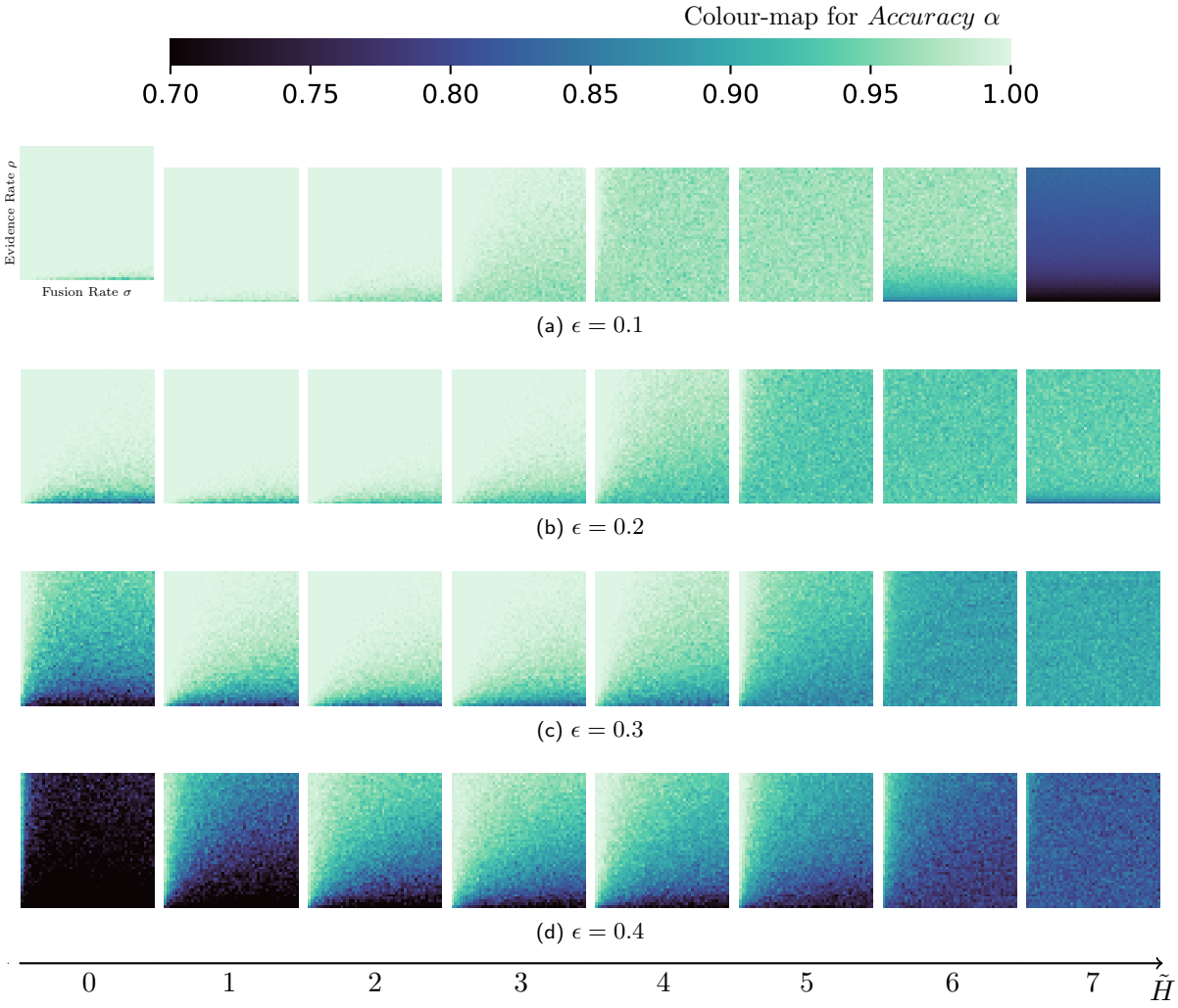

Figure 3.16: Average accuracy α at steady state for different evidence imprecision for different error rates $\epsilon \in \{0.1, 0.2, 0.3, 0.4\}$. From left to right: $\tilde{H} \in \{0, ..., 7\}$. In each heat map, the y-axis and x-axis respectively represent $\rho \in [0.02, 1)$ and $\sigma \in [0.02, 1)$. The axis labels for the heat maps are provided in the top left cell as an example. For higher error rates, an imprecise evidential updating threshold can improve the overall accuracy across different combinations of evidence and fusion rates.

the evidence rate, the learning accuracy is improved by increasing the Hamming threshold $\tilde{H}$ to different levels, depending on different error rates. Beyond the certain points, e.g. $\tilde{H} = 3$ for $\epsilon = 0.3$, additional increases in the Hamming threshold tend to reduce overall accuracy while making it more consistent across various regions of the parameter space. As the level of evidential imprecision increases, the performance across the parameter space becomes more uniform, displaying a moderate level of accuracy. There is a unique case in Figure 3.16a when $\tilde{H} = 7$, where the accuracy is uniformly low. This particular scenario will be further discussed and analysed in conjunction with the subsequent figures.

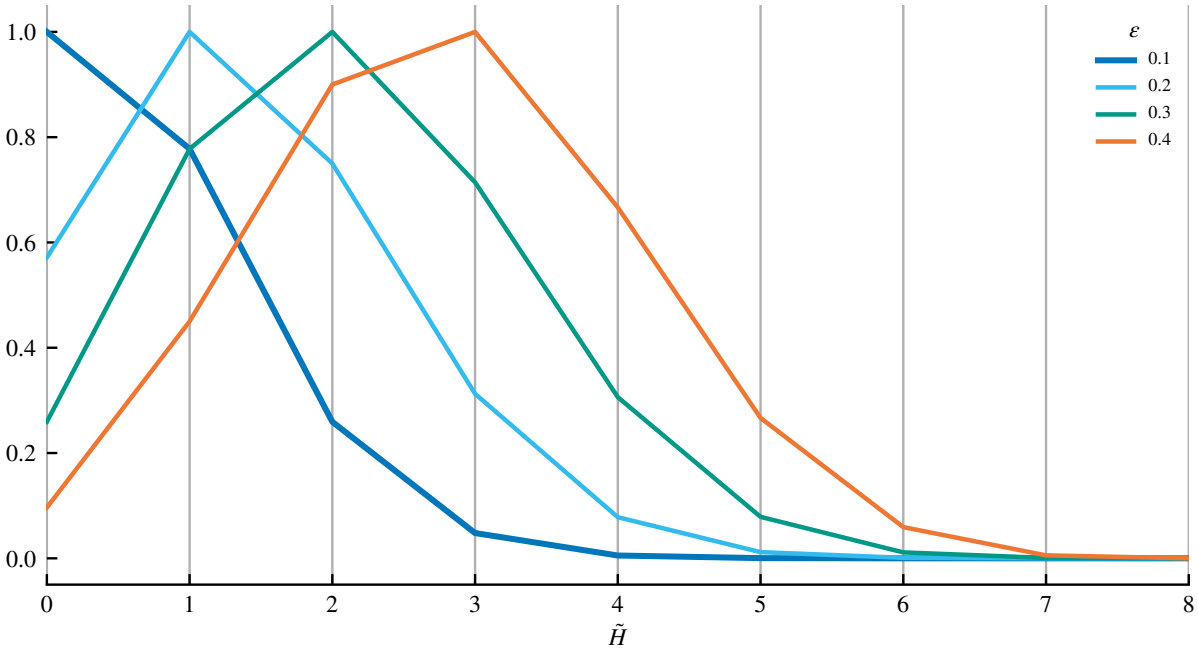

Figure 3.17: Normalised difference between probabilities of the evidence set including s^* and s_1 that is 1 bit away from s^* for error rate $\epsilon \in \{0.1, 0.2, 0.3, 0.4\}$. The difference between probabilities are maximised at a higher threshold for higher error rates.

From Figure 3.16 we see that the optimal Hamming thresholds for achieving the best performance vary depending on the error rates. In particular, when $\epsilon = 0.3$, from Figure 3.16c we see that accuracy is highest across the whole fusion and evidence rate parameter space when $\tilde{H} = 2$ or $\tilde{H} = 3$. For higher levels of imprecision there is then a relatively uniform decrease in performance across the parameter space; see particularly the first column from the right when $\tilde{H} = 7$. In general, these results indicate that highest overall accuracy is obtain for moderate levels of imprecision when using the proposed neighbourhood approach. For lower error rates, Figures 3.16a and 3.16b show that optimal performance is achieved with relatively low Hamming thresholds of $\tilde{H} = 1$ and $\tilde{H} = 2$ for $\epsilon = 0.2$, and $\tilde{H} = 0$ and $\tilde{H} = 1$ for $\epsilon = 0.1$. This suggests that at lower error rates, mroe precise evidence is effective for obtaining high accuracy in the system. In contrast, as shown in Figure 3.16d, at a higher error rate of $\epsilon = 0.4$, the model suggests that best performance is achieved with considerably higher Hamming thresholds of $\tilde{H} = 3$ and $\tilde{H} = 4$, i.e. in scenarios where the error rate is higher, more imprecise evidence may actually be advantageous for improving the overall accuracy of the learning system. Hence, in general these results suggest a pattern of performance in which the higher the error rate, the higher the level of imprecision at which the best accuracy is obtained.

One way to investigate the trade-off involved in the use of imprecise evidence in the form of Hamming distance thresholds, is to consider how increasing the threshold will increase both the probability that the true state of the world is included in the evidence, whilst also increasing

the probability that erroneous states are included as well. More specifically, it seems desirable to select a Hamming distance threshold such that the probability of true state of the world being in the evidence neighbourhood is high, while the probability of any state different from the true state being in the neighbourhood is low. Notice that the states which differ from the true state, which have the highest probability of belonging to the evidence neighbourhood, are those which have a different truth value for exactly one of the propositions under consideration. As above let s^* denote the true state of the world, and let s_1 denote one of the states that differ from s^* in exactly one proposition i.e. $H(s^*, s_1) = 1$. Also as above let s_e denote the estimated state of the world obtained through evidence collection. Then a desirable Hamming threshold $\tilde{H} = t$ could be one that maximises $P(s^* \in E(s_e, t)) - P(s_1 \in E(s_e, t))$. The probabilities of s^* and s_1 being in the imprecise evidential set $E(s_e, t)$ are as follows:

$$P(s^* \in E(s_e, t)) = P(H(s_e, s^*) \leqslant t) = \sum_{i=0}^{t} \binom{n}{i} \epsilon^i (1-\epsilon)^{n-i} \tag{3.5}$$

$$P(s_1 * \in E(s_e, t)) = P(H(s_e, s_1) \leqslant t) \tag{3.6}$$

$$= \epsilon(1-\epsilon)^n + \sum_{i=1}^{t} \binom{n-1}{i-1} \epsilon^{i-1} (1-\epsilon)^{n-i+1} + \sum_{i=1}^{t} \binom{n-1}{i} \epsilon^{i+1} (1-\epsilon)^{n-i-1} \tag{3.7}$$

Figure 3.17 shows the normalised difference between the two probabilities;

$$\frac{P(s^* \in E(s_e, t)) - P(s_1 \in E(s_e, t))}{\max\{P(s^* \in E(s_e, t)) - P(s_1 \in E(s_e, t)) : t\}} \tag{3.8}$$

for different threshold values t. Results suggest that the threshold which maximises this probability difference increases as the error rate increases, again suggesting that increasing imprecision may improve performance in high-inaccuracy scenarios. These results are broadly consistent with the simulation results shown in Figure 3.16

A common trade-off in social learning is between speed of learning and accuracy of learning; known as the speed vs. accuracy trade-off. This has been studied extensively across the collective intelligence literature from insect swarms to swarm robotics[5, 47, 80]. In the context of evidence neighbourhoods, we can consider the impact of different levels of evidential imprecision on time to convergence. We define convergence as all agents reaching a consensus on a singleton belief, i.e. all agents agree that the singleton belief represents the true state of the world s^*. Figure 3.18 shows the time steps to consensus for different Hamming threshold values and error rates, with lighter colours indicating less convergence time steps. A maximum limit of 20000 time steps is set for each simulation, i.e. this will be used as the convergence time for any simulation run that fails to convergence within 20000 time steps to get the average value. It is significant to note that the system exhibits increased robustness to varying evidence rates and error rates when the fusion rate is low, as demonstrated in Figure 3.16. However, a trade-off exists, as

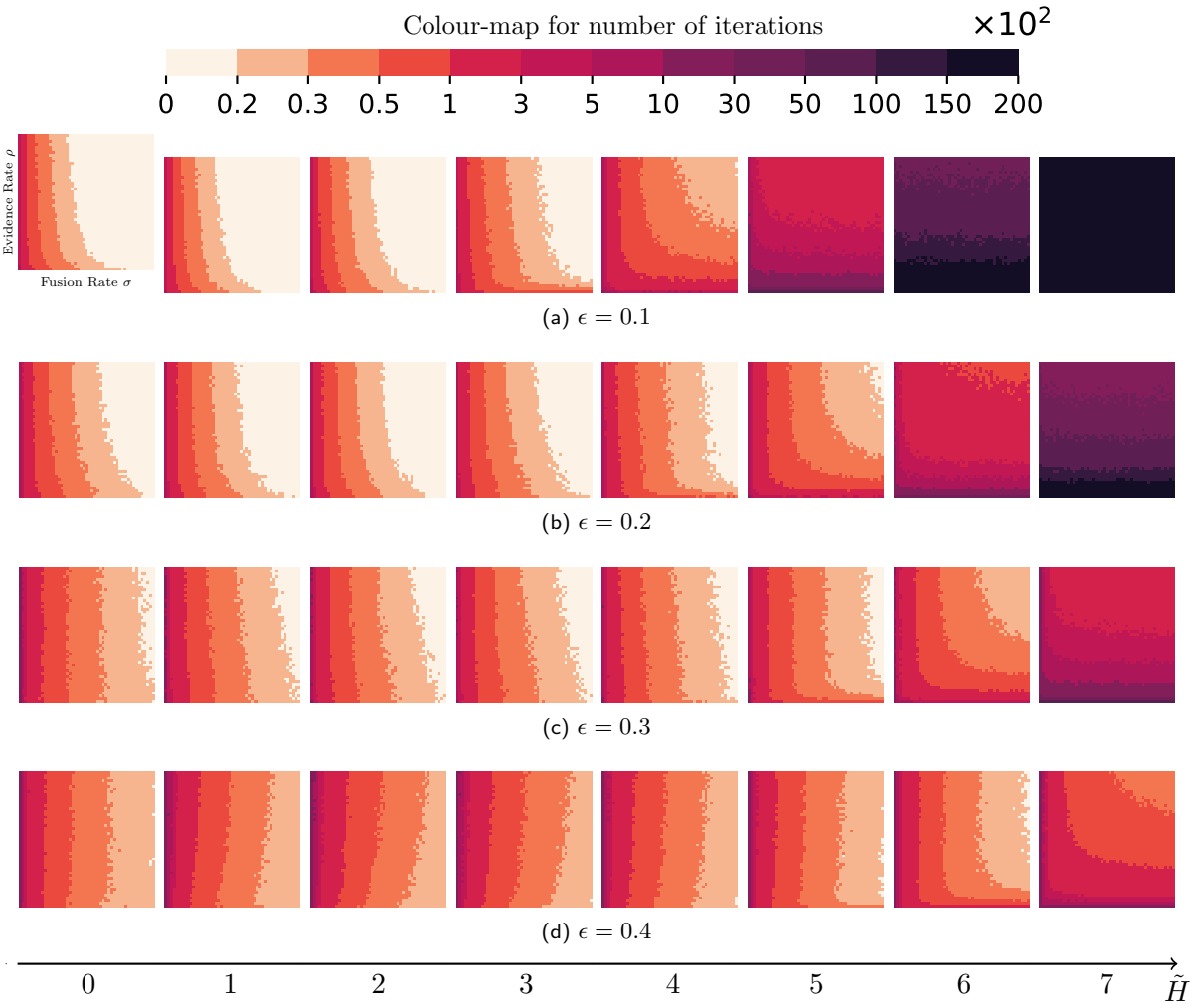

Figure 3.18: Average number of time steps until convergence τ at steady state for different evidence imprecision defined by various Hamming thresholds $\tilde{H}$ and error rate $\epsilon \in \{0.1, 0.2, 0.3, 0.4\}$, From left to right: $\tilde{H} \in \{0, ..., 7\}$. In each heat map, the y-axis and x-axis respectively represent $\rho \in [0.02, 1)$ and $\sigma \in [0.02, 1)$, The axis labels for the heat maps are provided in the top left cell as an example. The number of time steps to reach consensus is primarily determined by the fusion rate, except when the evidence rate is low or evidential updating is notably imprecise. For thresholds aimed at higher learning accuracy, the speed of reaching consensus is compromised compared to standard precise updating.

lower fusion rates requires a greater number of time steps for agents to achieve consensus, as shown in Figure 3.18. For example, for $\tilde{H} = 2$, comparing Figure 3.16c to Figure 3.18c, for low fusion rates ($\sigma \in (0, 0.1)$), agents reach consensus after 100 to 300 time steps with an accuracy close to 1, even for very low evidence rates. Whereas for low evidence rates and the highest fusion rates $\sigma \in (0.9, 1)$, the average accuracy is much lower (around 0.8) but a consensus is reached within just 20 time steps.

From Figure 3.18 we also see that the system exhibits slower convergence with increasing error rates when $\tilde{H} \leqslant 3$, whereas convergence accelerates with higher error rates when $\tilde{H} \geqslant 6$. For $\tilde{H} \in \{4, 5\}$, the most rapid convergence is observed at medium error rates, specifically when $\epsilon = 0.2$ for $\tilde{H} = 4$ and $\epsilon = 0.3$ for $\tilde{H} = 5$. One possible explanation for this phenomenon is that, under conditions of highly imprecise evidence and low error rates, agents are more likely to receive similar imprecise evidence at different time steps. Consequently, their beliefs remain imprecise following the fusion process. As a result, a greater number of time steps are required to accumulate sufficient variation through errors, which in turn drives the cardinality down and facilitates convergence. This insight highlights the intricate relationship between error rates, evidence imprecision, and system dynamics in the context of social learning models.

The heat maps presented suggest that the convergence speed is primarily influenced by the fusion rate under conditions of low to intermediate evidence imprecision and high error rates. In contrast, the impact of evidence becomes more significant when the error rate is low and the degree of evidence imprecision is high. For example, in Figure 3.18c, when $\tilde{H} < 6$, the speed of learning is mainly related to the fusion rate σ, i.e., the learning speed is slower for lower fusion rates. For $\tilde{H} \geqslant 6$, a high evidence rate ρ would also speed the convergence up. In addition, for a higher error rate, evidence rate ρ start to influence the convergence speed from a lower $\tilde{H}$, i.e., less imprecise evidence. For instance, in Figure 3.18a, the evidence rate starts to have a significant influence from $\tilde{H} = 4$ and for higher levels of evidential imprecision, the evidence rate has a much greater influence than the fusion rate. This underscores the need for a balanced approach to optimizing both fusion and evidence rates, particularly as the nature and degree of imprecision and error in evidence vary.

These heat maps also suggest that increasing evidential imprecision to a limited extent does not necessarily slow learning. For example, in Figure 3.18c, the agents reach consensus within 100 time steps for most evidence and fusion rate combinations for $\tilde{H} \leqslant 6$. Furthermore, the threshold values which result in highest accuracy do not slow convergence and sometimes faster than that of other thresholds. For example, in Figures 3.16b and 3.18b, both the highest overall accuracy and the fastest convergence is obtained when $\tilde{H} = 1$ or $\tilde{H} = 2$. In summary, certain levels of imprecision not only yield higher overall accuracy but also facilitate faster convergence, highlighting the potential benefits of incorporating hamming neighbourhood imprecisision to evidence for the social learning models.

3.5 Imprecision and robustness in social learning

Robustness to variation in underlying conditions is important in this social learning context since environments are often dynamic and our knowledge of them is usually limited. For example, evidence and fusion rates may be varying and difficult to predict in advance, since different factors may influence agents' capacity to collect evidence or interact with each other during the

learning process. In order to evaluate the influence of different levels of evidential imprecision on the robustness to different evidence and fusion rates, we can use aspects of info-gap theory proposed by [81]. Info-gap theory provides theoretical tools to aid decision making under severe uncertainty, by analyzing robustness to variation around a set of estimated parameter values representing the best available knowledge of the underlying conditions of the system. We apply the info-gap theory to evaluate the robustness of different levels of Hamming thresholds $\tilde{H}$ to the variation in the fusion and evidence rate, σ and ρ.

Suppose we have estimates of the evidence and fusion rates for a given social learning problem, denoted by $\hat{\rho}$ and $\hat{\sigma}$, respectively. Let $U(h)$ denote a neighbour of $(\hat{\sigma}, \hat{\rho})$ in the parameter space of size h. This is referred to in info-gap theory as an horizon of uncertainty.

$$U(h) = \{(\sigma, \rho) \in (0,1)^2 : |\sigma - \hat{\sigma}| \leqslant h, |\rho - \hat{\rho}| \leqslant h\} \tag{3.9}$$

The robustness at $(\hat{\sigma}, \hat{\rho})$ is then defined as the size of the largest horizon of uncertainty for which the average learning error $1 - \alpha$ is guaranteed to not exceed a critical maximum value δ. For different values of δ we then have the following robustness function:

$$\hat{h}(\delta) = \max\{h : m(h) \leqslant \delta\} \tag{3.10}$$

where $m(h) = \max\{|1 - \alpha(\sigma, \rho)| : (\sigma, \rho) \in U(h)\}$ is the maximum error across all parameter values in the horizon of uncertainty of size h.

Figure 3.19 illustrates the application of info-gap theory to the current context. Suppose that $\hat{\sigma}$ and $\hat{\rho}$ are at the centre of the parameter space i.e. $\hat{\sigma} = \hat{\rho} = 0.5$. Let $\hat{h}_1$ and $\hat{h}_2$ be robustness functions for two different algorithms. Then if $\hat{h}_1(\delta) \geqslant \hat{h}_2(\delta)$ for all δ we say that algorithm 1 robust dominates algorithm 2 at parameter estimates $\hat{sigma}$ and $\hat{\rho}$. In other words, for every tolerance level δ there is a larger neighbourhood of $(\hat{\sigma}, \hat{\rho})$ for which the error tolerance constraint is guaranteed to be met for algorithm 1 than there is for algorithm 2. This is a clear indication that under these conditions the performance of algorithm 1 is more robust to variation in fusion and evidence rates than algorithm 2 for all tolerance levels. On the other hand, if the robustness curves $\hat{h}_1$ and $\hat{h}_2$ cross then this suggests that there are some levels of tolerance at which algorithm 1 is more robust and some at which algorithm 2 is.

To better understand how varying levels of evidential imprecision interact with environments of different levels of evidential inaccuracy, we investigate the robustness of our imprecise evidence model at different error rates. In Figure 3.20, we show the robustness curves, denoted as $\hat{h}(\delta)$ for various Hamming thresholds $\tilde{H} \in \{0, 1, 2, 3, 7\}$ and different error rates $\epsilon \in \{0.1, 0.2, 0.3, 0.4\}$, under the assumption that $(\hat{\sigma}, \hat{\rho}) = (0.5, 0.5)$. In Figure 3.20a, the robustness curves for $\tilde{H} = 0$ and $\tilde{H} = 1$ (represented by the yellow and orange lines) are generally greater than those for other greater Hamming thresholds $\tilde{H}$, except when the error tolerance $\delta \in (0.06, 0.08)$. In this

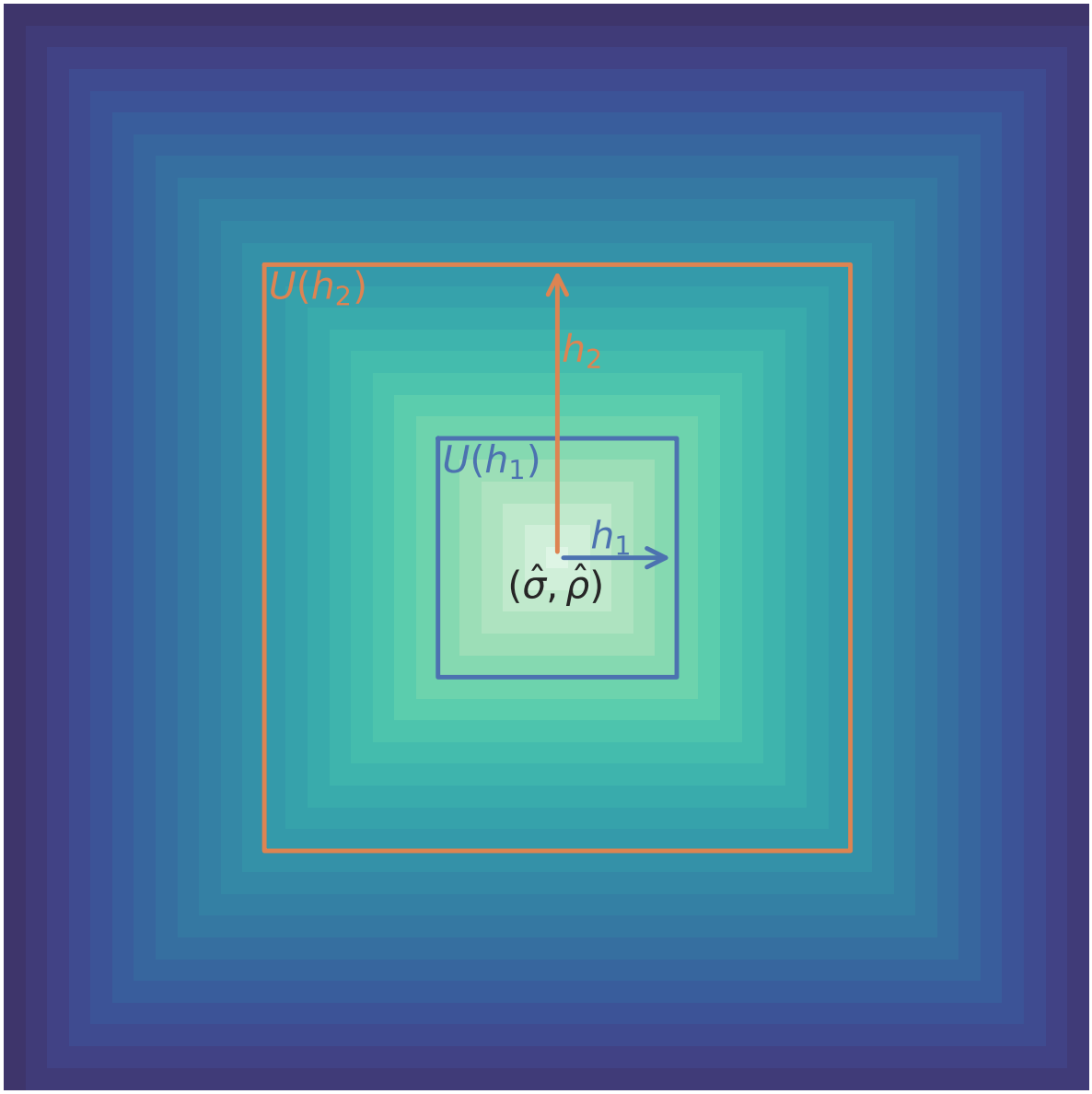

Figure 3.19: Diagram showing the horizon of uncertainty in Info-Gap Theory as a neighbourhood of the estimated fusion and evidence rates $(\hat{\sigma}, \hat{\rho})$.

specific range, curves for higher levels of evidential imprecision marginally exceed the curve for $\tilde{H} = 0$. For a specific tolerance of error $\delta = 0$, the system remains robust for $\tilde{H} = 0$ and $\tilde{H} = 1$, within the evidence and fusion rate ranges of $(0.5 - 0.35, 0.5 + 0.35)^2$ and $(0.5 - 0.36, 0.5 + 0.36)^2$, respectively. On the other hand, for higher thresholds $\tilde{H} = 2$ and $\tilde{H} = 2$, the level of system's robustness is significantly lower for low level of tolerance $\delta < 0.05$. Moreover, for higher levels of imprecise evidence, such as $\tilde{H} = 3$ and $\tilde{H} = 7$, the system is not robust to low error tolerance, $\delta < 0.02$, at all. In summary, for a low error rate $\epsilon = 0.1$, applying a Hamming neighbourhood to the evidence does not significantly enhance the system's robustness and therefore this form

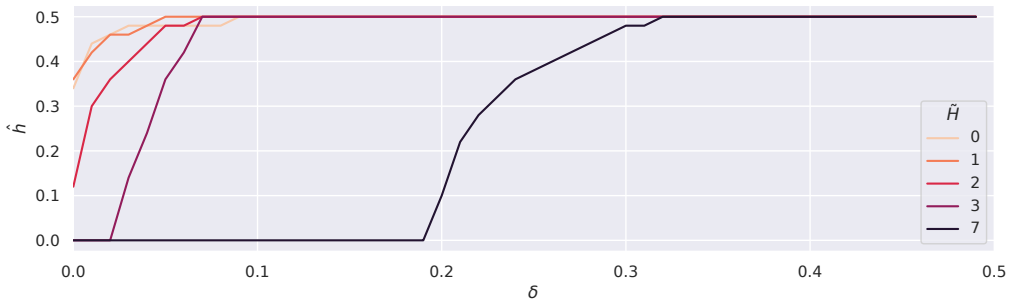

(a) $\epsilon = 0.1$

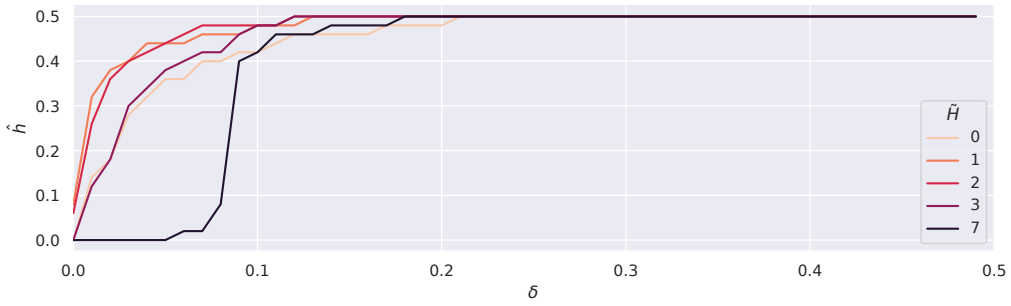

(b) $\epsilon = 0.2$

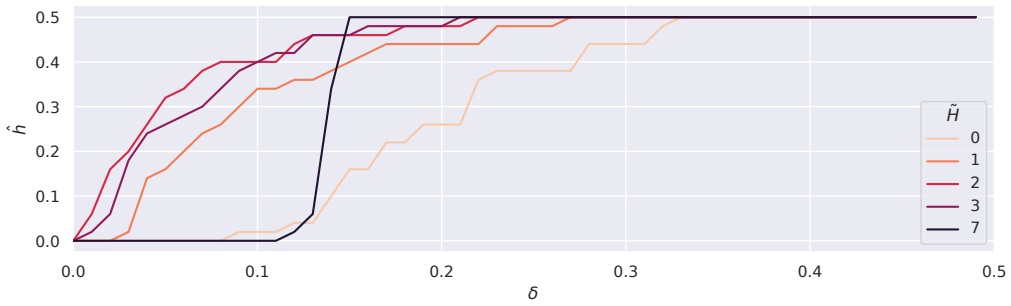

(c) $\epsilon = 0.3$

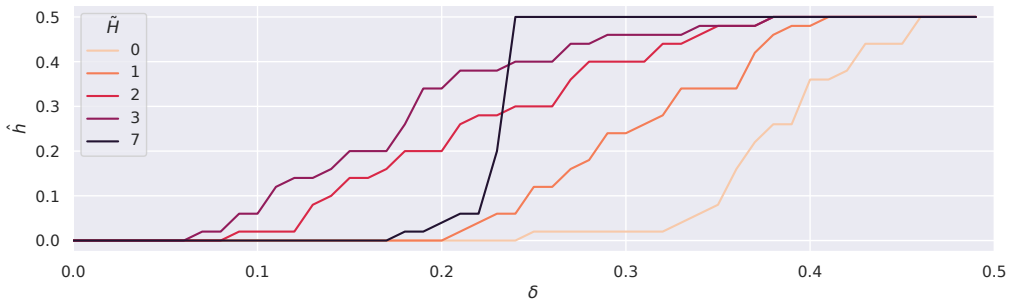

(d) $\epsilon = 0.4$

Figure 3.20: Robustness curves for various evidence imprecision levels, $\hat{\rho} = 0.5, \hat{\sigma} = 0.5$, and different error rates: (a) $\epsilon = 0.1$; (b) $\epsilon = 0.2$; (c) $\epsilon = 0.3$; (d) $\epsilon = 0.4$. The optimal imprecision for maximal robustness varies by error rate and tolerance — higher error rates/ tolerance require increased imprecision.

of imprecise evidence negatively impacts the system's ability to adapt to variations in both evidence and fusion rates.

For higher error rates $\epsilon \in \{0.2, 0.3, 0.4\}$, we see more significant advantage of applying imprecise evidential updating. From Figures 3.20b to 3.20d the robustness curves for $\tilde{H} = 1$(orange lines), $\tilde{H} = 2$(red lines), and $\tilde{H} = 3$ (purple lines) are everywhere greater than the curve for $\tilde{H} = 0$. This indicates that these moderate levels of imprecise evidence is more robust for all tolerance levels δ than the most precise evidence (when the Hamming threshold is not applied). We also observe a trend indicating that the system should employ higher levels of evidential imprecision to achieve greater robustness for higher error rates for low levels of error tolerance. Specifically, within the range of $\delta \in [0, 0.1]$, the greatest robustness is achieved by a threshold value of $\tilde{H} = 1$ or $\tilde{H} = 2$ for $\epsilon = 0.2$, by a threshold of $\tilde{H} = 2$ for a higher error rate $\epsilon = 0.3$, and by a threshold of $\tilde{H} = 3$ for a even higher error rate $\epsilon = 0.4$. In summary, our findings indicate that imprecise evidential updating contributes to enhanced robustness in social learning models in noisy environments.

Our findings also suggest the most imprecise evidence($\tilde{H} = 7$) can sometimes be the optimal level for robust system performance, as tolerance to error increase. In Figure 3.20b where the error rate is $\epsilon = 0.2$ the robustness curve for the high imprecision level of $\tilde{H} = 7$ is dominated by the robustness curves for $\tilde{H} \in \{1, 2, 3\}$ showing that it is the least robust model of these imprecise evidence models. On the other hand, it crosses the curve for $\tilde{H} = 0$ at $\delta = 0.1$ showing that it is slightly more robust than the most precise evidence model if the tolerance to error is higher than 0.1. However, in Figure 3.20c showing the higher error rate $\epsilon = 0.3$, the robustness curve for $\tilde{H} = 7$ crosses all other robustness curves so that there is a small range of higher tolerance values for which it is the most robust imprecise evidence model. Similarly, at an even higher error rate of $\epsilon = 0.4$ as shown in Figure 3.20d, the robustness curve for $\tilde{H} = 7$ not only intersects those for $\tilde{H} = 2$ and $\tilde{H} = 3$ but also surpasses the curve for $\tilde{H} = 1$, making it the most robust model for handling imprecise evidence in a range of error tolerance level. In other words, in these cases the highly imprecise model is more robust than other more precise evidential models if the tolerance to error is relatively high. Overall, this suggests that in noisy environments the level of error that is acceptable will play a role in deciding which level of evidential imprecision is most robust.

3.6 Conclusions

In this chapter we have emphasised the difference between imprecision and error (inaccuracy). The former in our set-based model can be modelled directly by the cardinality of the evidence sets while the latter describes the difference between the evidence gathered and the true state of the world s^* and can be modelled by a probabilistic parameter, the error rate ϵ.

The simulation results of the proposed set-based model have suggested that social learning

is robust to different levels of imprecise evidence. Furthermore, we have also suggested a multi-robot location classification type problem with smaller population size, in which the imprecision of evidence gathered by the robots may vary because of hardware or environment constraints. We then introduced a novel parameter N_u to limit the maximum number of locations that the robots can visit in an evidence collection episode, thereby changing the precision of the evidence. Using robot simulations described in Section 3.3.2, we found that in both moderately noisy scenarios and highly noisy scenarios ($\epsilon = 0.2$ and $\epsilon = 0.3$), our model was shown to be robust to noisy evidence, achieving an accuracy above that of the theoretical error for all upper-bound limits N_u. Under our model, we have shown that the robots' average accuracy is robust to different levels of imprecise evidence while there is a slight decrease at the most imprecise evidence scenario($N_u = 1$). We have also found that increasing the number of robots can decrease the variation of the system's average accuracy at different levels of imprecise evidence. The results of our robot simulation experiments show that our approach has strong potential to be applied to location classification tasks conducted by multi-robot systems.

The most significant advantage of the proposed approach is that it scales with scenarios in which the number of locations is greater than the number of robots(i.e. $k < n$). Moreover, in our approach each robot does not have to investigate every location for the system to reach consensus. there can be good performance in scenarios in which access to some locations is restricted, either by the range of the robots (e.g., due to power constraints) or a heterogeneous system possessing different levels of access or capabilities. One limitation of the proposed approach is that both the number and positions of the locations need to be known by the robots ahead of time. This is not a significant drawback for many tasks in which the environment is well-known or highly controlled, for example, search and rescue missions in mapped environments or warehouse robotics. Future work includes the ability to adapt to unseen or dynamic environments in which the robots discover the existence of new locations in an online manner. Another possible direction is to explore the effects of malfunctioning robots in the system.

For a certain type of imprecise evidence, where agents obtain an estimate of the true state of the world and then take a neighbourhood of that estimate, there can actually be benefits of imprecise evidence. The results showed that the overall best accuracy and fastest convergence speed can be obtained with an intermediate level of precision depending on the error rate. Furthermore, certain levels of imprecision can enable more robustness to variations in fusion and evidence rate than can be obtained from a precise evidence model. Indeed in high error scenarios there are even some levels of tolerance at which the most imprecise evidential model is also the most robust. Our probability model have showed that the proposed neighbourhood imprecise evidence model can increase the difference between the probability of s^* being included in the evidence sets and that of the distract states, which supports that this type of imprecise evidence can improve the system's accuracy.

In light of previous work on imprecise fusion described in Chapter 2, we intend to investigate

whether there are advantages in combining imprecision in both the fusion and evidential updating processes in Chapter 4. A best-of-n problem was explored in [12] using e-Pucks in a similar robotic setup. It would be intriguing to apply the probabilistic belief model to the location classification problem to further compare the effectiveness of different belief models. For example, a state of world can be associated with a probability of its being the true state of the world s^*. Agent's belief can then be represented as the probability distribution of s^*. Other types of belief models are also worth studying to further investigate the benefits of imprecision. For instance, for a probability-based belief model, an imprecise probability model, such as interval probabilities and upper and lower probabilities, can be applied to assess the impact of varying levels of evidential imprecision. Another avenue of future research will be to add communication constraints to the model, such as network connectivity or physical distance range. There are recent studies showing that limited connectivity can improve the performance of social learning [38] and that constrained communication of multi-agent systems can be more robust to the environment changes [8].

Chapter 4

Combining Imprecise Evidence and Fusion

In Chapter 3, we introduced a framework for representing evidence with varying levels of imprecision. We then employed both agent-based and robotic simulations to investigate social learning in the context of imprecise evidence. This demonstrated our model's robustness to imprecise evidence and its potential applicability in multi-robot systems. Subsequently, we introduced a Hamming neighbourhood approach to investigate the potential benefits of intentionally adding imprecision to the evidence. Our findings indicated that a low to medium level of evidence imprecision could improve the overall accuracy of social learning, depending on different levels of error rates, without compromising the speed of reaching consensus.

We have observed that incorporating imprecision in fusion or evidential updating can independently enhance the overall accuracy of social learning. In this chapter, we aim to provide a comprehensive analysis of a combined model by integrating the Jaccard operator (eq. (2.2)) into the Hamming neighbourhood model, in order to investigate the potential benefits of implementing imprecision in both processes simultaneously, potentially leading to a more effective and robust model. In this chapter, we present agent-based simulation experiments to investigate a version of our model with imprecision in both evidential and fusion processes. In order to thoroughly assess the model's performance, we consider various combinations of evidence (ρ) and fusion (σ) rates and distinct Hamming ($\tilde{H}$) and Jaccard (γ) thresholds.

We evaluate the model using the accuracy and robustness measures described in Chapter 3. It is important to note that the population may not converge to a shared singleton belief when γ is high, see Figure 2.10. To address this potential issue and further refine our understanding of the model, we also explore the cardinality of the agents' beliefs. Building on the findings in Chapter 2, which showed improved social learning accuracy with a low evidence rate using imprecise fusion, we hypothesise that combining this approach with an imprecise evidential updating strategy can further enhance accuracy when the evidence rates is low. This integrative framework aims to offer a comprehensive understanding of the dynamics involved in social

learning, particularly in terms of handling imprecise evidence and belief fusion.

4.1 Related Work

In this chapter, we introduce an integrated approach that combines the imprecise fusion models discussed in Chapter 2 and imprecise evidential updating in Chapter 3. As such, all the scholarly work cited in Section 2.1 and Section 3.1 continues to hold relevance and offers pertinent connections to the research proposed in this chapter.

4.2 Model

As in Chapter 2 and Chapter 3, we assume that the environment being learnt about can be described by a finite set of propositions $\mathcal{P} = \{p_1, ..., p_n\}$. A state s is a function $s : \mathcal{P} \to \{0, 1\}^n$. For notational convenience we represent a state s by the n-tuple $\langle s(p_1), \ldots, s(p_n)\rangle$. Uncertain beliefs are subsets of $\mathbb{S}$ with cardinality $|B| > 1$, while a singleton belief $B = \{s\}$ represents that an agent is certain that s is the true state.

As in Section 3.4, we assume the evidence collected by the agents precisely identifies a possible true state s_e, i.e., $s_e \in \mathbb{S}$ and $\mathrm{E} = \{s_e\}$. Error rate ϵ is also modelled the same way, agents receive $s_e(p_i) = s^*(p_i)$ with probability $1 - \epsilon$ and $s_e(p_i) = 1 - s^*(p_i)$ with probability ϵ for $i = 1, \ldots, n$. Agents will update their belief based on Equation (2.6) and Equation (3.4) as follows:

$$B|\,\mathrm{E} = \begin{cases} B \cap \mathrm{E}(s_e, \tilde{H}) : B \cap \mathrm{E}(s_e, \tilde{H}) \neq \emptyset \\ B : \textit{otherwise} \end{cases} \tag{4.1}$$

Agents fuse their belief pairwisely using Equation (2.2) as follows:

$$B_1 \odot_\gamma B_2 = \begin{cases} B_1 \cap B_2 & : \quad J(B_1, B_2) > \gamma \\ B_1 \cup B_2 & : \quad J(B_1, B_2) \leqslant \gamma \end{cases} \tag{4.2}$$

4.3 Agent-based Simulation Results

In this section, we present the results of the agent-based simulation results exploring the coherence of imprecise evidence, parameterised as $\tilde{H} \in [0, 7]$ and imprecise fusion, parameterised as $\gamma \in [0, 1]$. We conduct experiments exploring all eight possible $\tilde{H}$ values, as outlined in Chapter 3, and nine γ values, specifically $\gamma \in \{0, \frac{1}{8}, \frac{2}{8}, \ldots, 1\}$. There are 19949 potential γ values when considering a language size of $n = 8$ and hence an exhaustive sweep of parameter space as in Chapter 2 will not be possible. We explore various evidence rates and fusion rates in

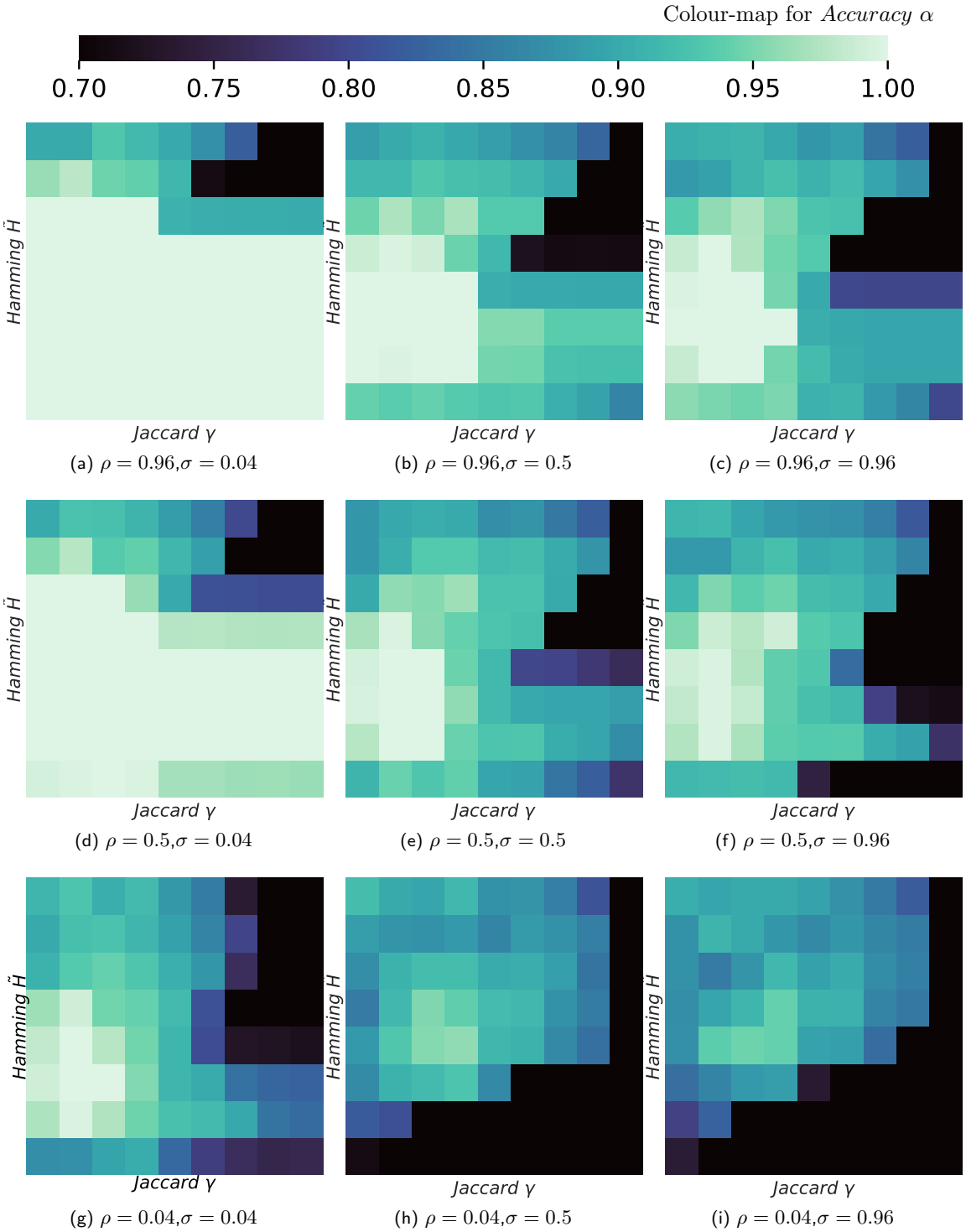

(a) $\rho = 0.96, \sigma = 0.04$ (b) $\rho = 0.96, \sigma = 0.5$ (c) $\rho = 0.96, \sigma = 0.96$

(d) $\rho = 0.5, \sigma = 0.04$ (e) $\rho = 0.5, \sigma = 0.5$ (f) $\rho = 0.5, \sigma = 0.96$

(g) $\rho = 0.04, \sigma = 0.04$ (h) $\rho = 0.04, \sigma = 0.5$ (i) $\rho = 0.04, \sigma = 0.96$

Figure 4.1: Average accuracy after 20000 iterations for $\tilde{H} \in \{0, \ldots, 7\}$ and $\gamma \in [0, 1]$, and various combinations of evidence and fusion rates. System robustness to imprecision hinges on the balance between evidence and fusion rates, with high evidence and low fusion rates achieving higher accuracy, while lower evidence or higher fusion rates demand moderate imprecision for optimal accuracy.

the range $\rho, \sigma \in [0.02, 1)^2$. This allows us to explore a broad range of parameter combinations while maintaining a manageable scope for the experiments. Throughout all the experiments in this chapter, we maintain the following fixed parameters: a population size of $k = 100$, a language size of $n = 8$, and an error rate of $\epsilon = 0.3$. To account for random variation, each combination of parameters is evaluated over 50 simulation runs. Additionally, a cap of 20000 time steps is set for each simulation run to ensure a reasonable time frame.

In Figure 4.1 we show the average accuracy for different combinations of Hamming thresholds $\tilde{H}$ and Jaccard thresholds γ, for various evidence and fusion rates. Each cell of the heat map display the average accuracy as defined by Equation (3.1). Lighter and darker colours indicate higher and lower accuracy, respectively. We see from Figure 4.1a that a low fusion rate and a high evidence rate can still be robust to the different levels of imprecision except when both evidence and fusion are highly imprecise ($\tilde{H} \geqslant 5$ and $\gamma \geqslant 0.5$). In other words, when the fusion rate is low and the evidence rate is high, neither imprecise evidential updating nor imprecise fusion are essential for improving learning accuracy. For lower evidence rates and higher fusion rates, the system is less robust to different combinations of $\tilde{H}$ and γ, i.e. fewer levels of evidential imprecision $\tilde{H}$ and fusion imprecision γ yield high accuracy. In these scenarios, a moderate level of both evidential and fusion imprecision tends to produce the best results. For example, in Figure 4.1g we see the best accuracy is obtained when $\gamma = \frac{1}{8}$ and $\tilde{H} = 2$ for a low evidence rate and a low fusion rate ($\rho = \sigma = 0.04$). In summary, the relationship between evidence and fusion rates directly impacts the system's robustness to different levels of imprecision in both evidence and fusion. Systems with high evidence rates and low fusion rates are generally more robust to imprecision, except in cases where both are extremely imprecise. On the other hand, systems with low evidence rates and high fusion rates are less robust of variations in evidential and fusion imprecision and in these cases a low to moderate level of imprecision of both evidential updating and belief fusion is required to achieve the highest accuracy.

To better understand how combined imprecision affects accuracy across varying evidence and fusion rates, we show Figure 4.2. This nested heat map shows the average accuracy for experiments conducted with various levels of imprecise evidence and imprecise fusion operators, as well as for different evidence rate $\rho \in [0.02, 1)$ and fusion rate $\sigma \in [0.02, 1)$. The child heat maps, contained within each cell of the parent heat map, display the average accuracy. Lighter and darker colours indicate higher and lower accuracy, respectively. For every $\tilde{H}$, the highest overall accuracy are achieved when $\gamma = 0.125$ among all fusion thresholds investigated and for $\gamma > 0.125$, the overall accuracy monotonically decreases as more imprecise fusion operator are applied.

In situations where more imprecise fusion operators are applied, the population does not always converge with an accuracy higher than $1 - \epsilon$ for certain combinations of evidence rate and fusion rate. Lower accuracy is visually represented by the dark areas in Figure 4.2. As the degree of imprecision in fusion increases, there are more combinations of evidence and

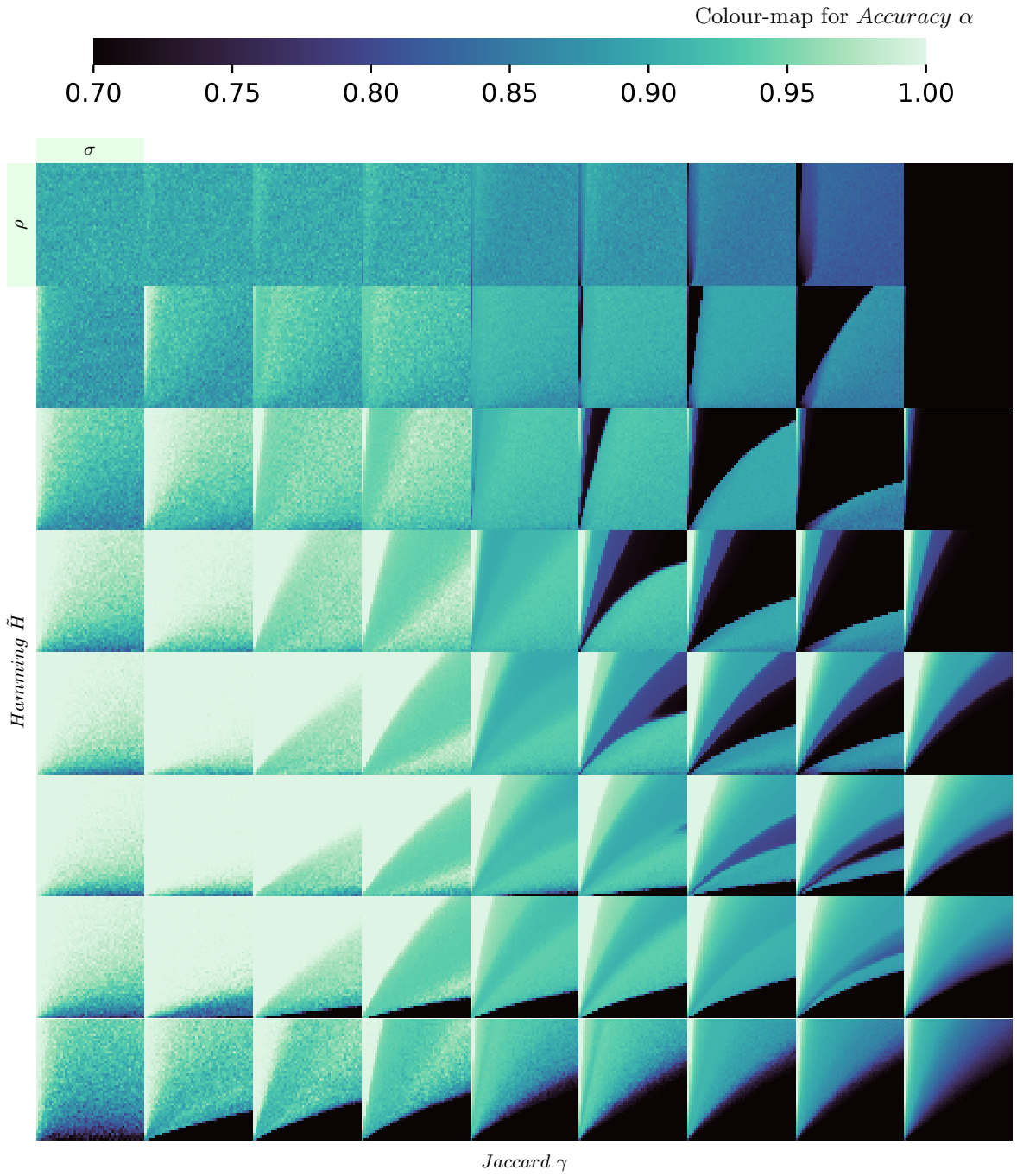

Figure 4.2: Average accuracy α at steady state for different evidence imprecision for $\epsilon = 0.3$. In each cell, the y-axis and x-axis respectively represent $\rho \in [0.02, 1)$ and $\sigma \in [0.02, 1)$. The axis labels for the heat maps are provided in the top left cell as an example. Overall learning accuracy across different combinations of evidence and fusion rates peaks at moderate levels of evidential and fusion imprecision ($\tilde{H} = 2, \gamma = 0.125$).

fusion rates that lead to poor performance, i.e. the dark area indicating poor performance grows. For fusion imprecision levels ranging from low to intermediate (i.e., γ in the interval $(0, 0.5]$), the application of imprecise evidential updating eliminates the poor performance. With more imprecise fusion operators, the size of the dark areas decreases for evidential updating thresholds upto $\tilde{H} = 2$. However, as the system employs more imprecise evidence updating, the dark areas progressively grow in size.

The location of the dark areas is also significantly influenced by the level of evidential imprecision. When the threshold for evidential updating, denoted as $\tilde{H}$, is low, the system accuracy is below $1 - \epsilon$ if the evidence rate is relatively lower than the fusion rate. In scenarios where both evidential updating and fusion are moderately imprecise, the system's performance is poor when the evidence rate and fusion rate are approximately equivalent. Conversely, in situations with significant imprecision in evidential updating, the system's performance deteriorates when the evidence rate is relatively high in comparison to the fusion rate, especially if the fusion process is also highly imprecise. When the fusion exhibits maximal imprecision, the population does not reach an accuracy over benchmark $(1 - \epsilon)$ for any pairs of evidence rate (ρ) and fusion rate (σ).

Consistent with the results using the standard fusion operator(i.e. $\gamma = 0$), the best performance is obtained when the evidence is low to intermediate imprecise, i.e. $\tilde{H} = 2$ or $\tilde{H} = 3$ for low imprecise fusion operators, e.g. for the imprecise level $\gamma = 0.125$ that the best performance is obtained. For more imprecise fusion operators, the variation of accuracy over the parameter space of ρ against σ shows more complex pattern. For $\gamma \in \{0.25, 0.375, 0.5\}$, we see that for moderately imprecise evidential updating, the accuracy is lower when the evidence rate and fusion rate are more similar. For more imprecise evidential updating, we see the poor performance area shift to greater evidence rates and smaller fusion rates. Therefore, in these cases, the best evidential threshold in terms of accuracy is dependent on the combination of certain evidence and fusion rates. When the difference becomes more significant, the system's performance becomes more accurate and a clear boundary can be observed between the low and high accuracy areas. For even higher thresholds, $\gamma > 0.5$, we see more bands and clearer boundaries between those bands, with various levels of accuracy, including the dark areas mentioned before.

In summary, our results suggest that the interaction between the level of imprecision in evidential updating and fusion processes significantly affects the overall system accuracy. The best performance is often observed at low to moderate levels of fusion and evidential imprecision. For high levels of imprecision, the system becomes increasingly sensitive to the balance between evidence and fusion rates, and the optimal combinations for these rates may vary depending on the level of imprecision.

There are two potential causes for the observed low accuracy: either the population reaches an incorrect consensus, or the population fails to achieve a consensus on a singleton belief,

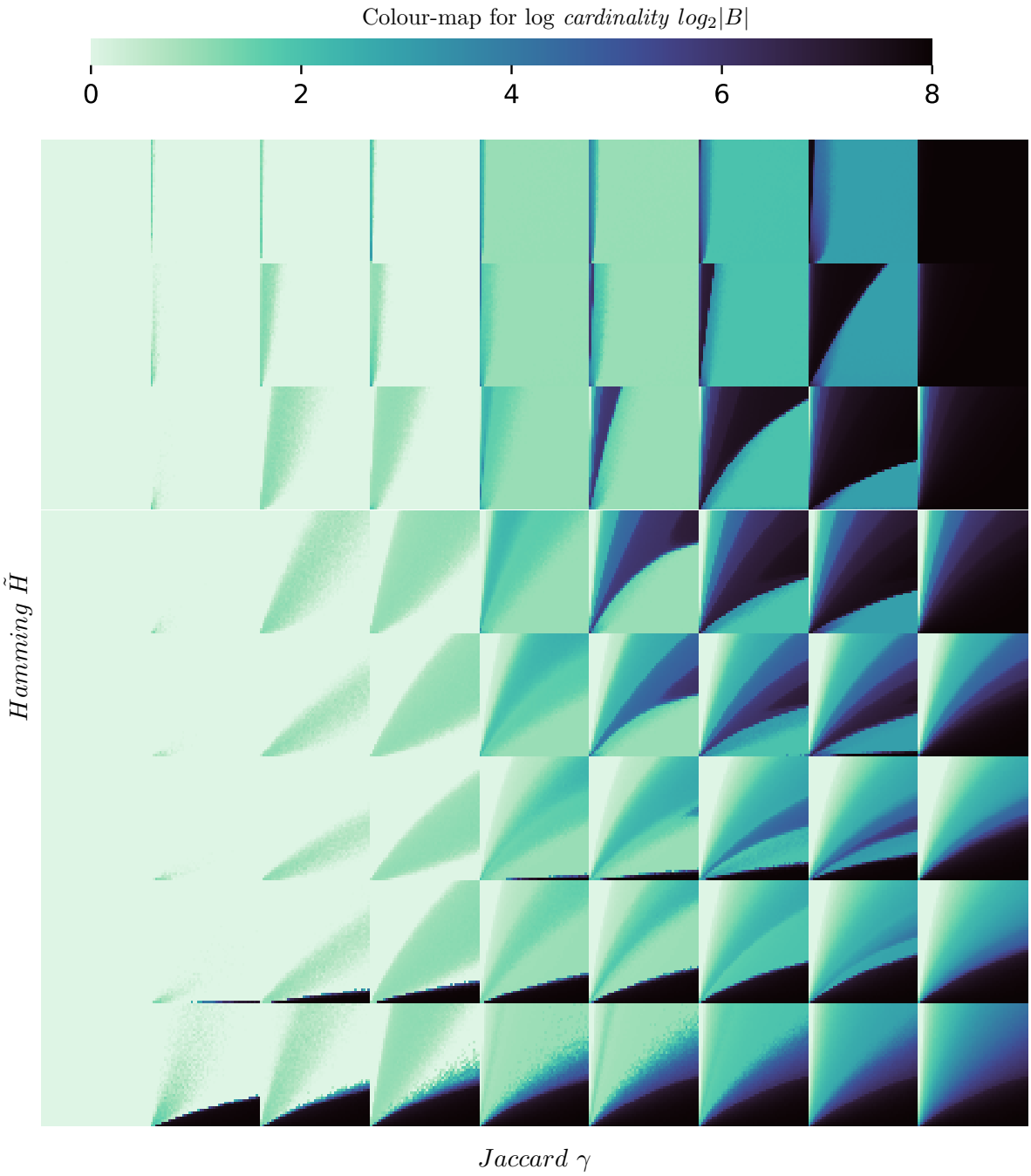

Figure 4.3: Average cardinality $|E|$ at steady state for different evidence imprecision for $\epsilon = 0.3$. In each cell, the y-axis and x-axis respectively represent $\rho \in [0.02, 1)$ and $\sigma \in [0.02, 1)$. More imprecise fusion operators tend to produce more imprecise final beliefs, i.e. the population struggling to reach a singleton belief with higher levels of fusion imprecision unless σ is relatively low compared to ρ.

indicating that the agents' final beliefs remain imprecise. To identify the root cause of the diminished accuracy represented in Figure 4.2, we present Figure 4.3, which demonstrates the average cardinality (expressed in a logarithmic scale) of agents' beliefs in the population following $20,000$ iterations, across 50 independent simulations. Lighter colours indicate lower cardinalities, for example 0 indicates the singleton belief $|B| = 1$ while darker colours represents higher cardinalities and more imprecise beliefs.

From Figure 4.3, we see that generally more imprecise fusion operators result in more imprecise final beliefs. When the most precise operator(the first column) is used, the population reaches a consensus on a singleton belief for every evidential imprecision. For imprecise fusion operators ($\gamma > 0$), the population fails to converge to a singleton belief within 20000 iterations in some scenarios. The average cardinality of the agents' belief is generally smaller for more imprecise evidential updating when low to intermediate imprecise fusion operators are applied ($\gamma \in [0.125, 0.5]$), and is greater when more imprecise operators ($\gamma \in [0.625, 1]$)are used.

For $\gamma \in [0.125, 0.375]$, the average cardinality can vary depending on different combinations of evidence and fusion rates. when the evidence rate is low compared to the fusion rate, the population's average belief cardinality is close to 2^8(in black) for less imprecise evidential updating. The latter is the cardinality of an ignorant belief that the agents initially hold before learning. In other words, the population learns very little about the state of the world on these occasions. For more imprecise evidential updating, the system ends with much lower cardinalities for any combination of ρ and σ. For $\tilde{H} \in [2, 4]$ we see that the system does not converge when ρ and σ is closer to each other and converges to singleton otherwise. For higher evidential imprecision, we see that the system converges to a singleton belief when the fusion rate is high enough.

The specific combination of imprecise fusion operators and the thresholds for evidence updating and fusion may introduce constraints and biases that shape the system's behaviour. These constraints can create distinct regimes where the system's performance is influenced primarily by the interaction between the evidence rate and fusion rate, resulting in the emergence of separated areas with uniform cardinality. For example, for imprecise operators $\gamma \in (0.5, 1)$, we see that the system converges to a singleton belief with much less combination of ρ and σ. Similar to less imprecise operators, for more precise evidential updating, the system barely learns anything when the evidence rate is low compared to the fusion rate. In contrast, for more imprecise evidential updating($\tilde{H} \in [5, 7]$), the system ends with a cardinality close to 2^8 when evidence rate is relatively high compared to the fusion rate. For moderately imprecise evidential updating, the convergence behaviours become complicated. For example, when $\tilde{H} = 3, \gamma = \frac{5}{8}$, see Figure 4.4, there are several 'contour line' of cardinalities starting from the bottom left; $(\rho, \sigma) = (0.02, 0.02)$. Counterclockwise, we see cardinality in log scale around 1, 6, 4, 2, 0.5 and 0. Further investigation into the underlying mechanisms governing the fusion process, the nature of evidence updating, and the interplay between these factors could shed more light on

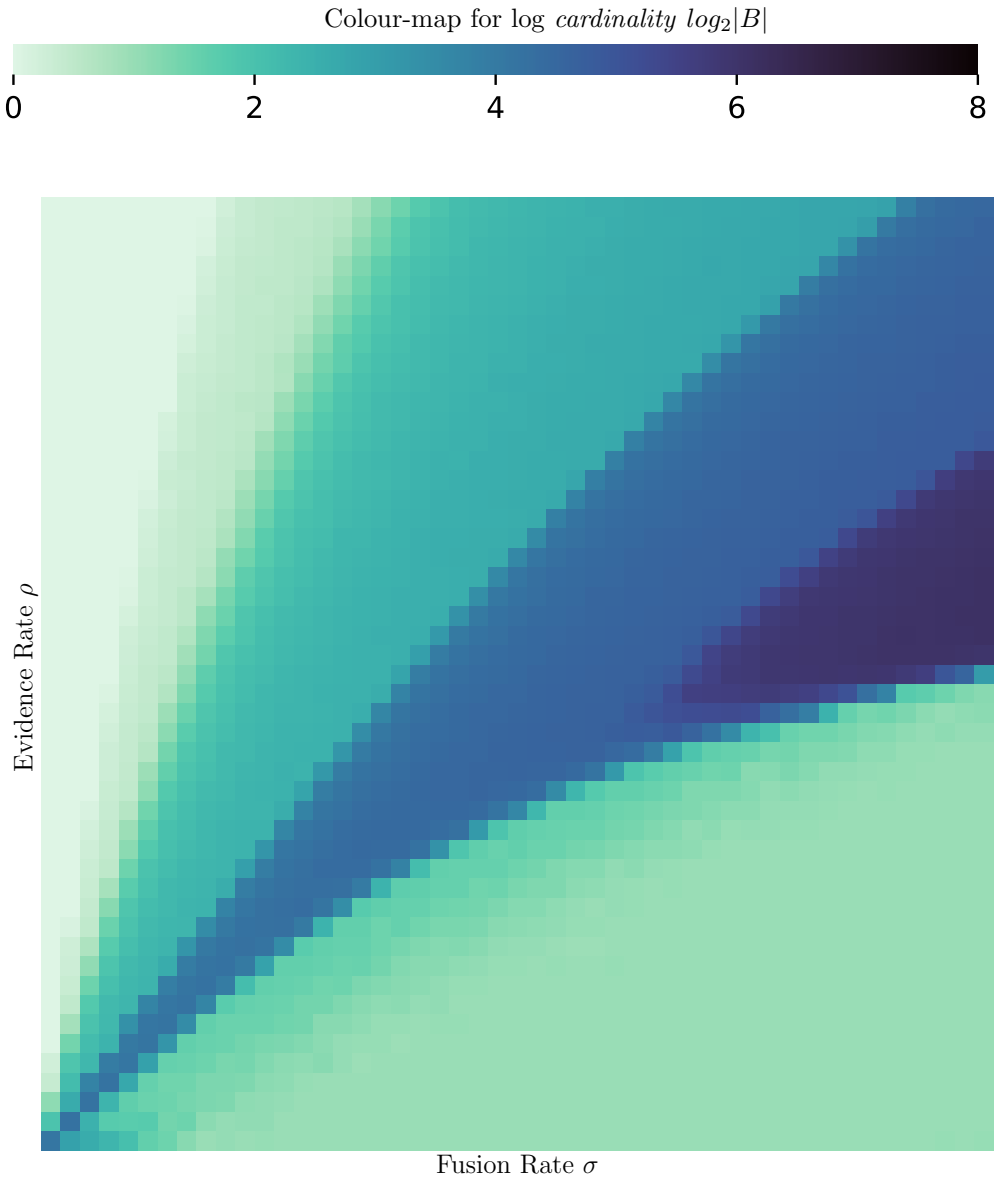

Figure 4.4: Average cardinality $|E|$ at steady state for different evidence imprecision for $\epsilon = 0.3$, $\sigma \in [0, 1)$, and $\rho \in (0, 1)$. The relative relationship between ρ and σ significantly influence the average cardinality of the population.

the precise reasons behind the observed pattern. Such research could contribute to a deeper understanding of the dynamics of imprecise fusion and its implications for decision-making systems.

Imprecise fusion also introduces the potential trade-off between the speed of learning and the accuracy of the learning outcome. To shed light on this trade-off, Figure 4.5 shows the average number of time steps required to achieve consensus across 50 independent simulations. Lighter colours here represents faster convergence and darker colours represents slower convergence.

In cases where the system fails to converge within 20000 time steps, we consider the number 20000 as the value for analysis purposes.

From Figure 4.5, it is evident that the model exhibits slower convergence when imprecise fusion operators are employed. When using the precise fusion operator, the model typically converges within 100 time steps, unless the most imprecise evidential updating ($\tilde{H} = 7$) is used or the fusion rate is significantly low. For the low imprecision fusion operators ($\gamma \in [0.125, 0.375]$), we see that the model converges faster with a higher fusion rate when highly imprecise evidential updating is applied. Conversely, for lower levels of evidential imprecision, the model converges faster when the fusion rate is relatively low compared to the evidence rate. When employing more imprecise fusion operators ($\gamma \geqslant 0.5$) and low levels of imprecise evidence, the model does not converge within 20000 time steps in most cases, unless the evidence rate is significantly higher than the fusion rate. Furthermore, in cases where both the evidential updating and belief fusion operator are highly imprecise, the model does not achieve convergence within 20000 time steps for any combination of evidence and fusion rates.

The speed-accuracy trade-off becomes apparent in cases where the precise fusion operator does not perform well in terms of accuracy, i.e. when the fusion rate is relatively higher than the evidence rate. Analysis of Figure 4.2 reveals that the best overall performance is achieved when using a fusion threshold of $\gamma = 0.125$ and evidential thresholds of $\tilde{H} \in \{2, 3\}$. However, Figure 4.5 demonstrates that for evidential thresholds of 2 or 3, the model requires more time steps to converge when using a fusion operator with a threshold of 0.125 compared to the precise fusion operator. Specifically, Figure 4.6 shows the average accuracy and time steps to convergence for $\gamma \in [0, 0.125, 0.25]$ and $\tilde{H} = 2$. From Figure 4.6c and Figure 4.6d we see that the system achieves higher accuracy when the fusion rate is high and the evidence rate is low with $\gamma = 0.125$ than with $\gamma = 0$, however, the model takes more time steps to achieve the higher accuracy, as shown in Figure 4.6a and Figure 4.6b. In other words, our results reveal a trade-off between the speed of convergence and the accuracy of the model when the fusion rate is high relative to the evidence rate, underscoring the need to carefully consider both accuracy and convergence speed in system optimisation in such scenarios.

In this section, we have shown the simulation results for various levels of imprecision of both evidence updating and belief fusion operators. The findings suggest that the optimal learning accuracy can be achieved by introducing a certain level of imprecision in both the evidence updating and belief fusion processes. It is important to note that convergence issues arise when highly imprecise fusion operators are applied, particularly in conjunction with higher levels of imprecise evidence. There exists a delicate balance between the level of imprecision and achieving accurate learning outcomes. In addition, the model exhibits slower convergence when employing imprecise fusion operators. The convergence behaviour is influenced by the specific combination of evidential updating and fusion rates, with various scenarios leading to slower or failed convergence within the given time frame of 20000 time steps. Therefore,

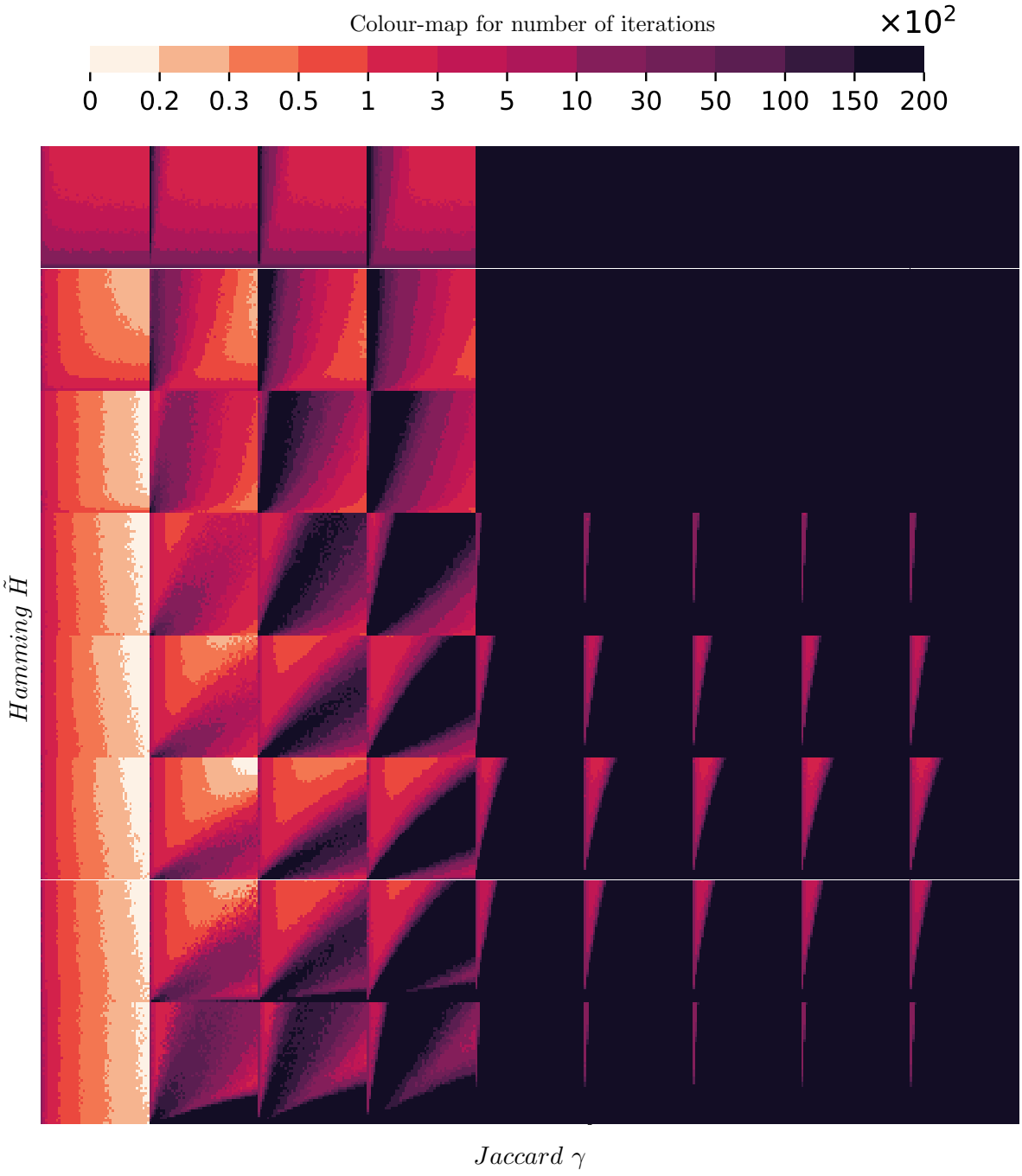

Figure 4.5: Average time steps to convergence α at steady state for different evidence imprecision for $\epsilon = 0.3$. In each cell, the y-axis and x-axis respectively represent $\rho \in [0.02, 1)$ and $\sigma \in [0.02, 1)$. Imprecise fusion requires more iterations to converge compared to standard precise fusion across all levels of evidential imprecision, indicating a trade-off between speed and accuracy.

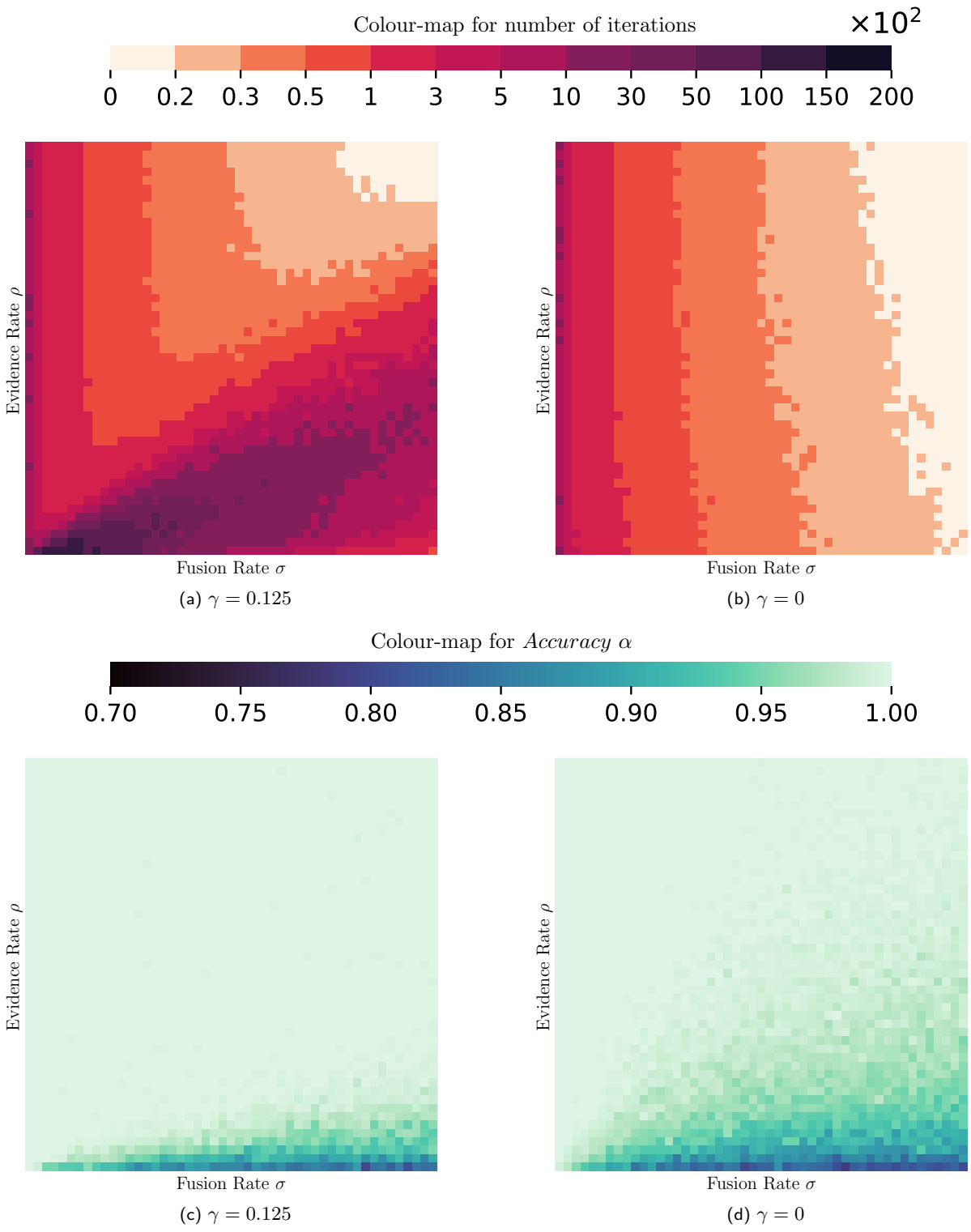

Figure 4.6: Average times steps to convergence and accuracy for $(\rho, \sigma) \in (0, 1)^2$, $\epsilon = 0.3$, and $\tilde{H} = 2$. Comparing imprecise and precise fusion, we see a speed-accuracy trade-off when σ is relatively high compared to the ρ

achieving this higher accuracy requires an imprecise fusion operator especially when the fusion rate is relatively high compared to the evidence rate but this increased accuracy comes at the cost of requiring more time steps to reach consensus. Hence, a careful consideration of the acceptable level of accuracy and the associated convergence time is crucial in the design and implementation of imprecise fusion mechanisms.

As discussed in Section 3.5, in real world applications of social learning, the evidence rate ρ and the fusion rate σ are both deeply uncertain and difficult to predict in advance, since the environments are often dynamic and agents' capacity to collect evidence and interact with each other can be influenced by many factors. To evaluate the robustness of the integrated model, we employ the info-gap theory again in Section 4.4.

4.4 Robustness of the Integrated Model

As discussed previously in Section 3.5, info-gap theory provides a useful framework for evaluation of robustness. In this section we use aspects of info-gap theory to further evaluate the impact of imprecise fusion operators and imprecise evidential updating on the robustness concerning variations in ρ and σ. We recall the formulation of our robustness model as follows:

Suppose we have estimates of the evidence and fusion rates for a given social learning problem, denoted by $\hat{\rho}$ and $\hat{\sigma}$, respectively. Let $U(h)$ denote a neighbour of $(\hat{\sigma}, \hat{\rho})$ in the parameter space of size h. This is referred to in info-gap theory as an horizon of uncertainty.

$$U(h) = \{(\sigma, \rho) \in (0,1)^2 : |\sigma - \hat{\sigma}| \leqslant h, |\rho - \hat{\rho}| \leqslant h\}$$

The robustness at $(\hat{\sigma}, \hat{\rho})$ is then defined as the size of the largest horizon of uncertainty for which the average learning error $1 - \alpha$ is guaranteed to not exceed a critical maximum value δ. For different values of δ we then have the following robustness function:

$$\hat{h}(\delta) = \max\{h : m(h) \leqslant \delta\}$$

where $m(h) = \max\{|1 - \alpha(\sigma, \rho)| : (\sigma, \rho) \in U(h)\}$ is the maximum error across all parameter values in the horizon of uncertainty of size h.

In Figure 4.7, we show application of info-gap theory to the integrated model for low to moderate levels of fusion imprecision $\gamma \in [0, 0.125, 0.25, 0.375]$ represented by the grey, blue, cyan, and orange lines, respectively. These robustness curves illustrate the system's robustness under different combinations of imprecision in the fusion and evidence updating processes. By examining the curves, we can gain insights into how changes in evidence and fusion imprecision affect the system's ability to maintain stable and accurate outcomes varying evidence and fusion rate.

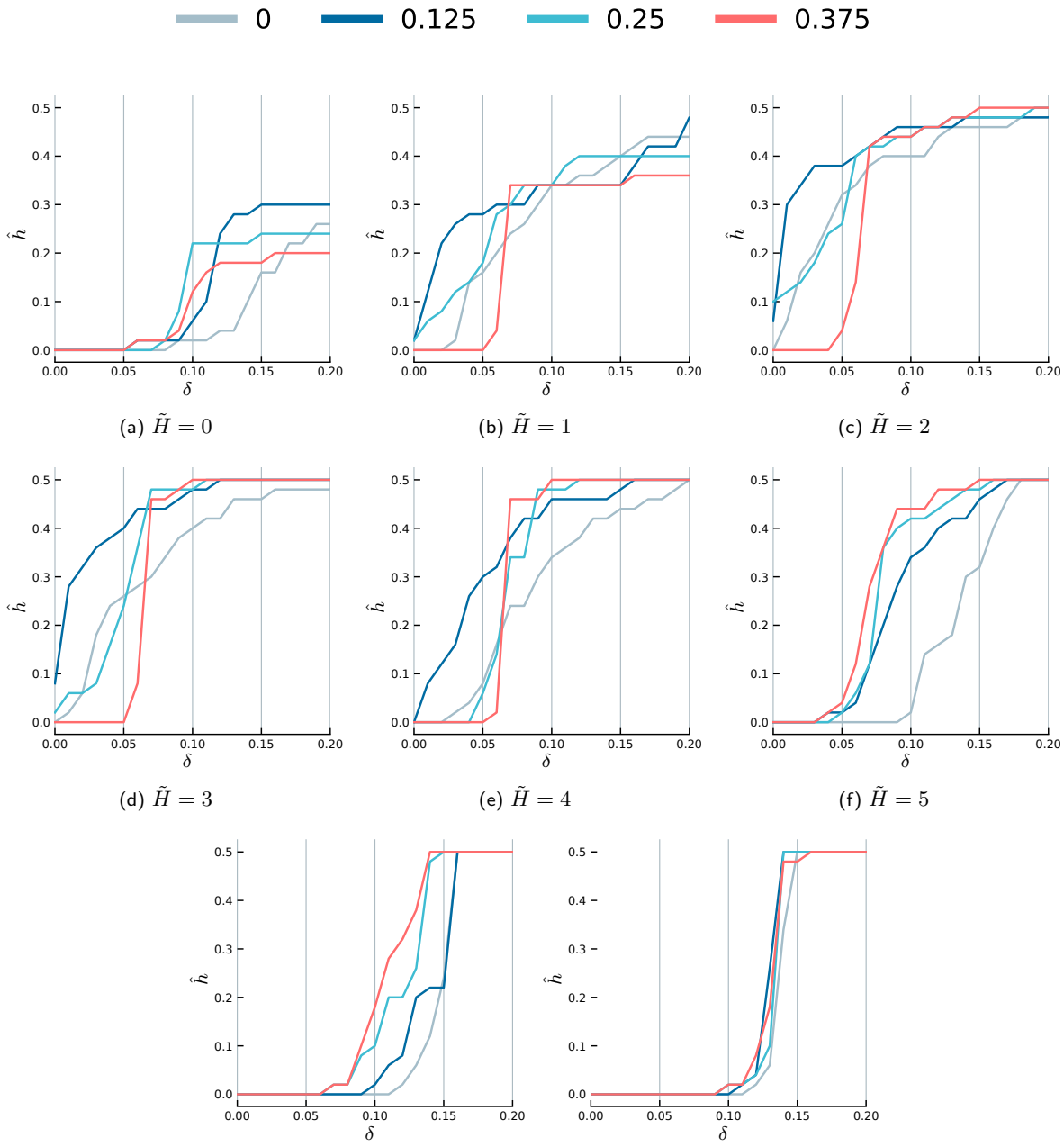

(a) $\tilde{H} = 0$ (b) $\tilde{H} = 1$ (c) $\tilde{H} = 2$

(d) $\tilde{H} = 3$ (e) $\tilde{H} = 4$ (f) $\tilde{H} = 5$

(g) $\tilde{H} = 6$ (h) $\tilde{H} = 7$

Figure 4.7: The level of robustness $\hat{h}$ against various levels of error tolerance $\delta \in [0, 0.2]$ for various levels of *evidence* and *fusion* imprecision, $\tilde{H} \in \{1, 2, \ldots, 7\}$ and $\gamma \in \{0, 0.125, 0.25, 0.375\}$, and for estimate evidence and fusion rates $(\hat{\rho}, \hat{\sigma}) = (0.5, 0.5)$, error rate $\epsilon = 0.3$. The robustness depends on the acceptable error tolerance δ, with most robust fusion imprecision thresholds γ varying across different $\tilde{H}$ and error tolerances.

From Figure 4.7a we see that the acceptable error level, represented by the tolerance δ, plays an important role in deciding which level of fusion imprecision is the most robust. For

example, if the system's acceptable error is $\delta = 0.1$, with $\gamma = 0.25$ the system will be the most robust. However, it crosses the curve for $\gamma = 0.125$ around $\delta = 0.12$, showing that $\gamma = 0.125$ is more robust for higher level of error tolerance $\delta > 0.12$. For $\tilde{H} = 1$, showing in Figure 4.7b, the system is the most robust with $\gamma = 0.125$ for low tolerance $\delta < 0.06$ and with more imprecise fusion operators, $\gamma = 0.25$ or $\gamma = 0.375$ for a higher tolerance $\delta \in (0.06, 0.1)$. In summary, the optimal fusion imprecision threshold γ values for system's robustness is highly dependent on the acceptable error tolerance δ.

The robustness of different levels of imprecise fusion operators also varies depending on the levels of evidential imprecision. Starting from $\tilde{H} = 2$, the acceptable level of error becomes less significant in determining the most robust fusion imprecision level. In Figures 4.7c to 4.7e, $\gamma = 0.125$ is the most robust for a low tolerance $\delta = 0.05$. For a higher tolerance, up to $\delta = 0.2$, all different levels of fusion imprecision are similarly robust. For medium high levels of evidential imprecision $\tilde{H} \in \{5, 6\}$, a higher level of fusion imprecision of $\gamma = 0.375$ becomes the most robust for all different tolerance δ, as shown in Figures 4.7f to 4.7g. In Figure 4.7h, where the most imprecise evidential updating is applied, the robustness of different levels of fusion imprecision becomes less distinct. All levels of fusion imprecision exhibit similar robustness, being non-robust for low tolerances and robust for tolerances exceeding $\delta = 0.15$.

In Section 3.5 we have demonstrated that the optimal evidential imprecision for the systems robustness also varies depending on the level of error tolerance. Building on this, and to offer a more comprehensive investigation of the combined effects of both imprecision, in Figure 4.8 we show the optimal combination of evidential updating threshold $\tilde{H}$ and fusion threshold γ (represented by colours) that achieves the greatest robustness to various evidence and fusion rates for error tolerance $\delta \in [0, 0.2]$. For small tolerances up to $\delta = 0.05$, the model with $\tilde{H} = 2$ and $\gamma = 0.125$ exhibits the highest level of robustness. However, for $\delta = 0$, this combination is slightly less robust compared to the case with $\gamma = 0.125$, also shown in Figure 4.7c. For moderate tolerances in the range of $\delta \in [0.05, 0.15]$, a higher level of evidential imprecision ($\tilde{H} = 3$) shows to be more robust. Regarding fusion thresholds, a range of values from $\gamma = 0.125$ to $\gamma = 0.375$ demonstrates similar levels of robustness, with minimal differences among these thresholds. For higher tolerances within the range of $\delta \in [0.15, 0.2]$, $\tilde{H} = 2$ remains optimal in terms of robustness, while more imprecise fusion operators $\gamma = 0.375$ are required. In summary, the analysis reveals that for higher tolerance levels, slightly more fusion imprecision can exhibit greater robustness compared to $\gamma = 0.125$. However, for small tolerances, $\gamma = 0.125$ remains the optimal choice for achieving the highest level of robustness.

4.5 Discussion and Conclusion

In this chapter, we have investigated social learning with the impact of both imprecise fusion operators and imprecise evidential updating at the same time. Through a series of simulations

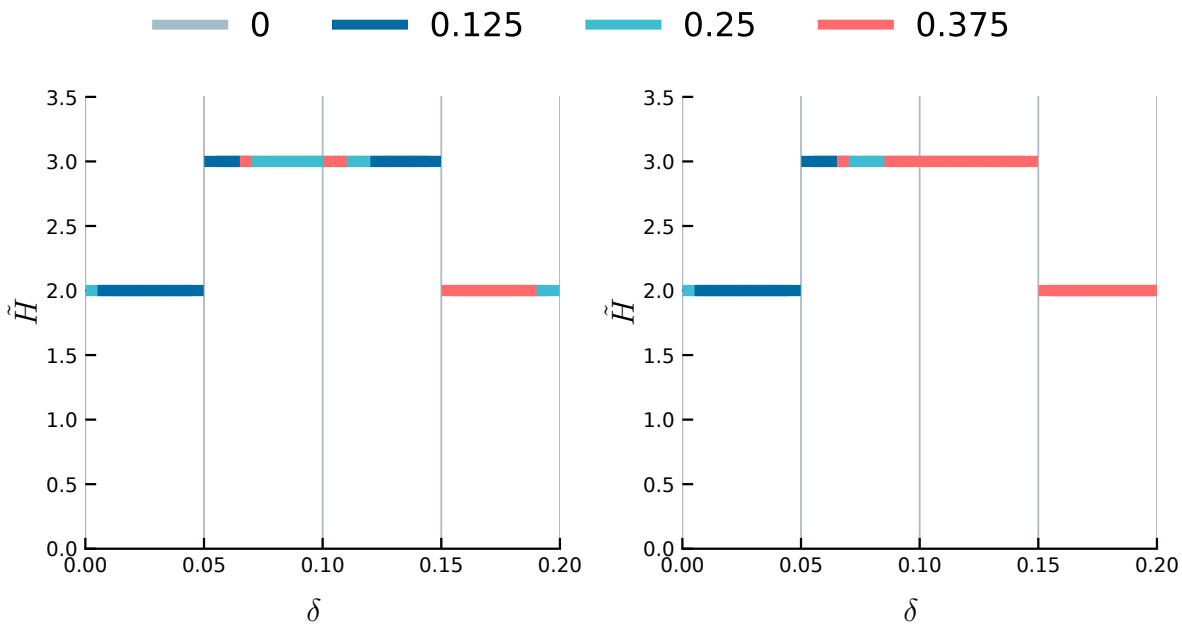

(a) Selects the most precise fusion threshold in a tie

(b) Selects the most imprecise fusion threshold in a tie

Figure 4.8: Evidence updating and belief fusion threshold ($\tilde{H}$ and γ) that achieve the most robust model for different levels of error tolerance ($\delta \in [0, 0.2]$); and for estimate evidence and fusion rates $(\hat{\rho}, \hat{\sigma}) = (0.5, 0.5)$, error rate $\epsilon = 0.3$. For different δ, the highest level of robustness is achieve by different combinations of γ and $\tilde{H}$.

and analysis, we have gained valuable insights into the trade-offs and dynamics involved in imprecise fusion and imprecise evidence in the context of social learning and decision-making.

One of the key findings is the social learning model can be improved under the joint influence of imprecision in evidential updating and imprecision in belief fusion. In noisy environment, adding a low to moderate level of imprecision to both the evidence updating and belief fusion process, can improve the accuracy of the learning outcome, compared to using imprecise evidential updating or imprecise belief fusion independently, especially when the evidence rate is relatively low compared to the fusion rate.

We have also found that the use of imprecise fusion operators introduces a trade-off between the speed of learning and the accuracy of learning outcomes. Compared with the standard precise fusion operators, by introducing imprecision to belief fusion process, the model tend to achieve higher accuracy but at the cost of slower convergence. The trade-off is more significant when the fusion rate σ is high and the evidence rate is low. This trade-off underscores the importance of carefully balancing the levels of fusion operators to achieve the desired learning outcomes.

We have also explored the concept of robustness in the context of imprecise fusion and imprecise evidence. By applying aspects of info-gap theory, we have evaluated the robustness of different parameter combinations and identified optimal thresholds for achieving reliable

and accurate outcomes. Our findings indicate that the choice of fusion imprecision level and evidence imprecision level depends on the acceptable error level (tolerance) and the specific requirements of the system.

Furthermore, we have explored the system's robustness to various evidence and fusion rate of this integrated model. Our results suggest that as the level of accepted error varies, the model need to use different levels of evidential and belief imprecision. Generally, more imprecise fusion fusion should be applied for higher levels of accepted error. For low and high levels of accepted error, the optimal level of evidential imprecision slightly lower than for moderate levels. These insights highlight the importance of adapting the imprecision levels based on the specific requirements and tolerance for error in the system.

For future direction an in-depth investigation into the impact of different error rates is warranted, as we have found in Chapter 3 that the optimal level of evidential imprecision is depending on the error rates. In addition, investigating real-time adaptation of imprecision levels in both fusion and evidential updating may be worthwhile. For instance, if an agent undergoes consecutive evidential updating processes without fusion, it could increase the fusion threshold, as this would not compromise speed when evidence is more frequent than fusion, vice versa. Understanding how to dynamically calibrate these settings could facilitate more efficient and accurate decision-making processes in social learning models.

In conclusion, this chapter has shed light on the interplay between imprecise fusion operators and imprecise evidential updating in social learning models. The integration of both aspects can enhance learning outcomes, with trade-offs in terms of speed and accuracy. Our findings emphasise the significance of selecting appropriate imprecision levels and strike a balance to achieve desired learning performance.

Chapter 5

From Existing to Novel: Evidential Updating Models

In Chapters 2 and 4, we investigated a fusion operator that allows for varying levels of imprecision in the fusion results, determined by specific thresholds. Our findings demonstrated that employing an imprecise operator with a certain level of imprecision can enhance the accuracy of the learning outcome. Compared to the standard operator, the fusion operator with the optimal threshold deems the beliefs of the fusion pair to be less reliable. As a result, it will take the union of them when their consistency falls below the level specified by the threshold, i.e. it will take union more frequently than the precise operator, especially in noisy environments. Traditional evidential updating, on the other hand, narrows an agent's belief when the evidence supports it and agent would not update their beliefs in the case that the evidence is inconsistent. The potential drawback is that this can result in the loss of inconsistent but potentially valuable information in evidence. In order to address this, this chapter explores the ways the keep the inconsistent information in the evidential updating process so that the agents will be able to retain a broader range of evidence. We expect this to be particularly significant in environments with high error rates, where agents are more likely to receive inconsistent evidence.

Specifically, we used a negative evidential updating strategy, which has proven to be effective in best-of-n problems [19] in previous chapters. By intersecting the evidence with the agent's belief, this updating method excludes options that are deemed incorrect by both sources, without increasing the belief cardinality or expanding the number of plausible states. In essence, this approach to evidential updating refines and narrows down the agent's belief space. In this chapter, we introduce the union operation into the evidential updating process. By incorporating union-based operations, we aim to expand the agent's belief space so as to allow for consider a broader range of possibilities when the agent's belief is inconsistent with the evidence received. We assume such an extension of the updating method allows for a more comprehensive exploration of potential solutions and enhances the agent's ability to adapt and learn in complex and uncertain environments.

We will begin this chapter by defining a new evidential update method that uses the Dubois&Prade operator, the standard precise belief fusion operator we have deployed in this thesis. Following this, we will present simulation results to investigate the implications and advantages of incorporating union-based evidential updating, compared with the original method. Additionally, we will introduce a novel approach to evidential updating, wherein agents update their belief using a hybrid approach in order to combine the strengths of the two methods. Simulation experiments will also be conducted to investigate and evaluate the efficacy of the proposed new method. Through these experiments, we aim to gain deeper insights into the performance and capabilities of the integrated approach, shedding light on its potential benefits and applications in social learning systems and decision-making processes.

5.1 Related Work

In this chapter we investigate different evidential updating approaches with various levels of evidential imprecision for the models presented in Chapter 3. As a result, the research presented in Section 3.1 remains relevant and connection to the proposed investigation. In addition, we also discuss and highlight various research studies that focus on different evidential updating methods. These studies investigate updating beliefs based on different types of evidence, and explore the implications of these methods in the context of social learning and decision-making.

In the context of the social learning literature, the evidence from the environment is often represented as quality values assigned to different options and the agents are required to identify the options with the highest qualities, e.g. [8, 13, 47]. In most cases agents update their beliefs by comparing the quality values of different options using a specified updating method. In [13] two methods are compared: one based on blind trust (direct comparison, DC) to the evidence, and the other based on a probabilistic approach where agents abandon previously collected evidence probabilistically (cross-inhibition). The latter makes decisions slower but can reach higher accuracy in the presence of evidential error. Inspired by these findings, [12] introduced a negative approach to utilizing evidence by enabling a comparison of quality values between two options. Following the principle of "the global best must be the local best" [12], the proposed negative updating aims to rule out certain options with lower quality values, by using probabilistic pooling and updating approaches. Furthermore, employing negative updating together with epistemic sets is shown to be able to solve problems with a much greater number of options upto 95 with a smaller number of 10 agents [19]. We applied the same updating method as [19] in both chapter 3 and chapter 4. In systems with set-based beliefs, negative updating involves taking the intersection with the evidence, which results in the elimination of inconsistent or less plausible states. On the other hand, positive updating entails taking the union, which allows for the inclusion of new potential best options or true states into agents' beliefs, incorporating them as supportive evidence. [26] compared a set of evidence

updating methods for a model in which agents' beliefs are modelled by mass functions based on Dempster-Shafer (DS) theory. The study shows that systems using positive and negative updating together (Dubois&Prade rule) are slower but more accurate than those using pure negative updating (Dempter's rule) when the evidence is easily available to agents. This differs from the findings observed in quality value based models. For set-based models, the impact of positive and negative updating on set-based beliefs requires further exploration to understand their implications in decision-making scenarios.

5.2 Combination operators for Evidence Updating

In this section, we compare two evidential updating methods, negative updating, which has been used in the previous chapters, and the updating using Dubois&Prade operator(DP updating). In particular, the only difference between the two methods is whether the agent update its belief by union with the inconsistent evidence or simply ignore it. By incorporating the union operation of the DP updating, we aim to let the agents increase the cardinality of their beliefs by accepting a wider range of plausible states during the evidential updating. We begin by providing a detailed description of the models and algorithms used in the simulation experiments. We then present the simulation results including the accuracy and speed of learning for the DP evidential updating approach. Through these investigations, we aim to shed light on the advantages and disadvantages of incorporating the union operation compared with the classic updating method and its potential applications in social learning and decision-making contexts.

5.2.1 Model

In order to investigate the impact of the DP updating to social learning, We revisit the fundamental assumption that the environment can be represented by a finite set of propositions $\mathcal{P} = \{p_1, ..., p_n\}$. Consequently, a state of the world is defined as a function s that maps these propositions to binary truth values. For notational convenience we represent a state by the n-tuple $\langle s(p_1), \ldots, s(p_n)\rangle$. We then assume that the evidence collected by agents precisely identifies a potential true state s_e and the error rate ϵ is incorporated to account for potential inaccuracies in the evidence, as in Chapters 3 and 4. For belief fusion we use the standard Dubois&Prade operator as describe by Equation (2.3). For evidential updating we use the Dubois& Prade (DP) operator, the same as the fusion operator of agents' beliefs, as follows:

$$B|E = B \odot E = \begin{cases} B \cap \mathrm{E} : B \cap E \neq \emptyset \\ B \cup E : \text{otherwise.} \end{cases} \tag{5.1}$$

From Chapter 3 we see that the precise evidence with only 1 state is not always the option that produces the most accurate learning outcome, especially when the error rate is high. Therefore, we will also explore imprecise evidence with different evidential thresholds $\tilde{H}$. The

rationale for varying the level of evidential imprecision when comparing negative and DP updating methods lies in the higher likelihood that more precise evidence will be inconsistent with an agent's beliefs, thereby, the differences between these two methods can be emphasised by varying the level of evidential imprecision.

5.2.2 Agent-based Simulation

In this section, we present the results of agent-based simulation experiments to explore the impact of different combination operators in evidential updating method. The simulations were conducted under the same conditions as those in *Section* 3.4. The parameters used include a population size of $k = 100$ agents, a language size of $n = 8$ propositions, and evidence rates and fusion rates $(\rho, \sigma) \in [0.02, 1)^2$. Each combination of parameters was subjected to a maximum limitation of 20000 iterations and was simulated with 50 independent runs to reduce the influence of random variations in the results.

In Figure 5.1 we show the the average accuracy of the population with error rates $\epsilon \in \{0.2, 0.3, 0.4\}$ for agents using negative updating and DP updating respectively. Note that Figures 5.1a, 5.1c and 5.1e is a repetition of Figures 3.16b to 3.16d. For a low error rate $\epsilon = 0.2$, in Figures 5.1a and 5.1b we see that both updating methods have reached similar levels of accuracy unless the evidence is updated with the more precise representation ($\tilde{H} = 0$). For $\tilde{H} = 0$ agents using DP updating achieve higher accuracy compared with those using negative updating. For a higher error rate $\epsilon = 0.3$, we see higher accuracy for a population applying DP updating for $\tilde{H} \leqslant 1$, a wider range of evidential imprecision. In addition, for $\tilde{H} = 0$ we see a more significant improvement on accuracy The population only achieves an accuracy close to 1.0 for a very low fusion rate when applying negative updating. On the other hand, agents applying DP updating can achieve high accuracy for higher fusion rates as long as the evidence rate is also high, as shown in Figure 5.1d. In summary, we have observed greater improvements in accuracy for higher error rates and more precise forms of evidence. One possible explanation for this trend is that with lower error rates, the evidence collected by agents is more likely to be consistent with their belief, and with a larger $\tilde{H}$, the evidence neighbourhood evidence has a higher chance of overlapping with the agents' belief sets. As a result, the probability of agents taking intersection during the updating process increases, leading to more similarity between Dubois&Prade updating and negative updating when the error rate is low and the evidence is imprecise.

For the highest error rate investigated, $\epsilon = 0.4$, we observe reduced differences between the two updating methods for highly imprecise evidence ($\tilde{H} \geqslant 4$) in Figures 5.1e and 5.1f. However, for $\tilde{H} < 4$, more noticeable differences emerge. In particular, in Figure 5.1f, the population using DP updating shows significantly lower accuracy ($\alpha < 0.7$) when the fusion rate is substantially lower than the evidence rate (the upper left corner of the heat maps) Moreover, agents employing the negative updating method achieve considerably higher accuracy

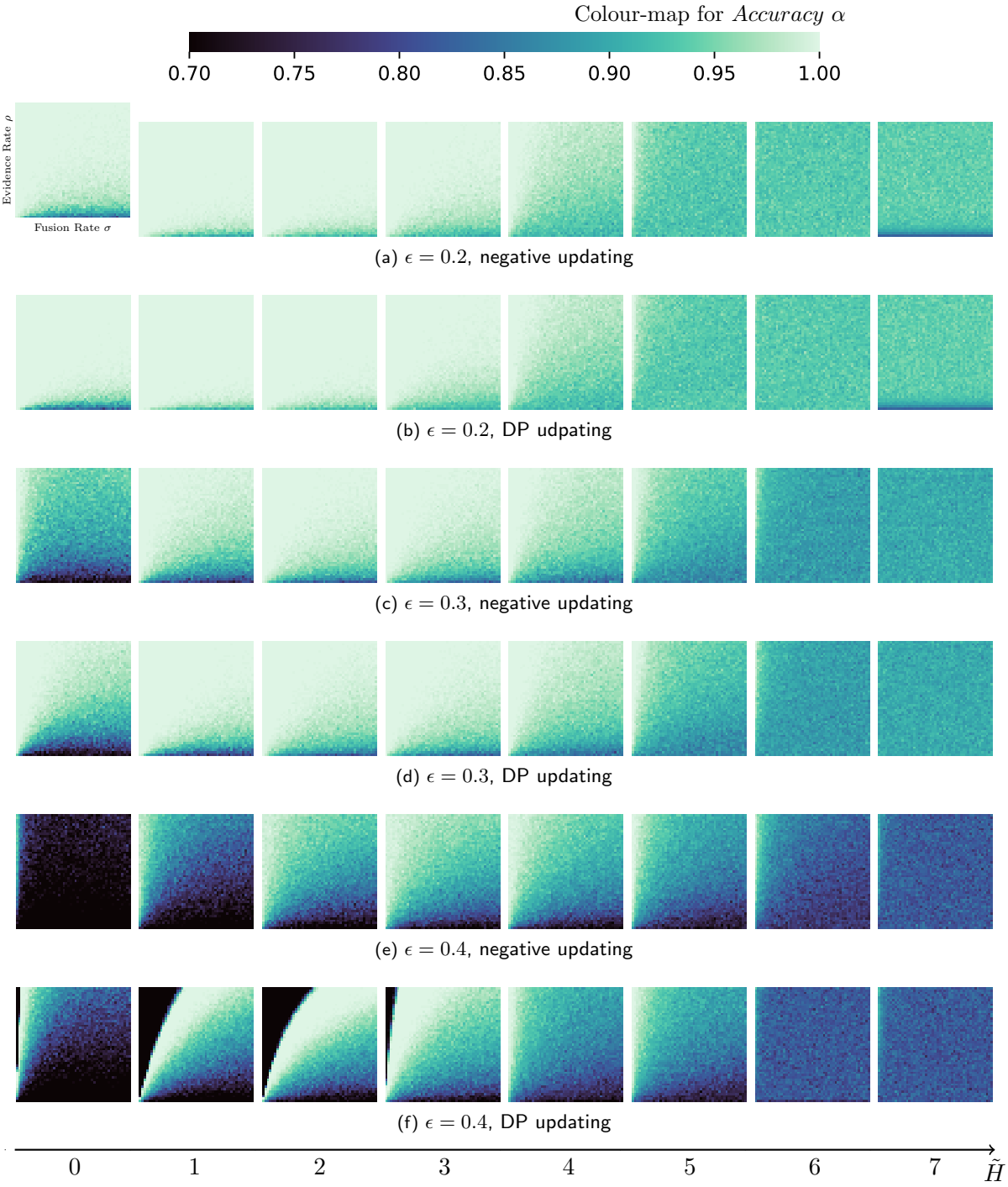

Figure 5.1: Average accuracy at steady state for different levels of evidential imprecision with negative updating or DP updating for different error rates $\epsilon \in \{0.2, 0.3, 0.4\}$, $\sigma \in [0.02, 1)$, $\rho \in [0.02, 1)$. From left to right: $\tilde{H} \in \{0, ..., 7\}$. The axis labels for the heat maps are provided in the top left figure as an example. At lower $\epsilon \in \{0.2, 0.3\}$ and low $\tilde{H}$, DP updating outperforms in accuracy, particularly in left-side heatmaps ($\tilde{H} = 0$). For $\epsilon = 0.4$, DP updating's performance declines, especially when σ is lower than ρ.

compared to agents using DP updating for the same fusion and evidence rate combinations. In adjacent regions, in other words, for higher fusion rates, agents with DP updating achieve higher accuracy values closer to 1.

In Figure 5.2, we present the average number of iterations used before the system converges to a consensus. The maximum limit of 20000 iterations also applies to ensure that the simulations do not run indefinitely. Darker colours represents slower convergence and lighter colours indicates faster convergence. For the majority of the scenarios investigated, the population is able to converge within 300 iterations while we see some exceptions where the error rate is high or the evidence is highly imprecise. For negative updating, The impact on the speed of convergence of different levels of evidential imprecision has been discussed in Chapter 3. For low and medium error rate $\epsilon \in \{0.2, 0.3\}$, for the most precise evidence, $\tilde{H} = 0$, agents using DP updating are slightly faster than agents using negative updating, see the left most figures of Figures 5.2a to 5.2b. For $\tilde{H} > 0$, there are no significant differences in the speed of convergence between the two methods; The number of iterations required for consensus for both update methods is smaller for a higher fusion rate when the evidence is not highly imprecise. For more imprecise evidence, $\tilde{H} \geqslant 5$, the impact of evidence rate on the speed of convergence become more significant and for $\tilde{H} = 7$ the speed of convergence is mostly dependent on the evidence rate.

For the higher error rate of $\epsilon = 0.4$, the number of iterations to convergence exhibits more significant differences between the two updating methods, particularly for less imprecise evidence with $\tilde{H} \leqslant 3$. Under DP updating, there is a region in which the fusion rate is notably lower than the evidence rate (the upper left region of the heat maps), resulting in the population failing to converge within 20000 iterations when $\tilde{H} \leqslant 3$, as shown in Figure 5.2f. On the other hand, negative updating demonstrates a higher level of robustness to different combinations of fusion and evidence rate. In addition, negative updating demonstrates a stronger dependence on the fusion rate, i.e. higher fusion rates lead to faster convergence. However, for DP updating, the speed of convergence is influenced by both the evidence rate and the fusion rate when $\tilde{H} = 2$ or $\tilde{H} = 3$, where faster convergence is observed only when both the evidence rate and fusion rate are high.

In summary, our findings suggest that in terms of accuracy DP updating performs slightly better than negative updating when the error rate is not high and the evidence is precise, without compromising time efficiency. However, when the error rate is high ($\epsilon = 0.4$), DP updating leads to convergence problems that prevent the population from reaching a consensus, particularly for more precise evidence, $\tilde{H} \leqslant 3$. This is worthy of further investigation, as apart from the combinations of σ and ρ where convergence is not achievable, the population achieves the highest accuracy for $\tilde{H} \in [2, 4]$. This indicates that the choice of updating method should consider the specific conditions of the system, such as error rate, evidence precision, and the desired level of accuracy. In the following section, we propose a new updating approach that aims to combine the strengths of both DP and negative updating methods, in order to overcome

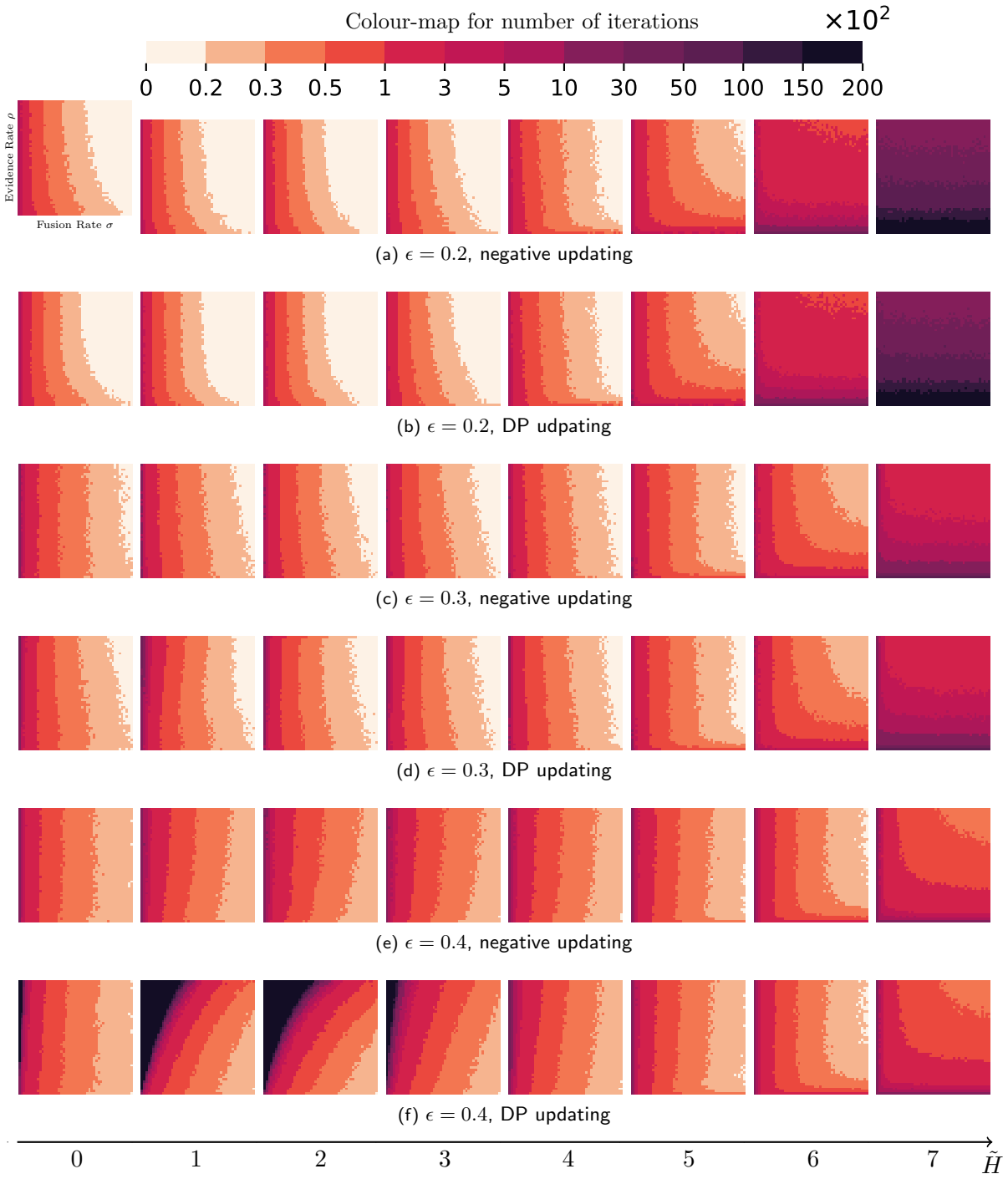

Figure 5.2: Average number iterations before convergence for different levels of evidential imprecision with negative or DP updating for different error rates $\epsilon \in \{0.2, 0.3, 0.4\}$, $\sigma \in [0.02, 1)$, $\rho \in [0.02, 1)$. From left to right: $\tilde{H} \in \{0, ..., 7\}$. The axis labels for the heat maps are provided in the top left figure as an example. For higher $\epsilon = 0.4$ and smaller $\tilde{H}$, systems using DP updating fails to reach a consensus.

the limitations observed and enhance the overall performance of the social learning model.

5.3 Hybrid Evidential Updating

In this section, we propose a novel updating approach that addresses the convergence problems observed with DP updating while enhancing the accuracy of negative updating under higher error rates. By adopting a hybrid updating strategy that combines the DP and negative updating under different conditions, we aim to achieve improved accuracy and convergence properties for a wide range of fusion and evidence rates. We then evaluate the performance of this new approach using agent-based simulations and compare it with DP and negative updating methods.

5.3.1 Model

In order to combine the strengths of the two methods, we introduce a new approach inspired by rough set theory [82] to represent the agents' belief as $B = \langle \underline{B}, \overline{B} \rangle$, where $\underline{B} \subseteq \overline{B}$. Here, $\underline{B}$ and $\overline{B}$ denote the lower and upper approximations of the possible true states of the world. We will apply this rough belief representation to the evidential updating process as follows:

$$B||\,\mathrm{E} = \langle \underline{B}, \overline{B} \rangle||\,\mathrm{E} = \begin{cases} \langle \underline{B} \cap \mathrm{E}, \underline{B} \cap \mathrm{E} \rangle : \underline{B} \cap \mathrm{E} \neq \emptyset \\ \langle \underline{B}, \underline{B} \cup \mathrm{E} \rangle : \text{otherwise} \end{cases} \tag{5.2}$$

In the proposed updating approach, we only use the lower belief $\underline{B}$ for the evidential updating operation. This means that in scenarios where agents consecutively receive two pieces of evidence—in other words when no fusion events occur between the two evidential updating processes—the second update will not retain the upper belief generated by the first update, if the initial evidence was inconsistent with the agent's existing beliefs. For example, consider an agent whose initial belief is denoted as $B = \{s_1, s_2\}$. Upon receiving a first piece of evidence $\rho = \{s_3\}$, the agent updates its beliefs to $\underline{B} = \{s_1, s_2\}$ and $\overline{B} = \{s_1, s_2, s_3\}$. Notably, the upper belief is expanded to incorporate the first piece of evidence, while the lower belief remains unchanged due to the inconsistency with the initial belief. Then, if the agent receives a second piece of evidence $\rho' = \{s_4\}$ before any fusion events occur, the agent will update its beliefs to $\underline{B} = \{s_1, s_2\}$ and $\overline{B} = \{s_1, s_2, s_4\}$.

In case that evidence collected by agents is inconsistent with their beliefs, both the original belief and the updated belief will be passed forward to fusion. Let $\underline{B}'$ and $\overline{B}'$ denote the fused lower and upper beliefs, respectively, then for rough belief fusion we apply the following fusion operator:

$$\underline{B}' = \overline{B}' = B_1 \otimes B_2 = \begin{cases} \overline{B}_1 \cap \overline{B}_2 & : \ \underline{B}_1 \cap \underline{B}_2 \neq \emptyset \\ (\underline{B}_1 \cup \underline{B}_2) \cup (\overline{B}_1 \cap \overline{B}_2) & : \ \underline{B}_1 \cap \underline{B}_2 = \ \emptyset \ and \ \overline{B}_1 \cap \overline{B}_2 \neq \emptyset \\ \overline{B}_1 \cup \overline{B}_2 & : Otherwise \end{cases} \tag{5.3}$$

The fusion operator ensures that the agent's upper and lower beliefs collapse to a single belief after fusion. Therefore, the agents' upper and lower beliefs can only differ after an updating event with inconsistent evidence and then collapses to a single belief set after subsequent updating based on consistent evidence or after fusion, which means that rough beliefs are 'temporary'; they persist only until a consistent evidential updating or a event of belief fusion. Assuming that two agents have undergone a single sequence involving one evidential updating process and one belief fusion process, the relationship between the fused beliefs obtained using the hybrid(B_h), negative(B_n), and DP(B_{dp}) updating methods is as follows:

$$B_h = B_n \cup B_{dp} \tag{5.4}$$

Equation (5.4) shows that the hybrid method yields beliefs that are equivalent to the union of those generated by the other two methods. A mathematical proof substantiating this claim can be found in Appendix B. The rationale for this hybrid approach is that agents' beliefs are generally more reliable than the evidence collected, particularly in highly noisy environments where the error rate ϵ is high. This is because agents' beliefs have undergone iterative fusion processes, i.e. error correct processes [26], which enhance their reliability. In Section 5.3.2 we show how the hybrid approach prioritises agents' beliefs over collected evidence in a single evidential updating and belief fusion sequence.

5.3.2 Comparison with the Negative and DP updating

In this section we compare the agents' fusion behaviours in a single evidential updating and belief fusion sequence between 3 different updating strategies. When both agents involved in the fusion have collected consistent evidence during the preceding evidential updating process such that $\underline{B}_1 = \overline{B}_1$ and $\underline{B}_2 = \overline{B}_2$, the new fusion operator becomes equivalent to a standard Dubois&Prade operator and all the 3 methods are equal in this case. However, the proposed hybrid approach in section 5.3.1 changes the fusion logic when at least one of the agents receives evidence which is not consistent with their lower beliefs ($\underline{B} \cap \mathrm{E} = \emptyset$) before the belief fusion.

We first assume that the lower belief of only one of the fusion pair of agents is different from its upper belief. For instance, there can be scenarios that one of the agent does not perform any evidential updating after the last fusion and the other receives evidence inconsitent with its lower belief. Additionally, there are also chances that both agents performs evidential updating but only one of the agent receives inconsistent evidence. Without loss of generality, we let

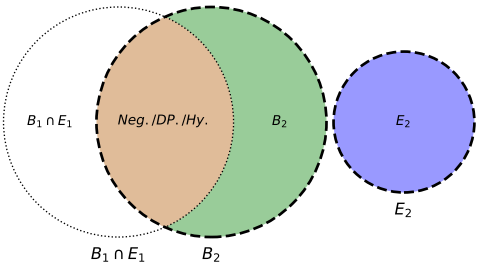

(a) Case 1a: $\underline{B}_1 \cap \underline{B}_2 = \overline{B}_1 \cap \overline{B}_2 \neq \emptyset$, in this case the outcome of all 3 methods are equal.

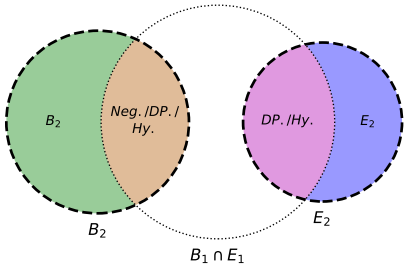

(b) Case 1b: $\emptyset \neq \underline{B}_1 \cap \underline{B}_2 \subset \overline{B}_1 \cap \overline{B}_2$, in this case the outcome of DP and Hybrid methods are equal and they are both super sets of the outcome of negative method

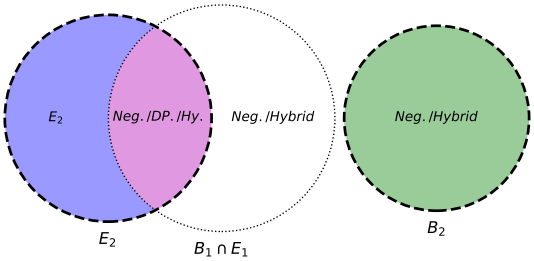

(c) Case 2a: $\underline{B}_1 \cap \underline{B}_2 = \emptyset, \overline{B}_1 \cap \overline{B}_2 \neq \emptyset$, in this case the outcome of negative and Hybrid methods are equal and they are both super sets of the outcome of DP method

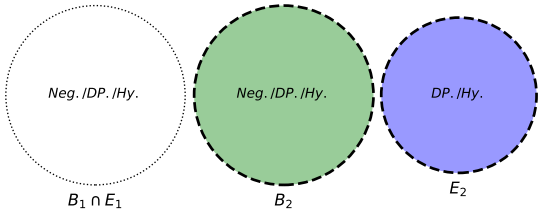

(d) Case 2b: $\overline{B}_1 \cap \overline{B}_2 = \emptyset$, in this case the outcome of DP and Hybrid methods are equal and they are both super sets of the outcome of negative method

Figure 5.3: The Venn diagrams illustrating various belief updating methods when one of the fusion pair receives inconsistent evidence, without loss of generality, we assume $B_1 \cap \mathrm{E}_1 \neq \emptyset$ $B_2 \cap \mathrm{E}_2 = \emptyset$. The dotted circle represents the evidential updated belief of B_1, i.e.$\underline{B}_1 = \overline{B}_1 = B_1 \cap \mathrm{E}_1$ and the dashed circle represents $\overline{B}_2$ of which the *green* circle represents $\underline{B}_2$ and the *purple* circles represents E_2. *Pink* regions represent the outcomes of $\underline{B}_1 \cap \underline{B}_2$; *Yellow* areas represent outcomes of $\overline{B}_1 \cap \overline{B}_2$.

$\underline{B}_1 \cap \mathrm{E}_1 \neq \emptyset$ and $\underline{B}_2 \cap \mathrm{E}_2 = \emptyset$, i.e. $\underline{B}_1 = \overline{B}_1$ and $\underline{B}_2 \neq \overline{B}_2$. Figure 5.3 shows that the outcome of the hybrid approach will always be the union of the outcome of the DP and negative methods. For example, in Figure 5.3b agents using the negative method will not include the consistencies between $\underline{B}_1$ and E_2 while the other two methods will; in Figure 5.3c agents using DP method will only include the consistencies between E_2 and $\underline{B}_1$ without including the more reliable agent's belief $\underline{B}_2$, while the other two methods will retain them. In other words, the hybrid approach will be able to maintain reliable beliefs as the negative method does and include consistent evidence as the DP method does.

We then show Figure 5.4 for another scenario where both agents involved in pairwise fusion have lower beliefs that differ from their upper beliefs. This indicates that they have both experienced evidential updating prior to fusion and have received inconsistent evidence, which is probable especially in noisy environments. Cases 1, 2, and 3 are corresponding to three distinct

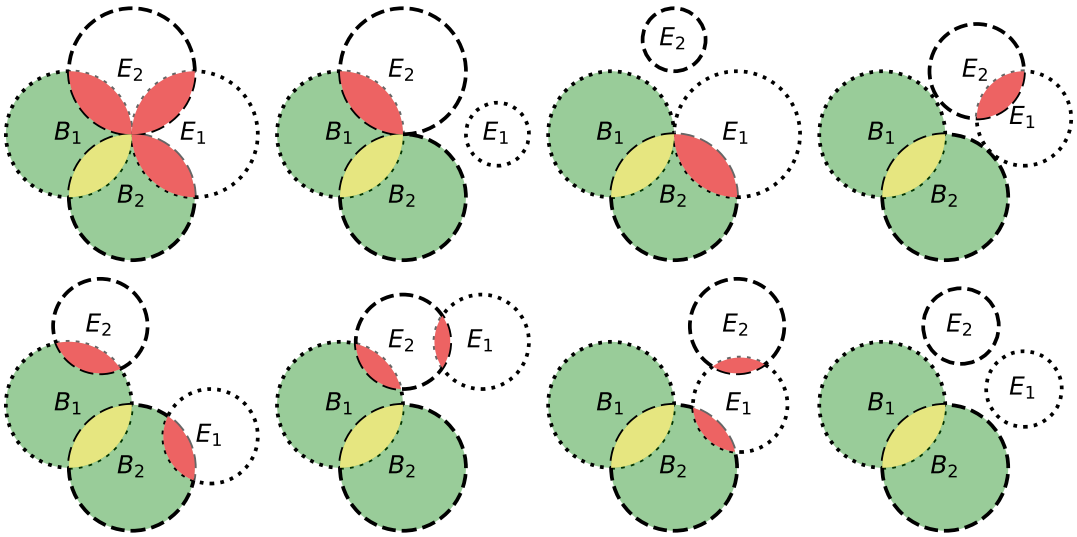

(a) Case 1: $\underline{B}_1 \cap \underline{B}_2 \neq \emptyset$; in this case the outcome of DP and Hybrid methods are equal and they are both super sets of the outcome of negative method.

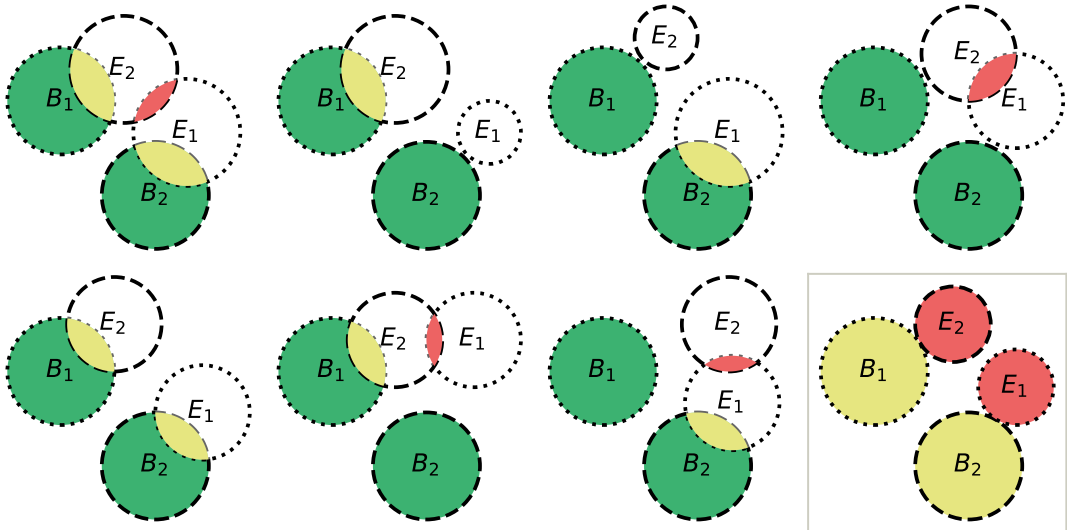

(b) Case 2: $\underline{B}_1 \cap \underline{B}_2 = \emptyset$, $\overline{B}_1 \cap \overline{B}_2 \neq \emptyset$ and Case 3 (bottom right): $\overline{B}_1 \cap \overline{B}_2 = \emptyset$; In Case 2 the DP method maintain the information from the evidence sets while the negative method maintain the information from the belief. In Case 3 the outcome of DP and Hybrid methods are equal and they are both super sets of the outcome of negative method

Figure 5.4: The Venn diagrams illustrating various belief updating methods when both agents receive inconsistent evidence. Each circle represents a set of belief or evidence and their overlap represents outcomes from different updating operations. *Light green* and *white* circles denote the initial beliefs held by the agent and evidence respectively; the 2 dotted circles and 2 dashed circles represents upper beliefs $\overline{B}_1$ and $\overline{B}_2$, respectively; *Dark green* areas indicate the results obtained from the negative method; *Red* regions represent the outcomes of DP updating; *Yellow* areas represent the overlap between outcomes of both negative and DP methods. The outcomes of hybrid method are represented by all yellow, dark green, and red coloured regions, i.e. the outcomes of hybrid method are the combined outcomes of DP and negative methods.

scenarios for the fusion operator applied to rough beliefs. Figure 5.4a represents Case 1, where the intersection between $\underline{B}_1$ and $\underline{B}_2$ is non-empty set. The bottom right figure of Figure 5.4b shows Case 3 where there are no intersections between E_1, evi_2, $\overline{B}_1$, and $\overline{B}_2$ is empty. In both instances, both the DP method and the hybrid method yield equivalent results, incorporating more information from the evidence sets compared to the negative method. We then show Case 2 in the rest of Figure 5.4b where the application of the DP method results in the exclusion of reliable information from the agents' beliefs. There are cases where the fusion results excludes information from the agents' beliefs prior to the most recent evidence collection episode. For example, this occurs in the scenario shown in the upper right figure of Figure 5.4b. In such scenarios, the fusion results are totally based on the evidence from a single collection but not on the agents' beliefs that are learnt from all previous iterations. In addition, from Figures 5.3 and 5.4 we see that for negative updating the agents will simply ignore any inconsistent evidence collected by agents while for the other 2 methods they bring the evidence to the fusion process, while the DP method sometimes lose valuable information of agents' beliefs and the fused belief is purely depending on noisy evidence. The hybrid method, in contrast, retains both consistent evidence and the agents' beliefs, which ensures that the beliefs carried by both agents in to the updating-fusion sequence is preserved in those scenarios. Agents will encounter such scenarios more frequently when the environment is more noisy. Therefore, we anticipate that the new approach will be particularly advantageous in scenarios where the evidence is highly noisy.

In summary, under the principle of agents' beliefs are more reliable than the evidence, the hybrid approach serves as a more versatile and adaptive evidential updating and fusion mechanism, particularly suited for environments with high levels of error rates. Unlike the DP methods, which may over-trust the evidence and discard valuable information in agents' beliefs, and the negative method, which under-trusts the evidence and excludes any information in the inconsistent evidence set, the hybrid approach strikes a balance. It effectively incorporates new evidence while also preserving existing beliefs. In the next section, we will use simulation experiments to investigate the properties of the newly proposed approach, assess its performance in terms of accuracy and time to convergence, and compare it with both DP and negative updating methods.

5.3.3 Agent-based Simulations

In this section, we present simulation results using the proposed approach under the same conditions as those used in Section 5.2.2 to maintain consistency . We recall the parameter settings as follows: population size $k = 100$ and language size $n = 8$. We conduct experiments in a noisy environment with varying error rates $\epsilon \in \{0.2, 0.3, 0.4\}$ and explore a range of evidence and fusion rates $(\rho, \sigma) \in [0.02, 1)^2$. We replicate the experiments for each combination of parameters 50 times and enforce a maximum iteration limit of 20000.

In Figure 5.5, the simulation results demonstrate the significant improvements on learning

accuracy achieved by the proposed new updating approach compared to DP updating and negative updating. For $\epsilon = 0.2$, the new approach consistently achieves an accuracy of 1 for all combinations of evidence and fusion rates for $\tilde{H} \leqslant 3$. It outperforms the other two methods, especially when the evidence rates are low. For $\epsilon = 0.3$, the new approach maintains high accuracy for $\tilde{H} \in \{1, 2, 3\}$, with only a few exceptions at extremely low evidence rates. For $\epsilon = 0.4$, the new approach effectively resolves the convergence issues of DP updating and also shows the most significant improvements of accuracy compared to the other 2 error rates. Furthermore, we see more improvements in scenarios with more precise evidence. As expected, in cases where agents update their belief with more imprecise evidence, the impact of the new updating method is relatively modest, given their higher probability that they update their belief by intersecting the evidence during the updating events in which all three approaches are equivalent. However, in situations involving precise evidence, our proposed approach effectively integrates these updating methods, demonstrating its efficacy in optimising the learning accuracy. Consequently, the optimal updating threshold for the new approach is likely to result in more precise options. For example, when $\epsilon = 0.4$, it shifts to $\tilde{H} = 2$ from $\tilde{H} = 3$ or $\tilde{H} = 4$ for negative updating. In summary, the results suggest that the proposed approach offers a potential alternative for evidential updating and belief fusion of social learning frameworks and can enhance the reliability of social learning in noisy environments.

However, while the proposed approach shows improvements in learning accuracy, it is important to note that these enhancements come at the expense of a lower speed of convergence. In Figure 5.6 we show the average iterations required for the agents reaching a consensus and the number 20000 will be used to calculate the average value for the runs that the agents fails to converge within 20000 iterations. Compared to negative and DP updating shown in Figure 5.2, the new approach requires more iterations for the agent to reach a consensus. For example, when the $(\rho, \sigma) = (0.98, 0.98)$ and $\tilde{H} = 1$, the new approach requires 20 to 30 iterations for the population to converge while the other two methods only need less than 20 iterations. Although the new approach exhibits slower convergence, the population still converges within 300 iterations for low and medium error rates $\epsilon \in \{0.2, 0.3\}$ and low to medium levels of evidential imprecision, $\tilde{H} \leqslant 4$, for which the best overall accuracy is obtained. More specifically, all approaches use similar numbers of iterations, in the range 100 to 300, to converge when the fusion rate is low.

Similar to negative and DP updating, we see in Figure 5.6c that convergence is slower for a higher error rate $\epsilon = 0.4$ when using more precise evidence representations, but faster when using more imprecise evidence representations. However, different to the other two methods, the convergence time depends on both evidence and fusion rate for relatively precise evidences $\tilde{H} < 3$, while the fusion rate plays the primary role for negative updating and DP for the same levels of evidential imprecision. For the highest error $\epsilon = 0.4$, we see much slower convergence and no convergence issues as we see in Figure 5.2b. Furthermore, from Figure 5.6 we also see

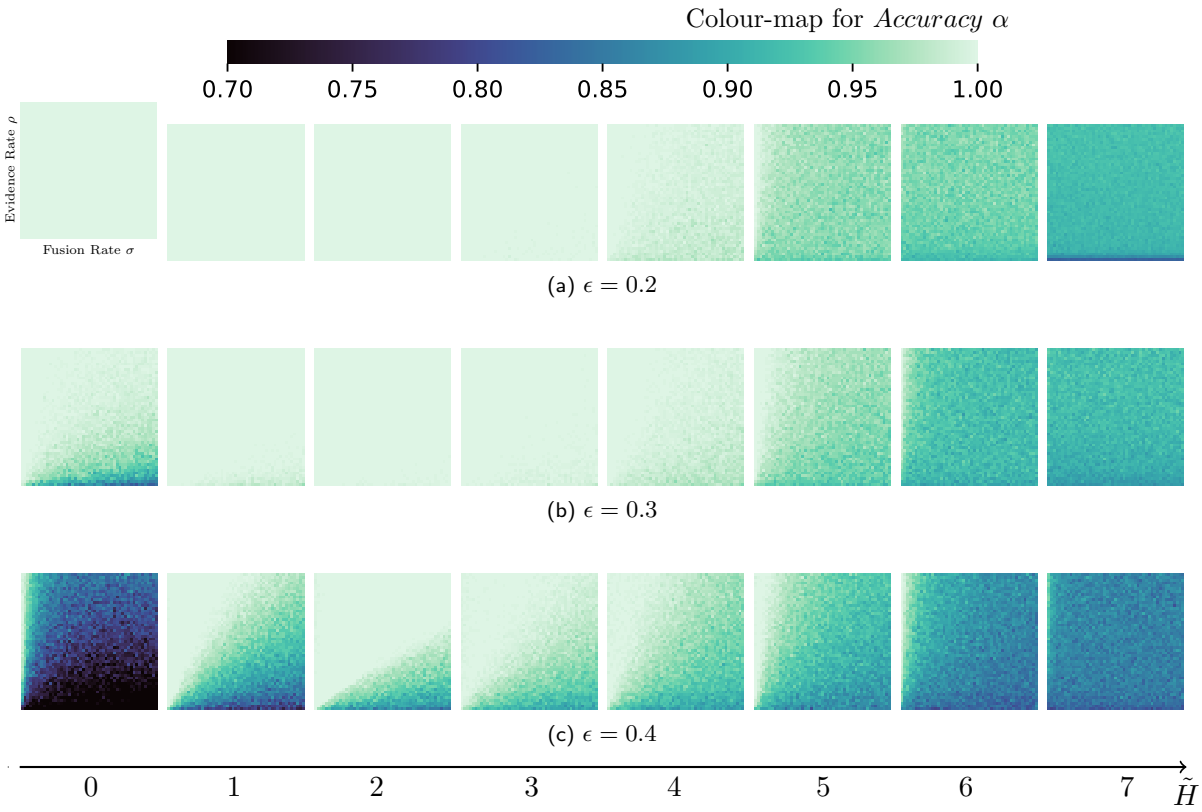

Figure 5.5: Average accuracy at steady state for different evidence imprecision for the hybrid approach and different error rates $\epsilon \in \{0.2, 0.3, 0.4\}$, $\sigma \in [0.02, 1)$, $\rho \in [0.02, 1)$. From left to right: $\tilde{H} \in \{0, ..., 7\}$. The axis labels for the heat maps are provided in the top left figure as an example. Comparing with Figure 5.1, this new approach outperforms both negative and DP updating, especially for higher ϵ.

that the fastest convergence is obtained by thresholds $\tilde{H} \in \{1, 2, 3\}$ for error rates $\epsilon \in [0.2, 0.4]$ respectively. These are consistent with the optimal Hamming thresholds for which agents achieves best overall accuracy with negative updating. In other words, when considering the time cost as well, $\tilde{H} = 1$ and $\tilde{H} = 2$ still appear to be the optimal thresholds for $\epsilon = 0.2$ and $\epsilon = 0.3$, respectively. However, for $\epsilon = 0.4$, there is a trade-off between $\tilde{H} = 3$ for faster convergence speed and $\tilde{H} = 2$ for higher accuracy.

In the case of $\epsilon = 0.4$, a notable trend emerges when $\tilde{H} = 2$ in Figure 5.6c, where we observe a distinct slowdown in the convergence speed when the fusion rate σ is relatively high compared to the evidence rate ρ. This slowdown of convergence come with decreased accuracy. From $\tilde{H} = 2$ in Figure 5.5c we see a transition from a constant high accuracy of 1.0 for combinations of ρ and σ, which lead to faster convergence to more varied values clustered around 0.92 for combinations that result in slower convergence. Figure 5.7 shows the average cardinality (logarithmically scaled) of agents' beliefs within the population at the 20000^{th} iteration. In

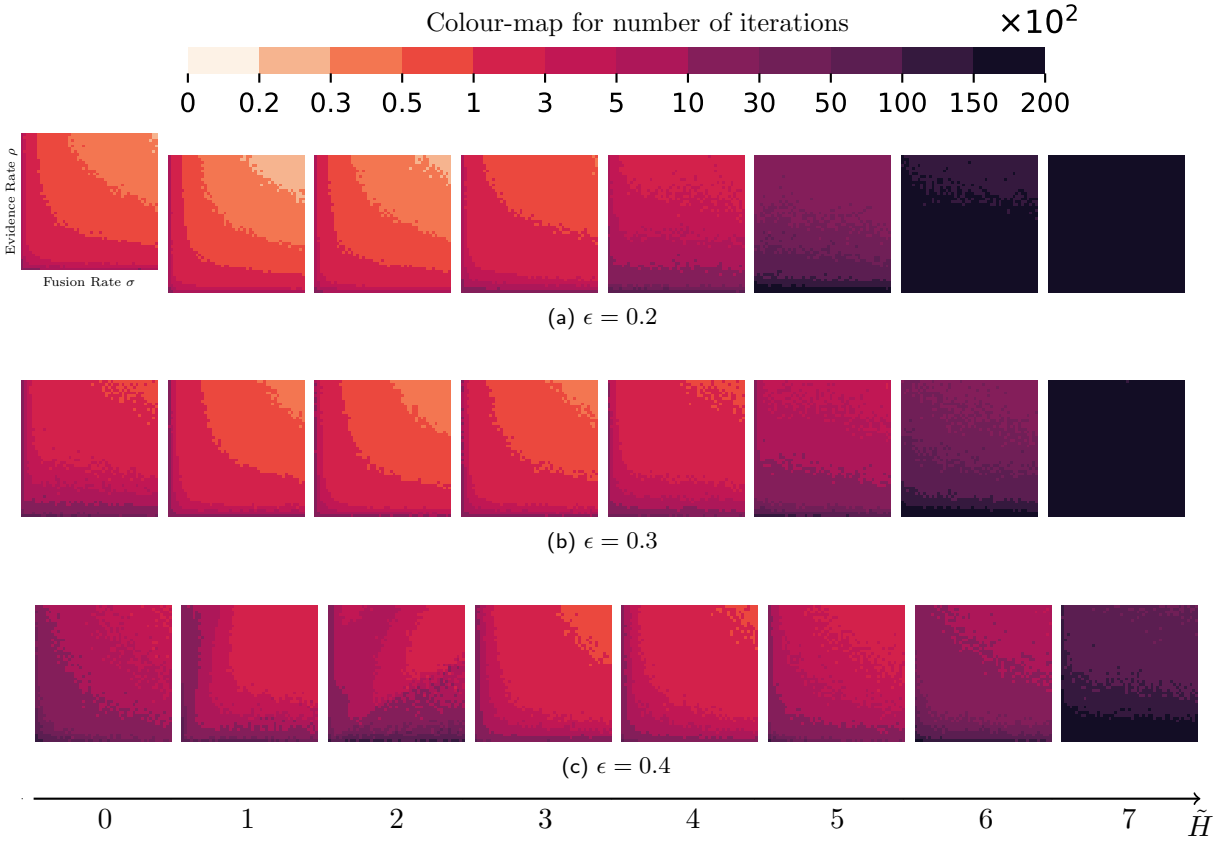

Figure 5.6: Average iterations before convergence or different evidence imprecision with the new approach for different error rates $\epsilon \in \{0.2, 0.3, 0.4\}$, $\sigma \in [0.02, 1)$, $\rho \in [0.02, 1)$. From the left to the right: $\tilde{H} \in \{0, ..., 7\}$. The axis labels for the heat maps are provided in the top left figure as an example.

Figure 5.7c we see that the average cardinality is between $2^{0.5}$ and 2 for $\tilde{H} = 2$ when the fusion rate is relatively high compared to the evidence rate. In contrast, for $\tilde{H} \in \{0, 1, 3, 4, 5, 6\}$ in Figure 5.7, the average cardinality eventually converges to 1 except for very low evidence rates, for which the average cardinality is between 1 and $1.07(2^{0.1})$. This may indicate that the population fails to converge to a singleton belief for some of the 50 runs. In addition, for the most imprecise evidential representation, $\tilde{H} = 7$, average cardinality is greater than 1 in most cases, as shown in Figure 5.7h. In summary, when the evidence rate is low or the evidence is extremely imprecise, 20000 iterations are not always sufficient for the population to reach consensus on a singleton belief.

In order to further investigate the speed-accuracy trade-off between different strategies, we present Figure 5.8 showing the average belief accuracy of the population in the first 3000 iterations for a high error rate $\epsilon = 0.4$. The error bands show the 0^{th} and 100^{th} percentile across all 50 independent simulations . We choose other parameters as follows: the error rate

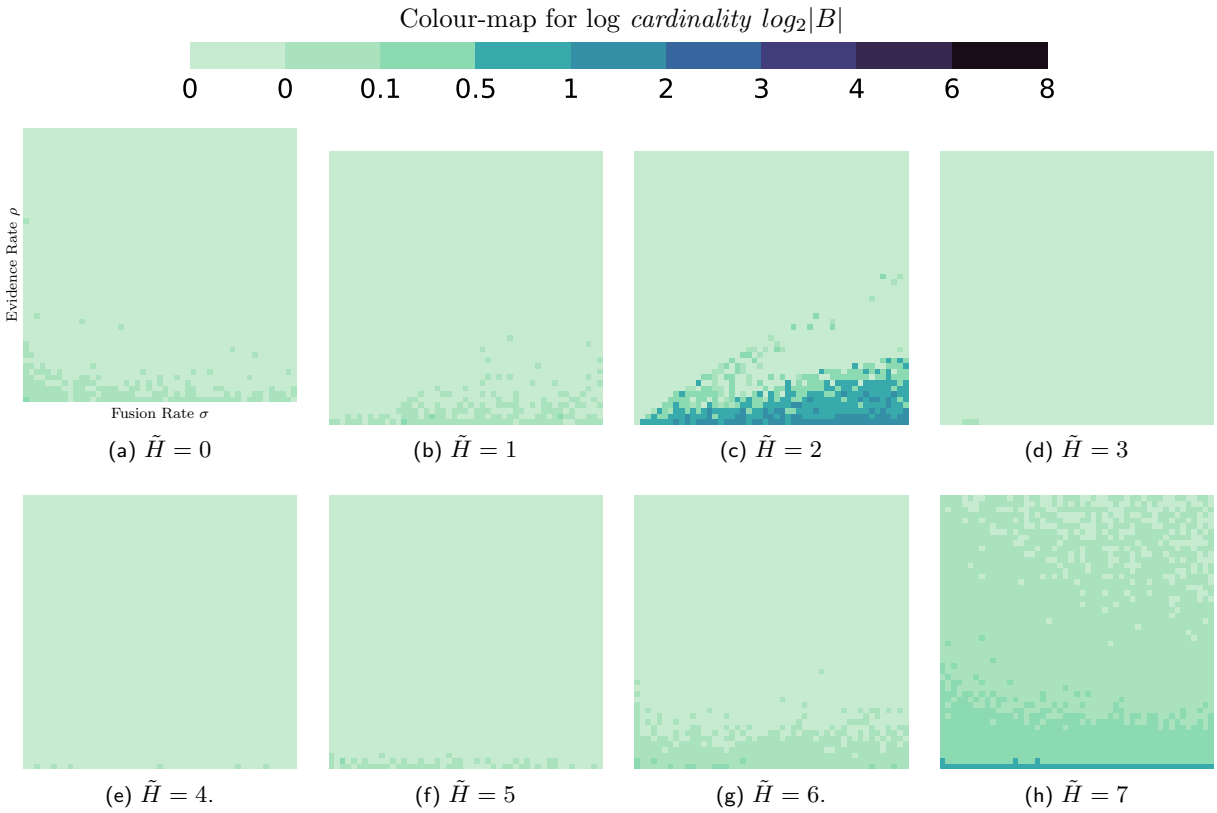

(a) $\tilde{H} = 0$ (b) $\tilde{H} = 1$ (c) $\tilde{H} = 2$ (d) $\tilde{H} = 3$

(e) $\tilde{H} = 4$. (f) $\tilde{H} = 5$ (g) $\tilde{H} = 6$. (h) $\tilde{H} = 7$

Figure 5.7: Average cardinality $log_2|B|$ at steady state for different evidence imprecision defined by various Hamming thresholds $\tilde{H}$ and $\epsilon = 0.4$, $\sigma \in [0, 1)$, and $\rho \in (0, 1)$. The axis labels for the heat maps are provided in the top left figure as an example.

$\epsilon = 0.4$ and the threshold $\tilde{H} = 2$, for which the performance using different methods varies the most. In Figure 5.8 we see the hybrid approach (green lines) consistently outperforms negative updating (orange lines) and DP updating (blue lines), showing both higher average accuracy and reduced performance fluctuation than its counterparts for all combinations of ρ and σ. The improvements are more significant when the evidence rate is low and the fusion rate is relatively high. In Figures 5.8h and 5.8i we see that the populations using the hybrid approach achieve accuracy over 0.9 while both the negative and DP updating methods showing similar performance, $\alpha \approx 0.75$. Although Figures 5.2e, 5.2f and 5.6c show that populations using the hybrid updating approach converge significantly slower than those using the other two methods for the same evidence and fusion rate combinations, the speed-accuracy trade-off is actually less significant as the new approach achieves higher accuracy than its counterparts before convergence. For example, the accuracy of the hybrid approach surpasses the other two methods within 200 iterations on average and reaches 0.9 at around 600^{th} iterations in Figures 5.8h and 5.8i. When the evidence rate is intermediate to high and the fusion rate is not higher than the evidence rate, in Figures 5.8a to 5.8e, we see that the populations using the hybrid

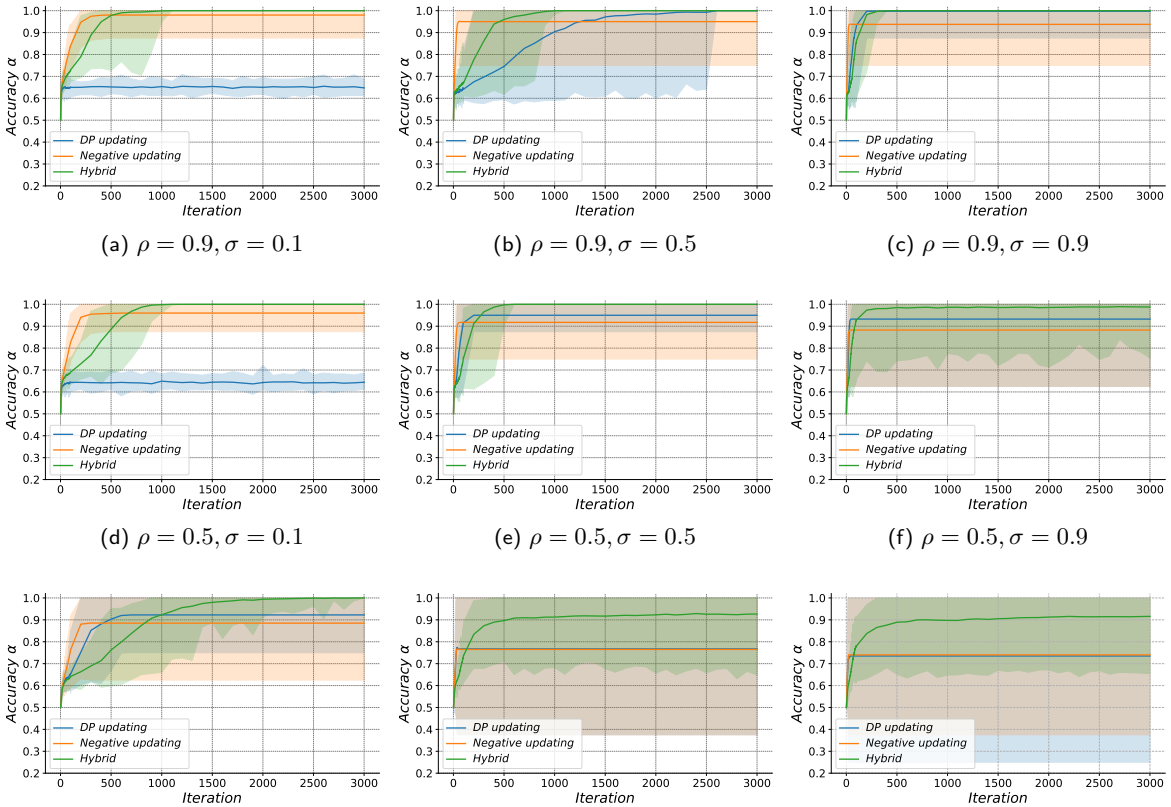

(a) $\rho = 0.9, \sigma = 0.1$ (b) $\rho = 0.9, \sigma = 0.5$ (c) $\rho = 0.9, \sigma = 0.9$

(d) $\rho = 0.5, \sigma = 0.1$ (e) $\rho = 0.5, \sigma = 0.5$ (f) $\rho = 0.5, \sigma = 0.9$

(g) $\rho = 0.1, \sigma = 0.1$ (h) $\rho = 0.1, \sigma = 0.5$ (i) $\rho = 0.1, \sigma = 0.9$

Figure 5.8: Average accuracy for the first 3000 iterations for evidence rate $\rho \in \{0.1, 0.5, 0.9\}$, fusion rate $\sigma \in \{0.1, 0.5, 0.9\}$, error rate ϵ=0.4, and evidential imprecision $\tilde{H} = 2$. The shaded error bands around the curve represent the 0^{th} and 100^{th} percentiles.

approach converge on the true state of the world for all 50 runs, whereas at least one of the other two methods also achieves high accuracy over 0.95 with some fluctuation. Furthermore, when both the evidence and fusion rates are low ($\rho = \sigma = 0.1$), we see in Figure 5.8g accuracy of systems using the hybrid approach overtake those using negative updating ($\alpha = 0.88$ from the 200^{th} iteration) after 800 iterations and then surpass those using DP updating ($\alpha = 0.92$ from the 600^{th} iteration) after 1000 iterations. In summary, more significant speed-accuracy trade-off is observed for lower evidence rates and fusion rates.

Additionally, we show Figure 5.9 for the average cardinality of the agents' beliefs during 20000 iterations. For a majority of the evidence and fusion rate combinations, the agents' average belief cardinality eventually converges to 1 for all three methods. Notably, when employing the DP updating strategy, there is a noticeable fluctuation in the average cardinality particularly when the evidence rate significantly outweighs the fusion rate, ranging from 4 to 16 from the 500^{th} to the 20000^{th} iteration, as observed in Figures 5.9a and 5.9d. The low accuracy observed in Figures 5.8a and 5.8d is likely to be a consequence of the difficult conditions under which

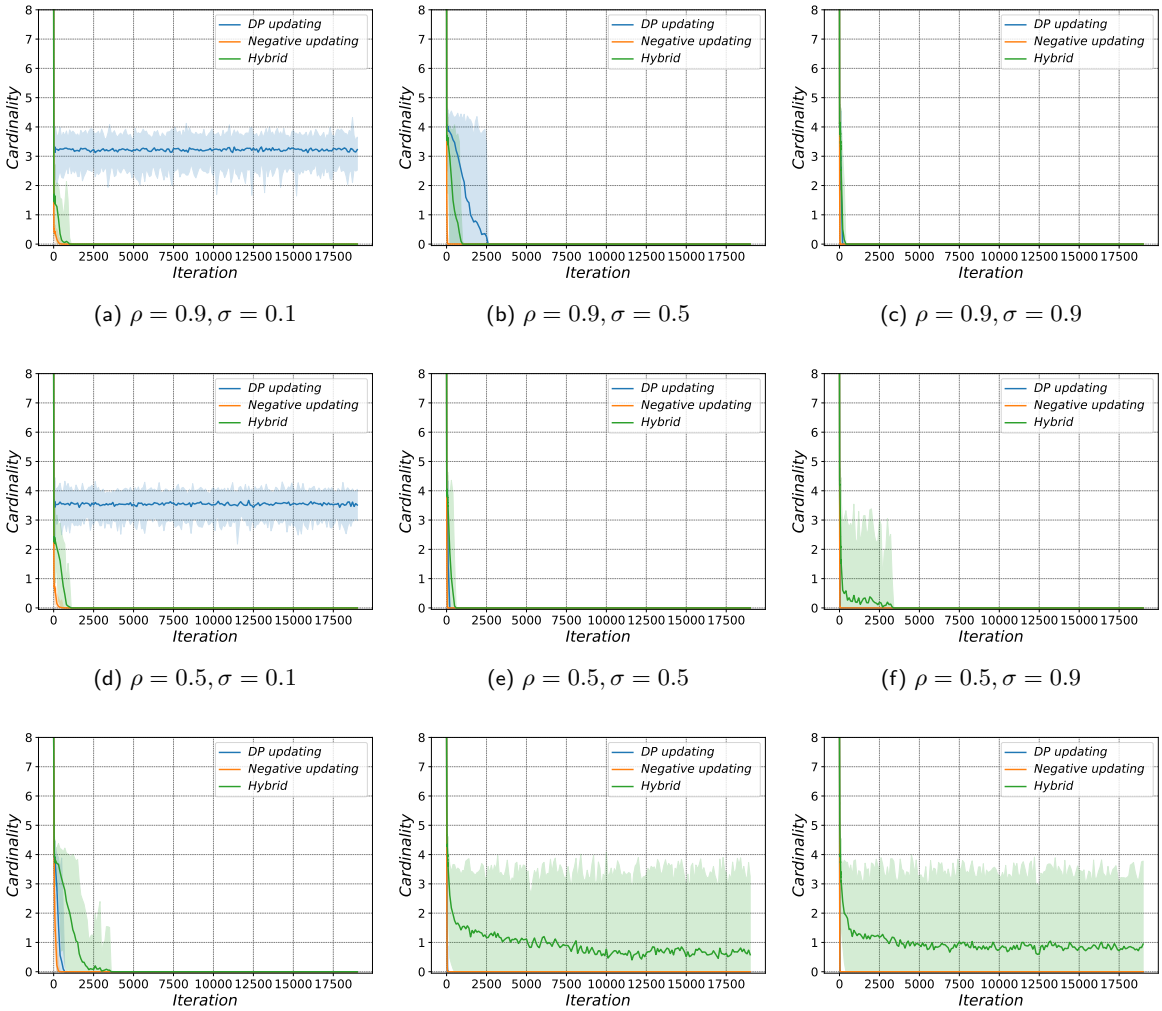

(a) $\rho = 0.9, \sigma = 0.1$ (b) $\rho = 0.9, \sigma = 0.5$ (c) $\rho = 0.9, \sigma = 0.9$

(d) $\rho = 0.5, \sigma = 0.1$ (e) $\rho = 0.5, \sigma = 0.5$ (f) $\rho = 0.5, \sigma = 0.9$

(g) $\rho = 0.1, \sigma = 0.1$ (h) $\rho = 0.1, \sigma = 0.5$ (i) $\rho = 0.1, \sigma = 0.9$

Figure 5.9: Average cardinality for evidence rate $\rho \in \{0.1, 0.5, 0.9\}$, fusion rate $\sigma \in \{0.1, 0.5, 0.9\}$, error rate ϵ=0.4, and evidential imprecision $\tilde{H} = 2$. The shaded error bands around the curve represent the 0^{th} and 100^{th} percentiles.

populations struggle to converge. The introduction of the hybrid approach effectively addresses these convergence challenges. Nonetheless, there are instances that the hybrid method itself experiences convergence issues, when the fusion rate is relatively high compared to the fusion rate, as shown in Figures 5.9h and 5.9i. In such scenarios, the agents' belief cardinality averages out at around 2 from the 2500^{th} iteration. Despite the convergence issues, the hybrid approach still consistently emerges as the most accurate strategy in such scenarios, as evidenced by Figures 5.8h and 5.8i.

5.4 Discussion and Conclusion

In this chapter, we have explored an evidential updating strategy for social learning models based on the Dubois&Prade combination rule and compared it with the classic negative updating strategy. In addition, we have also proposed a new approach using a integrated method of these two strategies of evidential updating. The proposed hybrid approach introduced the idea of rough beliefs to the evidential updating process and blurred the traditional boundary between evidential updating and belief fusion, by holding evidence that is inconsistent with the agent's belief by an upper belief to the fusion process.

Using agent-based simulation experiments, we have demonstrated that for a medium error rate $\epsilon = 0.3$ and for the optimal levels of evidential imprecision, populations using DP updating achieve higher accuracy when the evidence rate is low compared to the fusion rate than negative updating, i.e. DP updating is more robust to different evidence and fusion rates. For a lower error rate $\epsilon = 0.2$, we observed very similar performance of both accuracy and the time cost for both updating methods. However, when the error rate is high, i.e. $\epsilon = 0.4$, although systems using DP updating achieve higher accuracy for some combinations of evidence and fusion rates, they struggled to converge for low fusion rates and $\tilde{H} \in [0, 3]$ and the learning accuracy is extremely low in those scenarios. Further exploration into the convergence issue is required for future research.

To overcome the convergence failure of DP updating, we proposed a new approach that integrated both methods to gain the strength of both of them. By analysing the different dynamics of these methods by comparing them in different scenarios, we have demonstrated that the newly proposed approach can enhance the learning accuracy of the social learning model, especially in highly noisy environments, with slightly higher time costs. In addition to the increased time cost, another limitation of the proposed approach is that it might require more communication bandwidth to send over the upper and lower belief sets independently to other agents. Based on the study in this chapter and Section 3.3.2, the model can be further investigated with robotics applications to validate its efficacy and its time cost in practical applications.

Chapter 6

Conclusion

In Distributed AI and Multi-Agent Systems, social learning plays a critical role in enabling agents to adapt and make decisions collectively. In this thesis we have argued that intentionally increasing imprecision in the processes used by social learning models has a positive impact on the ability of the system to learn. From this perspective, we have proposed a propositional model where the imprecision of an agent's belief can be directly represented by the cardinality of their belief set. Based on this model, we have introduced imprecise evidential updating processes and imprecise belief fusion. We have then studied this model in simulation using both multi-agent systems and multi-robot systems and highlighted the strengths and limitations of the proposed approaches. In this chapter we will summarise the key contributions and findings of this thesis, which has focused on the role of imprecision in models for social learning. We will also discuss future research directions in the application of social learning in these systems.

In Chapter 2 we described the propositional model in a social learning context. The proposed model is distinct from other existing ones due to the agent's belief about the world being represented by a set of possible states of the world, consisting of an n-proposition tuple. The true state of the world is therefore one of the many possible states, and the agents must learn to identify which is the true state out of the set of all possible states. In other words, the population needs to identify the truth value for every proposition instead of the single, optimal option; such is the case in the best-of-n problem. We first introduced a set-based fusion operator for combining two, possibly conflicting, beliefs, and then conducted agent-based simulation experiments to study our proposed fusion operator. We find that the intersection-union fusion operator generally performs well in noisy environments with limited direct evidence. However, the effectiveness of social learning depends on the balance between the evidence rate ρ and the fusion rate σ. We further extended the study by introducing a parameterised imprecise fusion operator, allowing for the fusion process to produce fused beliefs with variable levels of imprecision. Our findings reveal that when the fusion rate σ is high compared to the evidence rate ρ, a less precise fusion operator leads to better outcomes. Importantly, it turns out that the ideal level of imprecision in the fusion operator is primarily dictated by the rate of belief

fusion and evidence gathering, rather than being significantly influenced by the degree to which the evidence is noisy.

In Chapter 3 we investigated the impact of imprecise evidence on the social learning model described in Chapter 2. We have emphasised the differences between imprecision and error in a set-based social learning model. Our agent-based simulations show that the model is robust to varying levels of imprecise evidence, as well as in the multi-robot location classification tasks. For the robotic classification task, the model scales well in situations where the number of locations is greater than the number of robots, and it performs effectively even with limited access to some locations. However, it requires prior knowledge of location positions. In addition, In addition, the performance of the system can be improved when a certain type of imprecise evidence is adopted; specifically, when the agents receive an estimate of the state of the world in the form of a singular, precise state and then use our Hamming neighbourhood approach to imprecisify the estimate to a set including multiple possibly-true states. The simulation results indicate that optimal accuracy and quickest convergence are achieved at a low-to-intermediate level of precision, and the optimal level of imprecision is influenced by the error rate. In higher error situations, the optimal level of evidential imprecision tend to be more imprecise. This type of imprecise evidence also make the system more robust to changes in fusion and evidence rates. For high error scenarios the most imprecise evidential model is also the most robust at a high tolerance level.

In Chapter 4 we explored how combining imprecise fusion operators, proposed in Chapter 2, and imprecise evidential updating, introduced in Chapter 3, can improve the performance of social learning models. Through agent-based simulation, we discovered that using a low-to-moderate level of imprecision in both evidence updating and belief fusion improves the accuracy of learning outcomes, especially when the evidence rate is low compared to the fusion rate. This results is consistent our conclusions in Chapters 2 and 3 in which imprecise fusion and imprecise evidential updating are applied independently. This combined approach also presents a speed-accuracy trade-off: higher accuracy is achieved at the expense of slower learning speed, which becomes more pronounced when the fusion rate is high and evidence rate is low. With respect to robustness, we found that selecting appropriate levels of imprecision depends on the acceptable error level. Additionally, we examined how the system's robustness varies with different evidence and fusion rates. Results showed that for higher levels of accepted error the systems should employ more imprecise fusion for more robustness to the changes in fusion and evidence rate, however, the optimal level of evidential imprecision differs based on the accepted error level. Finally, this chapter highlights the importance of carefully choosing and adapting imprecision levels to fulfill specific system requirements and tolerances for error, all while considering the balance needed to achieve the desired learning outcomes.

In Chapter 5, we compared the evidential updating strategy based on Dubois&Prade (DP) fusion operator with the traditional negative updating approach in social learning models.

We also introduced a hybrid method that combines both strategies. Through agent-based simulations, we found that DP updating performs better in terms of accuracy when the evidence rate is low compared to the fusion rate, specifically at a medium error rate. However, the method struggles to converge in high-error scenarios. To address this, we introduced a hybrid approach that combines the strengths of both DP and negative updating. This new model enhances learning accuracy, particularly in noisy environments, albeit with slightly higher time costs. We also noted that the hybrid model might require additional communication bandwidth, as it needs to send over both the evidence and belief sets to other agents. In light of these findings, we suggest that future research should focus on the underlying dynamics of the convergence issues associated with DP updating and explore the potential for applying our hybrid model in practical scenarios, such as the robotic location classification task introduced in Section 3.3.2. This will validate not only its efficacy but also its operational costs in real-world applications.

While our findings contribute to the understanding of the role of imprecise information in collective decision-making, they have also opened up a variety of research opportunities in the area of social learning in distributed AI and Multi-Agent Systems. These avenues for future research could be both extensions of the work already done or refinements that add precision, robustness, or scalability to existing models or frameworks. Incorporating these various elements into the existing framework could potentially transform it from a largely theoretical construct into a versatile tool for solving complex, real-world problems using distributed AI and multi-robot systems.

Firstly, the operator for belief fusion in the current framework is designed for pairwise interactions among agents. The pooling size of agents interaction has a significant impact on the speed and accuracy of collective decision-making task proposed in [63]. Therefore, one of the immediate extensions could involve expanding the model to facilitate belief fusion in larger pools of agents to investigate how the number of agents fusing their belief impacts on the learning outcome of our proposed model. A generalised version of the belief fusion operator (Equation (2.3)) was proposed in [15, Eq.4] using the idea of maximal-consistent subset [83], which can fuse n sources rather than just 2. By increasing the size of the pool, we might gain more rapid spread of information and faster learning, especially when individual agents have incomplete information. Therefore, the system could achieve more rapid convergence with greater pool size, which could be particularly useful in applications such as emergency response systems, where each agent might have a unique and critical piece of information. However, it should be noted that the increase of the agent pool could compromise the accuracy of learning outcomes [63]. This is an ongoing problem that requires further exploration.

The communication architecture in the current model assumes a fully connected network and we use a probabilistic fusion rate to model the real-world constrains. Recent studies shows that constrained communication can improve the performance of social learning [8, 38]. Our conclusion supports these findings; in our model the social learning is both more accurate and

rapid when the fusion rate is low. While the probabilistic model is useful for theoretical proofs and simulations, the actual network topologies of the system might be more complicated in practice. Therefore, a significant line of future work could focus on investigating the model's performance under different interaction network architectures, such as small-world or scale-free networks. Studying how these topological variations affect the speed and accuracy of social learning could bring us closer to practical implementations and a better understanding of the relationship between communication constraints and social learning performance.

In addition to factors like interaction network connectivity and physical communication range limitations, introducing a preference or hierarchy for fusion partners over random selection can enhance social learning performance. Currently, all agents are treated equally in belief fusion events. For the rationale of the potential of this direction, we show Figure 6.1 for preliminary results when removing the equality of agents during pooling. In non-random fusion, the agents are not randomised before entering the pairwise pooling process, leading to a deterministic selection of fusion partners. Specifically, agents are will combine beliefs with those that have smaller indices in the pre-arranged order, as opposed to the random fusion where agents have an equal probability of being paired with any other agent. For example, consider a pool of agents with indices $[1, 2, 3, 4]$; the fusion pairs would be deterministic, $[1, 2]$ and $[3, 4]$. If the pool were $[1, 3, 4, 5]$, the pairs would then be $[1, 3]$ and $[4, 5]$. From the figure we see that this modification improves overall accuracy when the fusion rates is high, for both the most precise evidence and at optimal levels of evidential imprecision.

Heterogeneity among agents can be further studied as well. Heterogeneity among agents could be beneficial or even crucial for the overall performance and adaptability of a multi-agent system. In a multi-armed bandit problem, the best performance is achieved by a population consisting of different types of social learning agents [84]. Varying the fusion and evidence-updating strategies within the population can also improve the robustness of the social learning model in dynamic environments [85]. Exploring variations in fusion and evidence thresholds across diverse agents offers a promising direction for improving the robustness and adaptability of multi-agent systems in future research.

Another future direction lies in the specifics of the Hamming neighbourhood model used for the imprecise evidential updating. As it stands, the agents in our model must require a complete estimate of the state of the world for the evidential updating event, i.e. they need to receive information about every proposition under consideration. However, in real-world scenarios, agents often have limited capacity and can only operate partial information, as the robotic simulation we investigated in Section 3.3.2. An extension to the current work could explore the dynamics of learning and decision-making based on incomplete estimates. This is not merely an academic exercise; it reflects the constraints of many real-world applications where full information is often unavailable or too costly to acquire. A model that can handle partial estimates could provide a more flexible and realistic framework for social learning

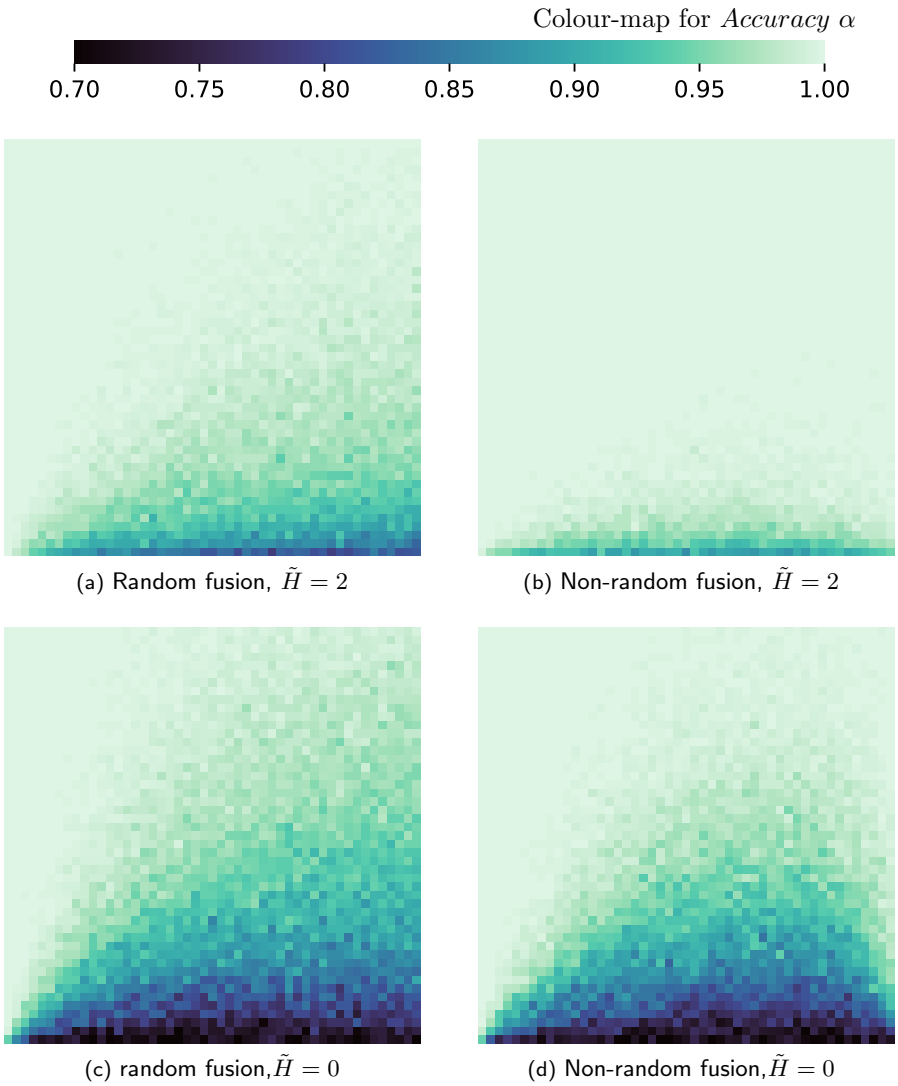

(a) Random fusion, $\tilde{H} = 2$ (b) Non-random fusion, $\tilde{H} = 2$

(c) random fusion,$\tilde{H} = 0$ (d) Non-random fusion,$\tilde{H} = 0$

Figure 6.1: Average accuracy at steady state for $(\rho, \sigma) \in (0, 1)^2$, $\epsilon = 0.3$, $\tilde{H} \in \{0, 2\}$, and for random fusion(left) and non-random fusion (right). In scenarios where fusion is non-random, systems with high fusion rates exhibit enhanced accuracy, in contrast to the diminished performance observed in random fusion contexts.

in distributed systems. Building on these directions, we can also further advance the social learning model into more robotic simulations. Specifically, the imprecise evidence model could be implemented within a robotic location classification task, with partial or complete information collected, depending on the parameter N_u. Furthermore, while the current model uses Hamming distance-based measure for evidential imprecision and Jaccard similarity coefficients for fusion imprecision, the door is open to experiment with other types of distance or similarity measures. For example, we can use the Jaccard operator for evidential udpating and Hamming distance based method for belief fusion.

The impact of physical movement of agents on the learning outcome can be further studied, for example, belief fusion event may occur when agents are in close proximity to one another rather than at fixed location as studied in Section 3.3.2. In other words, movement patterns can affect how information is disseminated among agents. For example, in a swarm of robots, their spatial arrangement and movement could influence how quickly and accurately they learn about their environment. The frequency and nature of interactions between agents can change depending on their movement. Agents that move and encounter different peers might have more diverse information, affecting the learning process and outcomes and leading to different learning outcomes. For example, agents that move randomly might learn slower than those following a strategic pattern to cover more area or interact with more peers. The idea of the proposed imprecise belief updating and fusion model may also be applied in the research of opinion dynamics. For example, how imprecision influences opinion formation, information diffusion, polarisation, consensus, and opinion cascades. Comparisons with existing models, real-world applications, and robustness assessments can further advance our understanding.

A notable limitation of the current algorithm is its assumption of a static environment, which may limit its applicability in scenarios where conditions and variables are subject to change over time. Addressing this limitation opens a promising avenue for research, particularly in the exploration of the algorithm's adaptability to dynamic environments. A structured approach to this exploration could involve introducing temporal variability into the propositions, thereby simulating the evolving nature of real-world environments. This modification would enable a systematic investigation into the algorithm's responsiveness and adaptability to changes, focusing on metrics such as the speed of response and the accuracy of decision-making in the face of fluctuating conditions.

In conclusion, this thesis has navigated a social learning model for multi-agent system, focussing on the role of imprecision in both evidential updating and belief fusion, as well as their combined effects. We have clarified the difference between imprecision and inaccuracy of evidence in noisy environment and demonstrated a pathway using imprecision toward enhanced robustness and accuracy of social learning, especially in scenarios where the evidence collect by agents are noisy. While our findings contribute to the understanding of the role of imprecise information in collective decision-making, they also raise further questions that beckon further investigation. As we have identified, the challenge of achieving a balance between the speed of learning and its accuracy remains a salient concern. The practical implications of our work are also worth noting, for example, our model has the potential to be useful in a location classification task, where robots often operate with incomplete or imprecise information. The applicability of our model in real-world scenarios, such as search and rescue operations involving robots, opens up exciting avenues for future research. Finally, this thesis contributes to the broader fields of multi-agent systems, social learning, and artificial intelligence by offering a new way to think about the use of imprecise information. We anticipate that this work will

spur further research, both theoretical and practical, in these important areas.

Appendix A

List of Notations

Propositions and states	
p	Propositions
s	States
$\mathbb{S}$	All possible states of the world
s^*	The true state of the world
s_e	States received as evidence
Evidence and belief	
E	Evidence
B	Beliefs
$\underline{B}$	Lower beliefs
$\overline{B}$	Upper beliefs

Beliefs after a updating-fusion sequence	
B_n	by negative updating
B_{dp}	by DP updating
B_h	by the hybrid updating
Probabilistic rates	
σ	Fusion rate
ρ	Evidence rate
ϵ	Error rate
Modelling parameters	
$\mathcal{A}$	A population of agents
n	Language size, the number of propositions
k	Population size, the number of agents
N_u	The maximum number of locations a robot can visit in a single evidence collection episodes

γ	Imprecise belief fusion threshold
$\tilde{H}$	Imprecise evidential updating threshold
H	Hamming distance
J	Jaccard similarity
Fusion operators and updating methods	
$\odot_\gamma$	Imprecise belief fusion operator
$\odot$	Intersection-union or Dubois&Prade operator
$\otimes$	Belief fusion operator for rough beliefs
$\|\|$	Hybrid updating
Evaluation	
α	Accuracy
θ	The average proportion of propositions about which agent are correct or uncertain about
F_β	F_β score
Robustness	
δ	Level of error tolerance
$\hat{h}$	Level of robustness
$\hat{h}(\delta)$	Function of robustness given δ

Appendix B

Proof of Relationships Between Different Evidential Updating Approaches

The objective of this appendix is to prove the relationship between the fused beliefs obtained using various methods, as outlined in equation Equation (5.4) of the main text. We will employ mathematical derivations to substantiate that the hybrid method, denoted as B_h, yields beliefs that are the union of those acquired through the negative B_n and DP B_{dp} methods.

We let $\{B_1, \mathrm{E}_1, B_2, \mathrm{E}_2\}$ be the beliefs before updating and the collected evidence of the two agents respectively. For notational convenience we let $I = (B_1 \cap \mathrm{E}_2) \cup (B_2 \cap \mathrm{E}_1) \cup (\mathrm{E}_1 \cap \mathrm{E}_2)$. We first consider the scenario where both agents receive inconsistent evidence and the updating-fusion belief transition functions is as follows:

Theorem B.1 (Negative updating and Dubois&Prade fusion)**.** *For* $\forall i \in \{1, 2\}, B_i \cap \mathrm{E}_i = \emptyset$*:*

$$B_n = B_1|\,\mathrm{E}_1 \odot B_2|\,\mathrm{E}_2 = B_1 \odot B_2 = \begin{cases} B_1 \cap B_2 & :\ B_1 \cap B_2 \neq \emptyset \\ B_1 \cup B_2 & : Otherwise \end{cases}$$

Theorem B.2 (DP updating and Dubois&Prade fusion)**.** *For* $\forall i \in \{1, 2\}, B_i \cap \mathrm{E}_i = \emptyset$*:*

$$B_{dp} = (B_1 \odot \mathrm{E}_1) \odot (B_2 \odot \mathrm{E}_2) = \begin{cases} (B_1 \cap B_2) \cup I & : B_1 \cap B_2 \neq \emptyset \\ I & : B_1 \cap B_2 = \emptyset \text{ and } I \neq \emptyset \\ B_1 \cup B_2 \cup \mathrm{E}_1 \cup \mathrm{E}_2 & : Otherwise \end{cases}$$

Theorem B.3 (The hybrid approach)**.** *For* $\forall i \in \{1, 2\}, B_i \cap \mathrm{E}_i = \emptyset$*:*

$$B_h = B_1||\,\mathrm{E}_1 \otimes B_2||\,\mathrm{E}_2 = \begin{cases} B_{dp} \supseteq B_n & :\ B_1 \cap B_2 \neq \emptyset \\ B_{dp} \cup B_1 \cup B_2 = B_{dp} \cup B_n & : B_1 \cap B_2 = \emptyset \text{ and } I \neq \emptyset \\ B_{dp} \supseteq B_n & : Otherwise \end{cases}$$

From Theorem B.1 to Theorem B.3 we show the transition models for scenarios where both agents receives evidence that is inconsistent with their beliefs during the preceding evidence collection episode. We have proven that $B_h = B_{dp} \cup B_n$ stands in these cases. We then consider the scenarios where only one of the agent receives inconsistent evidence. Without loss of generality, we assume that $\underline{B}_1 = B_1 \cap \mathrm{E}_1 \neq \emptyset$ and $B_2 \cap \mathrm{E}_2 = \emptyset$. The transition models are then as follows:

Theorem B.4 (Negative updating and Dubois&Prade fusion)**.** *Suppose* $B_1 \cap \mathrm{E}_1 \neq \emptyset$ *and* $B_2 \cap \mathrm{E}_2 = \emptyset$*:*

$$B_n = B_1|\,\mathrm{E}_1 \odot B_2|\,\mathrm{E}_2 = \begin{cases} \underline{B}_1 \cap B_2 & : \ \underline{B}_1 \cap B_2 \neq \emptyset \\ \underline{B}_1 \cup B_2 & : \mathit{Otherwise} \end{cases}$$

Theorem B.5 (DP updating and Dubois&Prade fusion)**.** *Suppose* $B_1 \cap \mathrm{E}_1 \neq \emptyset$ *and* $B_2 \cap \mathrm{E}_2 = \emptyset$*:*

$$B_{dp} = (B_1 \odot \mathrm{E}_1) \odot (B_2 \odot \mathrm{E}_2) = \begin{cases} \underline{B}_1 \cap B_2 \cup (\underline{B}_1 \cap \mathrm{E}_2) & : \ \underline{B}_1 \cap B_2 \neq \emptyset \\ \underline{B}_1 \cap \mathrm{E}_2 & : \ \underline{B}_1 \cap B_2 = \emptyset \ \mathit{and} \ \underline{B}_1 \cap \mathrm{E}_2 \neq \emptyset \\ \underline{B}_1 \cup B_2 \cup \mathrm{E}_2 & : \mathit{Otherwise} \end{cases}$$

Theorem B.6 (The hybrid approach)**.** *Suppose* $B_1 \cap \mathrm{E}_1 \neq \emptyset$ *and* $B_2 \cap \mathrm{E}_2 = \emptyset$*:*

$$B_1||\,\mathrm{E}_1 \otimes B_2||\,\mathrm{E}_2 = \begin{cases} B_{dp} \supseteq B_n & : \ \underline{B}_1 \cap B_2 \neq \emptyset \\ B_{dp} \cup \underline{B}_1 \cup B_2 = B_{dp} \cup B_n & : \ \underline{B}_1 \cap B_2 = \emptyset \ \mathit{and} \ \underline{B}_1 \cap \mathrm{E}_2 \neq \emptyset \\ B_{dp} \supseteq B_n & : \mathit{Otherwise} \end{cases}$$

From Theorem B.4 to Theorem B.6, we have proven that $B_h = B_{dp} \cup B_n$ holds in this case. For other scenarios, where both agents receive consistent evidence, these methods yield the same fusion results; therefore, $B_h = B_{dp} \cup B_n$ also holds. In conclusion, as we have demonstrated, this holds in all cases, whether agents receive consistent or inconsistent evidence.

Bibliography

[1] Cecilia M Heyes.
Social learning in animals: categories and mechanisms.
Biological Reviews, 69(2):207–231, 1994.

[2] Robert Boyd, Peter J Richerson, and Joseph Henrich.
The cultural niche: Why social learning is essential for human adaptation.
Proceedings of the National Academy of Sciences, 108(supplement_2):10918–10925, 2011.

[3] Bert Hölldobler and Edward O Wilson.
The ants.
Harvard University Press, 1990.

[4] Karl von Frisch.
The dance language and orientation of bees.
Harvard University Press, 1993.

[5] Nigel R Franks, Anna Dornhaus, Jon P Fitzsimmons, and Martin Stevens.
Speed versus accuracy in collective decision making.
Proceedings of the Royal Society of London. Series B: Biological Sciences, 270(1532): 2457–2463, 2003.

[6] PG Balaji, Gaurav Sachdeva, Dipti Srinivasan, and Chen-Khong Tham.
Multi-agent system based urban traffic management.
In *2007 IEEE Congress on Evolutionary Computation*, pages 1740–1747. IEEE, 2007.

[7] Virginia Bordignon, Vincenzo Matta, and Ali H Sayed.
Adaptive social learning.
IEEE Transactions on Information Theory, 67(9):6053–6081, 2021.

[8] Mohamed S. Talamali, Arindam Saha, James A. R. Marshall, and Andreagiovanni Reina.
When less is more: Robot swarms adapt better to changes with constrained communication.
Science Robotics, 6(56):1416, 2021.

[9] Dominik Deffner, Vivien Kleinow, and Richard McElreath.
Dynamic social learning in temporally and spatially variable environments.
Royal Society open science, 7(12):200734, 2020.

[10] Mauro S Innocente and Paolo Grasso.
Self-organising swarms of firefighting drones: Harnessing the power of collective intelligence in decentralised multi-robot systems.
Journal of Computational Science, 34:80–101, 2019.

[11] Mac Schwager, Philip Dames, Daniela Rus, and Vijay Kumar.
A multi-robot control policy for information gathering in the presence of unknown hazards.
In *Robotics research*, pages 455–472. Springer, 2017.

[12] Chanelle Lee, Jonathan Lawry, and Alan FT Winfield.
Negative updating applied to the best-of-n problem with noisy qualities.
Swarm Intelligence, pages 1–33, 2021.

[13] Mohamed S Talamali, James AR Marshall, Thomas Bose, and Andreagiovanni Reina.
Improving collective decision accuracy via time-varying cross-inhibition.
In *2019 International conference on robotics and automation (ICRA)*, pages 9652–9659. IEEE, 2019.

[14] Jonathan Lawry and Chanelle Lee.
Probability pooling for dependent agents in collective learning.
Artificial Intelligence, 288:103371, 2020.

[15] Didier Dubois, Weiru Liu, Jianbing Ma, and Henri Prade.
The basic principles of uncertain information fusion. an organised review of merging rules in different representation frameworks.
Information Fusion, 32:12–39, 2016.

[16] Jaakko Hintikka.
Knowledge and belief: an introduction to the logic of the two notions.
1962.

[17] M Vardi.
On the complexity of epistemic reasoning.
In *Proceedings. Fourth Annual Symposium on Logic in Computer Science*, pages 243–244, 1989.

[18] Enrique H Ruspini.
Epistemic logics, probability, and the calculus of evidence.

In *Proceedings of the 10th international joint conference on Artificial intelligence-Volume 2*, pages 924–931, 1987.

[19] Jonathan Lawry, Michael Crosscombe, and David Harvey.
Epistemic sets applied to best-of-n problems.
In *European Conference on Symbolic and Quantitative Approaches with Uncertainty*, pages 301–312. Springer, 2019.

[20] Gabriele Valentini, Heiko Hamann, Marco Dorigo, et al.
Self-organized collective decision making: the weighted voter model.
In *AAMAS*, pages 45–52, 2014.

[21] Michael Crosscombe, Jonathan Lawry, Sabine Hauert, and Martin Homer.
Robust distributed decision-making in robot swarms: Exploiting a third truth state.
In *2017 IEEE/RSJ International Conference on Intelligent Robots and Systems (IROS)*, pages 4326–4332. IEEE, 2017.

[22] Nicolas Schwind, Katsumi Inoue, Gauvain Bourgne, Sébastien Konieczny, and Pierre Marquis.
Belief revision games.
In *Proceedings of the AAAI Conference on Artificial Intelligence*, volume 29, 2015.

[23] Laurence Cholvy.
Opinion diffusion and influence: A logical approach.
International Journal of Approximate Reasoning, 93:24–39, 2018.

[24] Glenn Shafer.
A mathematical theory of evidence, volume 42.
Princeton university press, 1976.

[25] AP Dempster.
Upper and lower probabilities induced by a multivalued mapping.
The Annals of Mathematical Statistics, 38(2):325–339, 1967.

[26] Michael Crosscombe, Jonathan Lawry, and Palina Bartashevich.
Evidence propagation and consensus formation in noisy environments.
In *International Conference on Scalable Uncertainty Management*, pages 310–323. Springer, 2019.

[27] Rainer Hegselmann, Ulrich Krause, et al.
Truth and cognitive division of labor: First steps towards a computer aided social epistemology.
Journal of Artificial Societies and Social Simulation, 9(3):10, 2006.

[28] Igor Douven and Christoph Kelp.
Truth approximation, social epistemology, and opinion dynamics.
Erkenntnis, 75(2):271, 2011.

[29] Rodrigo J De Marco, Juan M Gurevitz, and Randolf Menzel.
Variability in the encoding of spatial information by dancing bees.
Journal of experimental biology, 211(10):1635–1644, 2008.

[30] Bernd Meyer, Cedrick Ansorge, and Toshiyuki Nakagaki.
The role of noise in self-organized decision making by the true slime mold physarum polycephalum.
PloS one, 12(3):e0172933, 2017.

[31] Audrey Dussutour, Madeleine Beekman, Stamatios C Nicolis, and Bernd Meyer.
Noise improves collective decision-making by ants in dynamic environments.
Proceedings of the Royal Society B: Biological Sciences, 276(1677):4353–4361, 2009.

[32] Li Zou, Xin Liu, and Yang Xu.
Resolution method of linguistic truth-valued propositional logic.
In *2005 International Conference on Neural Networks and Brain*, volume 3, pages 1996–1999. IEEE, 2005.

[33] Rosanna Keefe and Peter Smith.
Vagueness: A reader.
MIT press, 1996.

[34] Stephen Cole Kleene.
On notation for ordinal numbers.
The Journal of Symbolic Logic, 3(4):150–155, 1938.

[35] Davide Ciucci, Didier Dubois, and Jonathan Lawry.
Borderline vs. unknown: comparing three-valued representations of imperfect information.
International Journal of Approximate Reasoning, 55(9):1866–1889, 2014.

[36] Reza Olfati-Saber and Richard M Murray.
Consensus problems in networks of agents with switching topology and time-delays.
IEEE Transactions on automatic control, 49(9):1520–1533, 2004.

[37] Wei Ren, Randal W Beard, and Ella M Atkins.
A survey of consensus problems in multi-agent coordination.
In *Proceedings of the 2005, American Control Conference, 2005.*, pages 1859–1864. IEEE, 2005.

[38] Michael Crosscombe and Jonathan Lawry.
The impact of network connectivity on collective learning.
In *International Symposium Distributed Autonomous Robotic Systems*, pages 82–94. Springer, 2021.

[39] Jingying Ma, Maojiao Ye, Yuanshi Zheng, and Yunru Zhu.
Consensus analysis of hybrid multiagent systems: a game-theoretic approach.
International Journal of Robust and Nonlinear Control, 29(6):1840–1853, 2019.

[40] Isabelle Bloch, Anthony Hunter, Alain Appriou, André Ayoun, Salem Benferhat, Philippe Besnard, Laurence Cholvy, Roger Cooke, Frédéric Cuppens, Didier Dubois, et al.
Fusion: General concepts and characteristics.
International journal of intelligent systems, 16(10):1107–1134, 2001.

[41] Kaitlyn Preece and Madeleine Beekman.
Honeybee waggle dance error: adaption or constraint? unravelling the complex dance language of honeybees.
Animal behaviour, 94:19–26, 2014.

[42] David JT Sumpter.
The principles of collective animal behaviour.
Philosophical transactions of the royal society B: Biological Sciences, 361(1465):5–22, 2006.

[43] Manuele Brambilla, Eliseo Ferrante, Mauro Birattari, and Marco Dorigo.
Swarm robotics: a review from the swarm engineering perspective.
Swarm Intelligence, 7:1–41, 2013.

[44] Chris Parker and Hong Zhang.
Cooperative decision-making in decentralized multiple-robot systems: The best-of-n problem.
IEEE/ASME Transactions on Mechatronics, 14(2):240–251, 2009.

[45] Thomas Schmickl, Ronald Thenius, Christoph Moeslinger, Gerald Radspieler, Serge Kernbach, Marc Szymanski, and Karl Crailsheim.
Get in touch: cooperative decision making based on robot-to-robot collisions.
Autonomous Agents and Multi-Agent Systems, 18:133–155, 2009.

[46] Simon Garnier, Jacques Gautrais, Masoud Asadpour, Christian Jost, and Guy Theraulaz.
Self-organized aggregation triggers collective decision making in a group of cockroach-like robots.
Adaptive Behavior, 17(2):109–133, 2009.

[47] Gabriele Valentini, Eliseo Ferrante, Heiko Hamann, and Marco Dorigo.
Collective decision with 100 kilobots: Speed versus accuracy in binary discrimination problems.
Autonomous agents and multi-agent systems, 30(3):553–580, 2016.

[48] Gabriele Valentini, Eliseo Ferrante, and Marco Dorigo.
The best-of-n problem in robot swarms: Formalization, state of the art, and novel perspectives.
Frontiers in Robotics and AI, 4:9, 2017.

[49] Qihao Shan, Alexander Heck, and Sanaz Mostaghim.
Discrete collective estimation in swarm robotics with ranked voting systems.
In *2021 IEEE symposium series on computational intelligence (SSCI)*, pages 1–8. IEEE, 2021.

[50] Michael Crosscombe and Jonathan Lawry.
Collective preference learning in the best-of-n problem: From best-of-n to ranking n.
Swarm Intelligence, 15(1-2):145–170, 2021.

[51] Qihao Shan and Sanaz Mostaghim.
Noise-resistant and scalable collective preference learning via ranked voting in swarm robotics.
Swarm Intelligence, 17(1-2):5–26, 2023.

[52] Ercan Yildiz, Asuman Ozdaglar, Daron Acemoglu, Amin Saberi, and Anna Scaglione.
Binary opinion dynamics with stubborn agents.
ACM Transactions on Economics and Computation (TEAC), 1(4):1–30, 2013.

[53] Chanelle Lee, Jonathan Lawry, and Alan Winfield.
Combining opinion pooling and evidential updating for multi-agent consensus.
2018.

[54] Michael Crosscombe, Jonathan Lawry, and David Harvey.
Distributed possibilistic learning in multi-agent systems.
In *The 3rd International Symposium on Swarm Behavior and Bio-Inspired Robotics*, 2019.

[55] Peter Emerson.
The original borda count and partial voting.
Social Choice and Welfare, 40:353–358, 2013.

[56] Christophe Osswald and Arnaud Martin.
Understanding the large family of dempster-shafer theory's fusion operators-a decision-based measure.

In *2006 9th International Conference on Information Fusion*, pages 1–7. IEEE, 2006.

[57] Ryuichi Okada, Hidetoshi Ikeno, Toshifumi Kimura, Mizue Ohashi, Hitoshi Aonuma, and Etsuro Ito.
Error in the honeybee waggle dance improves foraging flexibility.
Scientific reports, 4(1):1–9, 2014.

[58] William F Towne and James L Gould.
The spatial precision of the honey bees' dance communication.
Journal of Insect Behavior, 1(2):129–155, 1988.

[59] Anja Weidenmüeller and Thomas D Seeley.
Imprecision in waggle dances of the honeybee (apis mellifera) for nearby food sources: error or adaptation?
Behavioral Ecology and Sociobiology, 46(3):190–199, 1999.

[60] Margaret J Couvillon, Hunter LF Phillipps, Roger Schürch, and Francis LW Ratnieks.
Working against gravity: horizontal honeybee waggle runs have greater angular scatter than vertical waggle runs.
Biology letters, 8(4):540–543, 2012.

[61] David A Tanner and Kirk Visscher.
Do honey bees tune error in their dances in nectar-foraging and house-hunting?
Behavioral Ecology and Sociobiology, 59(4):571–576, 2006.

[62] Charles Findling, Nicolas Chopin, and Etienne Koechlin.
Imprecise neural computations as a source of adaptive behaviour in volatile environments.
Nature Human Behaviour, 5(1):99–112, 2021.

[63] Chanelle Lee, Jonathan Lawry, and Alan Winfield.
Negative updating combined with opinion pooling in the best-of-n problem in swarm robotics.
In *International Conference on Swarm Intelligence*, pages 97–108. Springer, 2018.

[64] Yilun Shang and Roland Bouffanais.
Influence of the number of topologically interacting neighbors on swarm dynamics.
Scientific reports, 4(1):4184, 2014.

[65] Isabelle Bloch.
Fuzzy sets for image processing and understanding.
Fuzzy sets and systems, 281:280–291, 2015.

[66] Robin R Murphy.

Dempster-shafer theory for sensor fusion in autonomous mobile robots.
IEEE Transactions on Robotics and Automation, 14(2):197–206, 1998.

[67] Sébastien Konieczny and Ramón Pino Pérez.
Merging information under constraints: a logical framework.
Journal of Logic and computation, 12(5):773–808, 2002.

[68] Didler Dubois and Henri Prade.
Representation and combination of uncertainty with belief functions and possibility measures.
Computational intelligence, 4(3):244–264, 1988.

[69] Franz Dietrich and Christian List.
Probabilistic opinion pooling.
2016.

[70] Ronald R Yager.
On the specificity of a possibility distribution.
Fuzzy Sets and Systems, 50(3):279–292, 1992.

[71] Paul Jaccard.
The distribution of the flora in the alpine zone. 1.
New phytologist, 11(2):37–50, 1912.

[72] Steven Schockaert and Henri Prade.
An inconsistency-tolerant approach to information merging based on proposition relaxation.
In *Twenty-Fourth AAAI Conference on Artificial Intelligence*, 2010.

[73] Michael Crosscombe and Jonathan Lawry.
The benefits of interaction constraints in distributed autonomous systems.
arXiv preprint arXiv:2306.01179, 2023.

[74] Ricardo Mendonça, Mario Monteiro Marques, Francisco Marques, André Lourenco, Eduardo Pinto, Pedro Santana, Fernando Coito, Victor Lobo, and José Barata.
A cooperative multi-robot team for the surveillance of shipwreck survivors at sea.
In *OCEANS 2016 MTS/IEEE Monterey*, pages 1–6. IEEE, 2016.

[75] James A Preiss, Wolfgang Honig, Gaurav S Sukhatme, and Nora Ayanian.
Crazyswarm: A large nano-quadcopter swarm.
In *2017 IEEE International Conference on Robotics and Automation (ICRA)*, pages 3299–3304. IEEE, 2017.

[76] Jorge Pena Queralta, Jussi Taipalmaa, Bilge Can Pullinen, Victor Kathan Sarker, Tuan Nguyen Gia, Hannu Tenhunen, Moncef Gabbouj, Jenni Raitoharju, and Tomi Westerlund.
Collaborative multi-robot search and rescue: Planning, coordination, perception, and active vision.
Ieee Access, 8:191617–191643, 2020.

[77] Igor Douven.
Optimizing group learning: An evolutionary computing approach.
Artificial Intelligence, 275:235–251, 2019.

[78] Francesco Mondada, Michael Bonani, Xavier Raemy, James Pugh, Christopher Cianci, Adam Klaptocz, Stephane Magnenat, Jean-Christophe Zufferey, Dario Floreano, and Alcherio Martinoli.
The e-puck, a robot designed for education in engineering.
In *Proceedings of the 9th conference on autonomous robot systems and competitions*, volume 1, pages 59–65. IPCB: Instituto Politécnico de Castelo Branco, 2009.

[79] Valentino Braitenberg.
Vehicles: Experiments in synthetic psychology.
MIT press, 1986.

[80] G Valentini, H Hamann, and M Dorigo.
Efficient decision-making in a self-organizing swarm of simple robots: On the speed versus accuracy trade-off.
2014.

[81] Yakov Ben-Haim.
Info-gap decision theory: decisions under severe uncertainty.
Elsevier, 2006.

[82] Zdzisław Pawlak.
Rough sets.
International journal of computer & information sciences, 11:341–356, 1982.

[83] Nicholas Rescher and Ruth Manor.
On inferences from inconsistent premises.
Theory and Decision, 1(2):179–217, 1970.
doi: 10.1007/bf00154005.

[84] Anil Yaman, Nicolas Bredeche, Onur Çaylak, Joel Z Leibo, and Sang Wan Lee.
Meta-control of social learning strategies.
PLoS computational biology, 18(2):e1009882, 2022.

[85] Jonathan Lawry.
Heterogeneity and robustness in social learning.
In *ALIFE 2022: The 2022 Conference on Artificial Life*. MIT Press, 2022.